



**HAL**  
open science

## **Evidence for a new shallow magma intrusion at La Soufrière of Guadeloupe (Lesser Antilles). Insights from long-term geochemical monitoring of halogen- rich hydrothermal fluids**

Benoît Villemant, Jean-Christophe Komorowski, Celine Dessert, Agnès Michel, Olivier Crispi, Gilbert Hammouya, François Beauducel, Jean-Bernard de Chabalier

### ► **To cite this version:**

Benoît Villemant, Jean-Christophe Komorowski, Celine Dessert, Agnès Michel, Olivier Crispi, et al.. Evidence for a new shallow magma intrusion at La Soufrière of Guadeloupe (Lesser Antilles). Insights from long-term geochemical monitoring of halogen- rich hydrothermal fluids. *Journal of Volcanology and Geothermal Research*, 2014, pp.1-89. 10.1016/j.jvolgeores.2014.08.002 . hal-01064401

**HAL Id: hal-01064401**

**<https://hal.science/hal-01064401>**

Submitted on 16 Sep 2014

**HAL** is a multi-disciplinary open access archive for the deposit and dissemination of scientific research documents, whether they are published or not. The documents may come from teaching and research institutions in France or abroad, or from public or private research centers.

L'archive ouverte pluridisciplinaire **HAL**, est destinée au dépôt et à la diffusion de documents scientifiques de niveau recherche, publiés ou non, émanant des établissements d'enseignement et de recherche français ou étrangers, des laboratoires publics ou privés.

## Accepted Manuscript

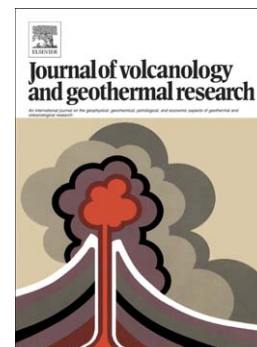
Evidence for a new shallow magma intrusion at La Soufrière of Guadeloupe (Lesser Antilles). Insights from long-term geochemical monitoring of halogen-rich hydrothermal fluids

B. Villemant, J.C. Komorowski, C. Dessert, A. Michel, O. Crispi, G. Hammouya, F. Beauducel, J.B. De Chabalier

PII: S0377-0273(14)00242-X  
DOI: doi: [10.1016/j.jvolgeores.2014.08.002](https://doi.org/10.1016/j.jvolgeores.2014.08.002)  
Reference: VOLGEO 5378

To appear in: *Journal of Volcanology and Geothermal Research*

Received date: 31 March 2014  
Accepted date: 2 August 2014



Please cite this article as: Villemant, B., Komorowski, J.C., Dessert, C., Michel, A., Crispi, O., Hammouya, G., Beauducel, F., De Chabalier, J.B., Evidence for a new shallow magma intrusion at La Soufrière of Guadeloupe (Lesser Antilles). Insights from long-term geochemical monitoring of halogen-rich hydrothermal fluids, *Journal of Volcanology and Geothermal Research* (2014), doi: [10.1016/j.jvolgeores.2014.08.002](https://doi.org/10.1016/j.jvolgeores.2014.08.002)

This is a PDF file of an unedited manuscript that has been accepted for publication. As a service to our customers we are providing this early version of the manuscript. The manuscript will undergo copyediting, typesetting, and review of the resulting proof before it is published in its final form. Please note that during the production process errors may be discovered which could affect the content, and all legal disclaimers that apply to the journal pertain.

Evidence for a new shallow magma intrusion at La Soufrière of Guadeloupe (Lesser Antilles). Insights from long-term geochemical monitoring of halogen-rich hydrothermal fluids.

Villemant B.<sup>(1\*)</sup>, Komorowski J.C.<sup>(2,3)</sup>, Dessert C.<sup>(2,3)</sup>, Michel A.<sup>(2)</sup>, Crispi O.<sup>(3)</sup>, Hammouya G.<sup>(3)</sup>, Beauducel F.<sup>(2,3)</sup>, De Chabaliér J.B.<sup>(2,3)</sup>

<sup>(1)</sup> Univ. P&M Curie, UPMC-Paris 06, UMR 7193, ISTE<sub>P</sub>, Laboratoire de Pétrologie, Géochimie, Volcanologie, 4 place Jussieu, 75230 Cedex 05, Paris, France.

<sup>(2)</sup> Institut de Physique du Globe de Paris, Sorbonne Paris Cité, Univ Paris Diderot, UMR 7154 CNRS, 1 rue Jussieu, 75238 Cedex05, Paris, France

<sup>(3)</sup> OVSG-IPGP, Observatoire Volcanologique et sismologique de la Soufrière de Guadeloupe, IPGP, Le Houélmont, 91173, Guadeloupe, France

\* *Corresponding author:*

*e-mail:* benoit.villemant@upmc.fr

*Phone#:* (33) 1 44 27 73 44

**Abstract :**

More than three decades of geochemical monitoring of hot springs and fumaroles of La Soufrière of Guadeloupe allows the construction of a working model of the shallow hydrothermal system. This system is delimited by the nested caldera structures inherited from the repeated flank collapse events and the present dome built during the last magmatic eruption (1530 AD) and which has been highly fractured by the subsequent phreatic or phreatomagmatic eruptions. Because it is confined into the low volume, highly compartmented and partially sealed upper edifice structure, the hydrothermal system is highly reactive to perturbations in the volcanic activity (input of deep magmatic fluids), the edifice structure (sealing and fracturing) and meteorology (wet tropical regime).

The current unrest, which began with a mild reactivation of fumarolic activity in 1990, increased markedly in 1992 with seismic swarms and an increase of degassing from the summit of the dome. In 1997 seismic activity increased further and was accompanied by a sudden high-flux HCl-rich gas from summit fumaroles. We focus on the interpretation of the time-series of the chemistry and temperature of fumarolic gases and hot springs as well as the relative behaviours of halogens (F, Cl, Br and I). This extensive geochemical time-series shows that the deep magmatic fluids have undergone large changes in composition due to condensation and chemical interaction with shallow groundwater (scrubbing). It is possible to trace back these processes and the potential contribution of a deep magmatic source using a limited set of geochemical time series: T, CO<sub>2</sub> and total S content in fumaroles, T and Cl<sup>-</sup> in hot springs and the relative fractionations between F, Cl, Br and I in both fluids.

Coupling 35 years of geochemical data with meteorological rainfall data and models of ion transport in the hydrothermal aquifers has allowed us to identify a series of magmatic gas pulses into the hydrothermal system since the 1976-1977 crisis. The contrasting behaviours of S- and Cl-bearing species in fumarolic gas and in thermal springs suggests that the current activity is the result of a new magma intrusion which was progressively emplaced at shallow depth since ~1992. Although it might still be evolving, the characteristics of this new intrusion indicate that it has already reached a magnitude similar to the intrusion that was emplaced during the 1976-1977 eruptive crisis. The assessment of potential hazards associated with evolution of the current unrest must consider the implications of recurrent intrusion and further pressurization of the hydrothermal system on the likelihood of renewed phreatic explosive activity. Moreover, the role of hydrothermal pressurization on the basal friction along low-strength layers within the upper part of the edifice must be evaluated with regards to partial flank collapse. At this stage enhanced monitoring,

research, and data analysis is required to quantify the uncertainties related to future scenarios of renewed eruptive activity and magmatic evolution.

Keywords: hydrothermal system; geochemical monitoring; halogens; magma intrusion; magma degassing; volcanic hazard.

ACCEPTED MANUSCRIPT

## Highlights:

- We analyze data from high-resolution geochemical monitoring of fluids over 35y.
- We determine the evolution of fluids from magma source to fumaroles and hot springs.
- Halogen and S species provide evidence for a recent magmatic signature since 1992.
- The present unrest conditions are likely the result of stalled magmatic intrusions.
- The data suggest an increase in volcanic hazard at La Soufriere of Guadeloupe.

ACCEPTED MANUSCRIPT

## 1. Introduction:

Long term monitoring of geochemical and geophysical parameters of shallow hydrothermal systems has been undertaken at numerous active volcanic areas (Newhall and Dzurisin, 1988), such as Flegrean Fields (Chiodini et al., 2003), Long Valley caldera (Sorey et al., 2003), Yellowstone (Lowenstern et al., 2006, Hurwitz et al., 2007), Mt Baker (Crider et al., 2011) and La Soufrière of Guadeloupe (Villemant et al., 2005). In these volcanic areas, unrest events have been interpreted as driven by magmatic processes at depth, involving the transfer of heat and fluids from magma intrusions to the shallow hydrothermal system. However numerous processes not directly related to magmatic activity may lead to similar changes in hydrothermal systems. These complex processes increase the difficulty of interpreting monitoring data (see e.g., Todesco et al., 2008, 2009, Moretti et al., 2013). The composition of magmatic and hydrothermal fluids collected in active volcanic areas is highly sensitive to the magma source composition and degassing processes at high temperature, but also to their lower temperature evolution and interactions with the surrounding hydrothermal systems during their shallow transfer paths (see e.g. Giggenbach, 1987, 1988, Symonds et al., 2001 among others). Monitoring the background composition, temperature and fluxes of magmatic and hydrothermal fluids over long periods of time thus constitutes a major tool for short-term hazard evaluation during unrest conditions.

The last major magmatic eruption at La Soufrière of Guadeloupe occurred in 1530 AD (Boudon et al., 2008; Komorowski et al., 2008) and possibly in 1635 (Hincks et al., 2014). Six historical phreatic eruptions have occurred since 1635 AD, namely in 1690, 1797-98, 1812, 1836-37, 1956, and 1976-77 (Komorowski et al., 2005). The July 1976 - March 1977 eruption was particularly violent and complex (Feuillard et al., 1983; Komorowski et al., 2005). The lack of adequate monitoring and knowledge of the eruptive past contributed significantly to scientific uncertainty and the difficulty of reaching a consensual expert scientific judgement on the likely scenarios for the evolution of the crisis (Komorowski et al., 2005; Feuillard, 2011; Hincks et al., 2014; Beauducel, Soufrière 1976-77 web page). Hence, the study and management of this eruption was particularly difficult for scientists and national authorities. Since this eruption, La Soufrière of Guadeloupe has become one of the best monitored volcanoes in the world, with a network of pluridisciplinary methods that are implemented by the “Observatoire Volcanologique et Sismologique de La Soufrière de Guadeloupe” (OVSG-IPGP). Permanent networks monitor seismicity and ground deformations. Sampling and analysis of the physico-chemistry of thermal springs, fumaroles and acid ponds on a fortnightly base since 1979 has provided a continuous data record over ~35 years (see OVSG-IPGP 1978-2012 and 1999-2013). This large extended baseline

dataset is a unique opportunity to analyse in details the long term evolution of the magmatic-hydrothermal system of a seldomly erupting explosive andesitic volcano.

The 1976-1977 crisis has been interpreted either as a failed magmatic eruption (Feuillard et al., 1983), or as triggered by the pulsatory behaviour of the surficial hydrothermal system (Boudon et al., 1989, Zlotnicki et al., 1992). The geochemical surveys from 1979 to 2000 evidenced a series of major geochemical anomalies in thermal springs around the dome. These anomalies have recently been interpreted as the consequence of the intrusion of a small volume of andesitic magma at shallow depth which triggered the phreatic explosions in 1976-1977 and then, through a slow crystallisation -degassing process, episodically injected gas pulses into the shallow hydrothermal system (Villemant et al., 2005, Boichu et al., 2008, 2011). This model is supported by Cl isotopes investigations (Li et al., 2012). More recently, on the basis of noble gas and C isotopes studies, Ruzié et al. (2012, 2013) have proposed a similar model where the gas flux generated by a new fresh magma injection at depth is modulated by the shallow hydrothermal system and the sealing of the edifice.

Since 1976, the geochemical anomalies recorded in hot springs have progressively decreased with time and vanished for most springs between 1992 and 1995. The sustained fumarolic activity that developed on and around the dome during the 1976 crisis vanished initially very rapidly from the dome summit in 1977 and then decreased more progressively at the base of the dome to disappear almost completely in 1981. From 1992, though the geochemical anomalies in hot springs continued to decline, fumaroles at the summit of the dome were progressively reactivated, and a persistent high flux of HCl-rich H<sub>2</sub>O vapour appeared in late 1997 (Komorowski et al., 2001, Bernard et al., 2006). Two small intermittent acid ponds were emplaced during that period at the summit of the dome (Komorowski et al., 2005). From 2006, as most springs reached a steady composition, a single spring, Galion, registered a new series of Cl anomalies culminating in 2009. Heat flux that is mainly driven by the main summit fumaroles increased by a factor of ~3 from 2005 to 2010 (Beauducel Pers. Com. see also Allard et al., 2014). In parallel, since the end of the 1976-1977 crisis, the seismic activity rapidly decreased (<10 earthquakes/month from 1984-1985) to reach a minimum in 1990 (OVSG-IPGP website). No other major anomalous geophysical signals were recorded between the end of 1977 and 1992. Since the end of 1992 the monitoring system has recorded a progressive increase in shallow and low energy seismicity (VT, LP), and a slow rise of temperature of thermal springs close to the dome (OVSG-IPGP and IPGP website). This situation of unrest at La Soufrière of Guadeloupe and its related phenomenology is not clearly understood at the present time. A magmatic origin cannot be excluded. How to identify the possible intrusion of a new magma batch as seems to have occurred during the 1976-1977 volcanic crisis?

Numerous studies have shown that geochemical monitoring provides valuable insights as to processes in the deep magmatic system that can be responsible for unrest recorded at the surface (Symonds et al., 2001, Stimac et al., 2003, Crider et al. 2011, Melian et al. 2012, Chiodini et al., 2010, Moretti et al., 2013). Halogens are of particular interest because they display simple behaviours at high temperature during magma degassing at relatively shallow level and gas transfer to the surface (Symonds and Reed, 1993, Villemant et al., 2003, 2005, Balcone et al., 2010). Halogens (F, Cl, Br and I) display simple behaviours during magma differentiation and degassing because they generally have low mineral/melt partition coefficients and high H<sub>2</sub>O vapour-melt partition coefficients. Experimental data show that halogens are highly soluble in silicate melts in the absence of an exsolved H<sub>2</sub>O vapour phase and that their volatile behaviour is mainly controlled by H<sub>2</sub>O degassing (Webster et al., 1999; Aiuppa et al. 2008 and references therein). Cl, Br and I are extracted as halogen acids (HCl, HBr, HI) from the magma with similar vapour-melt partition coefficients, whereas F is not significantly extracted and remains concentrated in silicate melts (Villemant and Boudon, 1999, Balcone et al., 2010). Halogen contents in magmatic gases are almost not modified by decompression, gas- wall rock interactions or cooling (down to temperatures ~120°C) during ‘dry transfer path’, i.e. without interaction with a shallow hydrothermal system or atmospheric gases (Symonds and Reed, 1993). If gas interacts with hydrothermal or phreatic waters (‘wet transfer path’) halogen acids are completely dissolved (‘scrubbing effect’) and transported as conservative ions in low temperature aqueous systems (Symonds et al., 2001, Villemant et al., 2005). From these properties it is inferred that halogen abundance ratios (Cl/Br/I) of the degassing magmas are preserved in gases from high to intermediate temperatures (T >120°C) when they are transferred through a ‘dry path’ to the surface as observed, for example, in Mt Etna fumaroles (Aiuppa et al., 2005). These halogen ratios can also be preserved when halogen acids are completely dissolved in phreatic and hydrothermal systems. However, halogens may be highly fractionated during low temperature gas condensation (<120°C), boiling of acid or ion-rich waters or precipitation of halides in highly concentrated brines (see e.g. Berndt and Seyfried, 1997 and references therein). Halogens speciation in the gas plume may also be highly modified by mixing with oxidizing atmospheric gas and photocatalytic reactions (Bobrowski et al., 2003; Gerlach, 2004; Millard et al., 2006; Oppenheimer et al., 2006; Villemant et al., 2008; Aiuppa et al., 2008; Von Glasow et al., 2009). Thus halogen systematics in volcanic fluids provide an efficient tool for identifying their origin and transfer histories, including condensation-evaporation and dissolution-precipitation processes, which is the goal of geochemical surveys of active volcanoes.

In this paper we present and interpret the geochemical time-series data (temperature and chemical compositions) that was measured during about 35 years of sampling of hot springs,

fumaroles and acid ponds between 1979 and the end of year 2012. It extends the 1979-2003 data series from hot springs only that was discussed by Villemant et al. (2005) and focuses more specifically on halogens (F, Cl, Br, I) and temperature records. The interpretation of gas monitoring data remains a specific challenge because these are often marred by large errors caused by numerous difficulties in fumaroles sampling as well as the analytical protocols. The approach used here is to combine all the information (gas and hot spring water geochemistry, phenomenology) to overcome this difficulty and to extract an interpretative scheme that is as consistent as possible with all available geochemical data. On the basis of the entire monitoring data set we propose a general model for the evolution of the surficial hydrothermal system since 1976 and its relationship with deep magmatic activity.

## 2. Geological setting and phenomenology of the hydrothermal activity at La Soufrière of Guadeloupe

The last magmatic activity at La Soufrière, dated at 1530 AD, produced pyroclastic pumiceous tephra fallout and pyroclastic flows and built an andesite lava dome (Boudon et al., 2007, 2008, Komorowski et al., 2008). This dome is located in a complex horseshoe-shaped structure (Fig. 1) inherited from recurrent flank collapse events (11500 and 3500 B.P.) that affected the summit area of the Carmichael volcano which is part of La Soufrière - Grande Découverte volcanic complex (Boudon et al., 1989, 2008, Komorowski et al., 2005). The historic activity since 1635 has been limited to six explosive phreatic eruptions without participation of magma. The most violent eruptions were those of 1797-1798 and 1976-1977, the latter of which has been interpreted as a failed magmatic eruption (Feuillard et al., 1983, Komorowski et al., 2005; Villemant et al., 2005; Boichu et al., 2008; 2011; Ruzié et al., 2012).

The co-existence of an active magma chamber and abundant ground-water fed by a tropical climate regime with abundant rainfall (mean value for 1983-2010:  $10 \pm 2$  m/yr) has led to the occurrence of numerous permanent thermal springs and permanent to intermittent fumarolic degassing on the summit and at the periphery of the dome (Bigot et al., 1987, Zlotnicki et al., 1992, Villemant et al., 2005, Komorowski et al., 2005, Fig. 1). Interaction of the more active summit fumaroles with perched aquifers favours the formation of intermittent acid ponds (Cratère Sud and Tarissan). Historical observations show that the nature, distribution and intensity of hydrothermal activity have considerably varied over time (Komorowski et al., 2005, Bernard et al., 2006).

The large development of intense and recent fumarolic activity on the volcano is also evidenced by numerous zones of hydrothermally altered volcanic material. These alteration zones generally consist of elongated areas varying in size from tens to hundreds of meters (Fig. 1a). They

are located at the summit of the dome (Faille du Nord, Tarissan, Cratère Sud, Lacroix) and on its flanks (Collardeau, Carbet Echelle, Col de l'Echelle-Chaudières, La Ty fault) and generally correspond to the main fracture systems. All of the altered zones have been historically active, but at present, only the fumarolic fields of the La Ty fault and the dome summit are active. This fumarolic alteration affects massive dome lavas (Faille du Nord) or pyroclastic material (scoria and ashfall deposits at La Ty fault, at the summit of the dome and at Col de l'Echelle for example) and mainly consists of the development of smectite at the expense of the magmatic glass and the precipitation of sulfates and sulfides (Salaün et al., 2011). Frequent partial edifice-collapse events (at least ten in the last 15 000 years) have affected the La Soufrière-Grande Découverte volcanic complex and emplaced debris-avalanche deposits which contain abundant fragments of hydrothermal alteration products (Komorowski et al., 2005; Salaün et al., 2011). Finally, the six historical phreatic eruptions emitted large amounts of ash which contain abundant hydrothermally altered material (Feuillard et al., 1983) and were easily altered after deposition by fumarolic and hydrothermal activity (Salaün et al., 2011).

Although the fumarolic fields at the periphery of the dome (Collardeau, Carbet-Echelle, Chaudière-Souffleur, Morne-Mitan) were active before the 1976 - 1977 volcanic crisis, their activity increased markedly after the onset of the eruption which began with a violent phreatic explosion in July 1976 (Feuillard et al., 1983; Komorowski et al., 2005). The eruption ended in April 1977 after a series of ~26 explosive events. A progressive decline of fumarolic activity started in May 1997 (summit) and gradually reached peripheral fumaroles which ceased to degas sequentially (Carbet in 1979; Collardeau in 1982; Col de l'Echelle and Lacroix in 1984; Komorowski et al., 2005). Only residual low temperature degassing remained at the La Ty fault and Morne-Mitan fumaroles between 1984 and 1992. Fumarolic activity progressively returned at the summit, starting in 1990 at Cratère Sud, progressing to the Napoleon fumarole in 1997, Tarissan in 2000, the Gouffre 1956 crater in 2007, and finally recently the Lacroix Superieur fumarole in 2012. However, temperature and degassing flux significantly increased in late 1997 at the Cratère Sud fumarole, which has been characterised, since early 1998, by a persistent high flux of HCl-rich H<sub>2</sub>O vapour (up to 1M HCl) that forms plumes visible at large distance from the dome (Komorowski et al., 2001; 2005; OVSG-IPGP, 1999-2013). No significant fumarolic activity has been maintained at the base of the dome except persistent weak and non pressurized emanations at Morne Mitan and La Ty fault. Boiling ponds of extremely acid water were emplaced at Cratère Sud and Tarissan in late 1997 and 2001 respectively. The Cratère Sud pond is not easily accessible and likely intermittent, and Tarissan pond is permanent but its level (ca. 87 m below the summit surface: Kuster et al., 1997) is highly variable in time (Beauducel pers. com., Allard et al., 2014).

Thermal springs are concentrated around the base of the dome mainly in the SW, S and NE sectors (Fig. 1a). This distribution is controlled by the structure of the volcanic edifice and the extensive development of argilic hydrothermal alteration along preferential zones (Fig. 1b). The basement of the volcanic structures (caldera and flank collapse craters), to which the recent volcanic activity has been confined, forms preferential zones of shallow ground-water circulation such as the Cratère Amic structure. Most springs are located at high altitudes (950 to 1170m) within or at the exit of the Cratère Amic around the dome (at a maximum distance of 1.2 km from the summit): Carbet Echelle (CE), Tarade (Ta), Bains Jaunes (BJ), Pas du Roy (PR), Galion (Ga) and Ravine Marchand (RM) and Ravine Roche (RR). The flow rate and the temperature at CE has strongly decreased over the past years, to reach ambient temperature and eventually to cease at the beginning of 2010. Three other springs are located outside the Cratère Amic structure, either on the eastern flank of the Grande Découverte volcano: at Chute du Carbet (CC) or on the western flank at Bains Chauds du Matouba-Eaux Vives (BCM-EV) and Habitation Revel (HR). CC is located at much lower altitude (~ 600 m) at a distance of around 2.5 km east of the summit. HR is located at ~ 3.5 km east of the dome at an altitude of ~ 600 m and BCM is located at ~ 1km north-west and at an altitude of ~ 1050 m. Eaux-Vives (EV) is in fact the catchment of BCM spring water transported through a pipe: EV waters have a chemical composition identical to those of BCM but the temperatures are systematically shifted by ~ -10°C. The geochemical survey from 1979 documented temporary compositional anomalies for the springs located in the sector delimited by the Cratère Amic structure within which La Soufrière dome has been built (Villemant et al., 2005). CC spring, which displays similar geochemical anomalies, is located on the fault system of the Chutes du Carbet, suggesting that its phreatic system is related to that developed inside Cratère Amic. The absence of geochemical anomalies in waters collected in the last ~35 years in the other springs located outside the Cratère Amic (HR and BCM-EV) indicate that they are isolated from the direct influence of volcanic activity. The major chlorine and temperature anomalies evidenced after the 1976-1977 volcanic crisis for hot springs within the Cratère Amic have progressively decreased with time at a rate decreasing with distance to the dome: CE spring, which is the closest to the dome (~100 m), has reached a steady composition in 1992, whereas CC spring, which is the furthest one (~2.5 km), reached its steady composition in 2004. However since 2006, a single spring, Galion (Ga) has registered a new series of Cl anomalies which culminated in 2009.

### 3. Geochemical survey of gas plume, fumaroles, acid ponds and thermal springs

#### 3.1 Sampling and analytical methods

A very complete and systematic survey of the volcanic activity of La Soufrière has been progressively developed after the 1976-1977 volcanic crisis by the Observatoire Volcanologique et Sismologique de Guadeloupe (OVSG-IPGP), which is part of the Institut de Physique du Globe de Paris (Feuillard et al., 1983, Bigot et al., 1994, and OVSG-IPGP website.). It includes geophysical (seismicity, ground deformation, magnetic measurements, heat flux, gravimetry) and geochemical monitoring (physico-chemistry of thermal sources and fumaroles, soil degassing) and offers one of the most complete and continuous data records over a long period of time (~35 years) on the same volcano. Beginning in 1979, hot springs and fumaroles of La Soufrière have been regularly sampled twice monthly, and their temperature and major element compositions determined by the OVSG-IPGP. From 1979 to 1994 only 5 hot springs were systematically sampled (CE, BJ, Ga, CC and BCM-EV); then, from 1995 to 2000, 3 hot springs inside Cratère Amic structure were added to the systematic survey: PR, Ta and RM. Since 1997 and the marked increase of fumarolic activity at the summit of the dome, systematic sampling of gases and condensates have been performed. To determine the concentration of gas species on a dry basis ( $\text{CO}_2$ ,  $\text{H}_2\text{S}$ ,  $\text{SO}_2$ ,  $\text{CO}$ ,  $\text{CH}_4$ ,  $\text{H}_2$ ,  $\text{N}_2$ ,  $\text{O}_2$ ), sampling is performed using evacuated bottles containing powdered  $\text{P}_2\text{O}_5$  or a reactive solution of  $\text{NaOH}$ . Gas compositions were determined by gas chromatography and, since 2001, by quadrupole mass spectrometry at OVSG-IPGP. To determine the concentration of minor reduced gas species ( $\text{CO}$ ,  $\text{H}_2$ ,  $\text{CH}_4$ ) and for  $\text{H}_2\text{S}$  -  $\text{SO}_2$  measurements,  $\text{P}_2\text{O}_5$ - bottles are preferred to  $\text{NaOH}$ - bottles because the former better preserves the redox conditions (Delorme 1983, Bernard et al., 2006). Gas compositions are also corrected for air pollution ( $\text{N}_2$  or  $\text{O}_2$ ) but samples displaying evidences for large air/gas ratios (e.g.  $\text{N}_2 > 5$  mol%) are discussed separately.  $\text{H}_2\text{O}$  and  $\text{HCl}$  are measured in gas condensates (by gravimetric and ion chromatography methods at the OVSG-IPGP and by IC-ICP-MS at the LGSV-IPGP). Additional measurements of halogens (F, Cl, Br and I) contents are also performed by IC and ICP-MS at the LGSV-IPGP (Michel and Villemant, 2003). When sampling is possible, acid pond compositions are determined with the same methods as those used for thermal springs. The specific field conditions of La Soufrière fumaroles and particularly their low temperature, which is near the boiling point, lead to significant difficulties for gas sampling and analysis. Sampling and analytical methods are described in details on the OVSG WebObs website (Beauducel et al., 2004, 2010) and in Villemant et al. (2005). Mean temperature and major element compositions of springs and acid pond waters and fumaroles condensates collected between 1979 and the present day are reported in Table I. Mean temperature and major gas compositions of fumaroles (dry gas basis) are reported in Table II. Temperature and major elements compositions for more limited periods have also been reported in Villemant et al. (2005) and Chen et al. (2013). Complete data sets (temperatures, springs and gas compositions in major elements) are included in

the OVSG-IPGP database (WebObs website, Beauducel et al., 2004, 2010; see also OVSG-IPGP and IPGP -public access- websites). A comprehensive consistent data set for halogens data and CSC gas composition is available as Supplementary Material .

### 3.2 Main geochemical characteristics of thermal springs, acid ponds and fumaroles

#### 3.2.1 Thermal springs:

All springs have relatively high flow rates ranging from some Kg/s to 100 Kg/s for BCM. Temperature ranges are moderate (25-45°C) except for CE and BCM springs. BCM spring displays a constant and high (60°C) temperature over the last 35 years. CE spring temperature has decreased from ~70°C (1<sup>st</sup> measurement in 1979, after the end of the 1976-1977 volcanic crisis) down to the mean ambient air temperature (~20°C) in 2010. On the basis of their Na, Ca, Mg, SO<sub>4</sub>, Cl and HCO<sub>3</sub> contents (Giggenbach's diagrams, Fig. 2) the thermal springs can be divided in 3 main types: Ca-SO<sub>4</sub> waters (BJ, CE, Ga, Ta, RM, PR, BCM), a Ca-Na-HCO<sub>3</sub> water (HR) and a Ca-Na-Cl water (CC) (Table Ia). F contents are always very low: ~0.1 10<sup>-3</sup> Mol/L in BCM and <0.05 10<sup>-3</sup> Mol /L in other springs. The slightly SO<sub>4</sub>-rich acidic waters may result from mixing between meteoric water and oxidised H<sub>2</sub>S-bearing magmatic fluids (Bigot et al., 1994, Brombach et al., 2000); they are all located within the Cratère Amic structure. CC waters could be the result of mixing between Ca-SO<sub>4</sub> waters and Na-Cl waters found in the deep geothermal system of Bouillante on the eastern coast of Basse Terre (Traineau et al., 1997). However, CC waters cannot be considered as a simple mixing between these two components because of the large Cl<sup>-</sup> enrichment counterbalanced by Ca<sup>++</sup> and Mg<sup>++</sup> (in the 1:1 ratio, Villemant et al., 2005). BCM-EV waters differ from the other Ca-SO<sub>4</sub> waters in having very low Cl contents. HR waters could correspond to shallow groundwaters with compositions close to that of regional cold springs heated by magmatic heat transfer. Large Cl enrichments are characteristic of springs inside or connected to (CC) the Cratère Amic structure.

#### 3.2.2 Acid ponds.

The acid ponds are emplaced inside dome summit fractures at Cratère Sud and Tarissan at depths of ~ 20 m and ~100 m respectively and are not easily accessible. These acid ponds are almost permanent since 1997 and 2001 respectively, but their depth may rapidly vary with time (±50 m at Tarissan). Physical and chemical characteristics of Tarissan acid pond are permanently monitored by OVSG-IPGP. Its temperature varies slightly around 97°C (Table Ib) which is the ebullition temperature of ion poor aqueous solutions at this altitude (~1400 m). Water boiling is sufficient to explain the vapour flux at the Tarissan vent (D. Gibert and S. Vergniolle., pers. com.). Ponds waters

are highly acid, turbid and lightly coloured yellow indicating large ion contents due to interaction with host andesite. Unlike temperatures, compositions of acid ponds strongly vary with time. Ion contents in Tarissan acid pond reached their highest values during the 2007-2009 period with maximum contents as high as 10 wt% Cl<sup>-</sup> (2.9 mol/L) and 3500 ppm in Ca<sup>++</sup>. Mg<sup>++</sup> and Na<sup>+</sup> reached concentration values of ~1200 ppm. Their normalised Mg-Ca-Na compositions plot within the composition field of the active hot springs (Fig. 2). However, SO<sub>4</sub><sup>-</sup> and HCO<sub>3</sub><sup>-</sup> contents of acid ponds are much lower and even negligible relative to their Cl<sup>-</sup> contents contrary to most hot springs, which typically have more SO<sub>4</sub><sup>-</sup> than Cl<sup>-</sup>. Acid ponds compositions define the Cl-rich end-member towards which most waters of active springs are trending.

### 3.2.3 Fumaroles.

The gas temperatures are generally close to the boiling point, inevitably leading to H<sub>2</sub>O condensation along the sampling line which dissolves mainly HCl and to a lesser degree some sulphur species and little CO<sub>2</sub> (see Giggenbach et al., 2001 and references therein). In addition, mixing with air within the gas plume may modify redox conditions (e.g. lowering the H<sub>2</sub>S/SO<sub>2</sub> ratio or to a lesser extent the CO/CO<sub>2</sub> ratio), but these reactions are kinetically limited. For these reasons large amounts of gas and condensates are collected, minimising condensation effects on dry gas measurements. Solid S may also occur as deposits around the summit fumarole vents or as precipitates in sample condensates, leading to underestimation of the total S/ total C ratio. The most robust gas data are mainly total S/total C ratio, minimum gas temperatures, and Cl (and other halogen) contents measured in gas condensates; other 'dry gases' currently have to be interpreted with caution (see discussion below).

CSC is the most active summit fumarole and the most continuously sampled; it mainly consists of H<sub>2</sub>O vapour containing CO<sub>2</sub>, H<sub>2</sub>S and HCl with only minor SO<sub>2</sub> and H<sub>2</sub>, as well as traces of CH<sub>4</sub> and CO, with temperature varying between 96 and 130 °C (Table II). Low temperature gases (T = 94-95°C) were collected just before the renewal of the fumarolic activity in 1997 at both the summit of the dome and the La Ty fault (Brombach et al., 2000). They mainly consisted of water vapour (93-97 mol % H<sub>2</sub>O) with minor CO<sub>2</sub>, H<sub>2</sub>S and H<sub>2</sub> (Fig. 3) and no significant amounts of SO<sub>2</sub> and HCl and other reduced species (CO, CH<sub>4</sub>). These compositions do not directly derive from a pure magmatic gas. Isotopic compositions of He, C, H and O indicate that all these fluids are mixtures between atmospheric, meteoric and magmatic components and likely result from boiling hydrothermal aqueous solutions equilibrated at low temperatures (Allard et al., 1998, Brombach et al., 2000, Ruzié et al., 2012, 2013). The fumarolic field at the base of the dome (LaTy and Route de la Citerne - RC-) has not been significantly modified in composition and temperature since 1997.

The fumarolic activity at the summit of the dome (Cratère Sud Central and North - CSC and CSN- and Tarissan fumaroles) has increased considerably since 1997. Maximum vapour fluxes were observed between 2000 and 2010. Vapour fluxes at Cratère Sud were estimated on the basis of direct gas speed determination in 2005 and through remote thermal imagery in 2010 (Dupont, 2010, Beauducel Pers. Com): they have increased from ~500 to ~1600 T/day. This represents the major part of present day heat loss at la Soufrière, estimated at around 60 MW (Beauducel Pers. Com.). Compared to pre-1998 fumaroles, the summit fumaroles have also high H<sub>2</sub>O contents (93-98%) but relatively lower contents of CO<sub>2</sub> and H<sub>2</sub> and are higher in H<sub>2</sub>S, SO<sub>2</sub> and CO. They are also characterised by significant amounts of HCl (up to 0.5 mol% in total gas), which has only been observed in summit fumaroles during the 1976-1977 volcanic crisis (Table II). These compositions suggest an increasing contribution of a S- and HCl- rich component of magmatic origin. Conversely there is no evidence for changing CO<sub>2</sub> input from the deep magmatic systems (Ruzié et al., 2013).

#### 4. Temperature and composition time series of hot springs and fumaroles

##### 4.1 Thermal springs: long term variations

Major element composition evolution of springs define three distinct groups (Table II). Most springs outside the Cratère Amic structure (HR, BCM-EV) display no significant chemical variations over 35 years. Most springs inside the Cratère Amic structure display large composition variations for the period 1979-1994 and then reach an almost steady composition. Two springs, Ga and CC, respectively inside and outside the Cratère Amic structure, display distinctive time series features. For CC spring chemical data are reported for the periods 1979-2005 and 2005-present day. Ga spring displays a 3-fold time series evolution, the first two being similar to those of other springs located inside the Cratère Amic. Since 2006, a series of Cl anomalies are observed in this spring, culminating in 2009 with an intense and long lasting anomaly. The composition time series of the first regime (1979-1995) have been interpreted in previous papers (Villemant et al., 2005, Boichu et al., 2011) and we will here mainly focus on the second period (1995-present day).

##### *4.1.1 Major element composition variations.*

Time series of hot spring compositions are reported in Fig. 4 and in Supplementary Material. They display long term and short term (months to one year) variations. The short term variations have similar frequency characteristics for all ion species in all springs, but with very different amplitudes. The short term variations are of low amplitude in springs outside Amic Crater and of higher amplitude for springs inside the structure and in particular the sources at higher altitude (CE,

Ta, Ga). Springs outside the Cratère Amic (HR, BCM –EV), except CC, do not display significant long term variations in their chemical compositions over the entire sampling period (~35 years). Cation contents of springs inside Cratère Amic and CC generally display a slight and regular decrease over the whole sampling period (Fig. 5 a and Supplementary Material, Fig. B). On the contrary the long term variations in anionic species are large with at least two distinct periods of evolution. Cl is generally the most abundant and most variable anionic species ( $1 - 20 \cdot 10^{-3}$  Mol/L, Fig. 4b). It varies generally at constant  $\text{SO}_4^{2-}/\text{HCO}_3^-$  ratios (linear arrays trending towards the Cl apex of Fig. 2). The variations in Cl contents are the largest in CE spring during the 1979-1995 period and in Ga spring during the 2002- present day period. CC spring also displays a very large Cl anomaly during the period 1980-2005. Charge balance in Cl rich waters is maintained by correlative increases in the bulk cation content, with no dominant variation of a specific cation as already observed by Villemant et al. (2005).  $\text{F}^-$  does not display variations.  $\text{SO}_4^{2-}$  and  $\text{HCO}_3^-$  display variable, smooth and of low amplitude (generally less than 1 mMol/l) changes, except for  $\text{HCO}_3^-$  in CE during the period 1979-1995 (no data are however available for  $\text{SO}_4^{2-}$  during this period).

Thermal springs located inside the Cratère Amic and close to the dome (mainly CE, BJ and Ga, sampled since 1979, and likely PR, RM and Ta springs which, however, were not sampled before 1995) display two distinct evolution regimes over the 1979-1994 and 1995-present day periods. The first regime is characterised by series of large Cl positive anomalies, the intensities and extents of which are more pronounced for the springs closest to the dome (as CE located ~100 m from the dome). In CE spring the pre-1995 Cl anomalies are also correlated to increases in  $\text{SO}_4^{2-}$ ,  $\text{HCO}_3^-$  and in  $\text{Na}^+$  (and likely in other cations, but these were not determined before 1987). CC spring displays a unique Cl anomaly extending over a very large interval of time (~25 y), with a maximum occurring in 1990. Since ~1995 most springs inside the Cratère Amic have displayed low and almost constant ion contents (total ion content  $\sim 15 \cdot 10^{-3}$  Mol/L) with a relatively homogeneous composition which corresponds to the Ca(Mg)- $\text{SO}_4$  type with low Cl content ( $\text{Cl} < 3 \cdot 10^{-3}$  Mol/L; Fig. 4a,b, Table I). Two springs however, Ta and Ga, display specific variations: Ta spring, since the beginning of sampling in 1995, displays short term oscillatory variations for all ions, whereas Ga spring, since 2001, displays large Cl anomalies lasting up to some months.

#### *4.1.2 Temperature variations.*

Time series of hot springs are reported in Fig. 4b, c. All hot springs located outside the Cratère Amic structure (including CC) display steady or slightly decreasing temperatures ( $\Delta T < 5^\circ\text{C}$ ) since 1979. BCM remains at a remarkably high and constant temperature ( $58.5 \pm 0.5^\circ\text{C}$ ). Hot springs located inside the structure, except CE, are characterised by almost constant or slightly variable

temperatures before 1995 and a slow increase in temperature since 1995 ( $\Delta T \sim 5^\circ\text{C}$  in average over  $\sim 15$  years). Ta and Ga springs display the largest temperature increases since 1995 ( $\sim 7^\circ\text{C}$  and  $\sim 6^\circ\text{C}$  respectively). CE spring displays a very large temperature decrease between 1979 and 2010. In this spring, from 1979 to 1992, some small temperature spikes (1 to  $3^\circ\text{C}$ ) lasting  $\sim 3$ -4 months were observed and are clearly synchronous to the largest Cl spikes of this period (Fig. 4c). Later, the temperature smoothly decreases down to the ambient air temperature ( $\sim 20^\circ\text{C}$ ). It is to be noticed that temperatures of the springs located inside the Cratère Amic structure tend, at least since 1995, to increase towards higher values closer to the steady temperatures of springs located outside the structure.

#### 4.2 Thermal springs: short term variations

The large chemical and thermal variations at short time scales observed in springs located inside the Cratère Amic structure during the 1979-1995 period (mainly CE spring and to lesser extents BJ and Ga springs) have been described in details by Villemant et al. (2005). These variations have no periodic character and the delay between two Cl (and T) pulses progressively increases with time. They have been interpreted as the result of the pulsatory degassing of a magma intrusion (Villemant et al., 2005, Boichu et al., 2008, 2011). This regime ended in  $\sim 1995$ . In the recent period most springs evolve towards steady compositions and temperatures, but two springs, Ta and Ga, display large composition and temperature variations at short time scales (some months).

Since the beginning of sampling in 1995, Ta spring displays correlated short period variations in both temperature and bulk major element composition, with a clear periodic character (Fig. 5a). Fourier transform analysis of T and Cl variations indicates a dominant period of  $\sim 12$  months, which corresponds to the annual variations in rainfall regime. The T- and Cl- maxima correspond (with a delay varying in time between 1 and 3 months) to rainfall minima at the dome summit, suggesting that runoff and rain water infiltration represent the major control of the temperature and composition variations of Ta spring. The rain-fall regime recorded since 1992 at the dome summit (meteorological station 'VOLCAN') is compared to the temperature- and major elements- time series of Ta spring in Fig. 5a, and to the temperature and Cl- time series for BJ and Ga springs in Fig. 5b. To match the main characteristics of both rainfall- and T- time series, different time delays characteristic of each spring have to be applied. These time delays must also vary in a stepwise fashion. The delays are calculated using a simple best fit of the rainfall – temperature correlations over some time windows. The delays increase with time from  $\sim 1.2$  to 3 months for Ta spring and from 3.8 to 4.5 months in Ga spring. The shifts in delay values are relatively sharp and occur for

both springs at the end of 1998 and in May 2005. This increase suggests a significant decrease in edifice permeability, which is more compatible with progressive bulk sealing of the host-rock than with any significant meteorological or seismic event occurring at that period. The 21 Nov. 2004 Les Saintes regional earthquake (Mw 6.3; Beauducel et al., 2011, Feuillet et al., 2011) might have been expected to enhance fluid circulation and thus shorten the delay between rainfall maxima and T and Cl minima, but this was not observed. In BJ spring, the delay is approximately constant (~2 months) over the whole record period. This delay is consistent with that obtained by hydrologic tracing of rain water transfer from the dome summit to the BJ spring (2-3 months) performed in 1993 by Bigot et al. (1994). Cl- time series of Ta spring is also well correlated with the delayed rainfall regime, but for the other springs (BJ and Ga) the agreement is poor. Runoff and infiltration of the intense rainfalls on the summit area of La Soufrière volcano (~ 10 m/year) are thus major direct contributors to hydrologic and thermal budgets of the springs which are the closest to the dome summit. In addition, EC spring which has a similar position to Ta spring relative to the dome and is thus fed by a small summit aquifer. The large variations in composition observed from 1979 to 1985 could also be explained by the rainfall regime. However, unlike Ta spring, there is no correlation between composition variations and rainfall (Fig. C, Supplementary material) and the main source of these fluctuations in composition must be found in magma or hydrothermal deep sources (see Villemant et al., 2005, Boichu et al., 2011). For all other springs there are no significant correlations between temperature- or composition- time series and rain fall regime over the whole sampling period, especially for springs outside the Cratère Amic structure and far from the dome (BCM-EV, HR, CC).

Since 2001, the evolution of Ga spring composition is characterised by a series of significant Cl anomalies which are a-periodic and of increasing intensity with time: Feb. 01, Nov. 02, Oct. 03, Nov. 04, Aug. 05, June 07 and the largest one culminating in October 2009 (Fig. 4a). Cl enrichments are large (from ~7  $10^{-3}$  Mol/L in 2001 and 2003 up to 20  $10^{-3}$  Mol/L in October 2009, relative to a background of ~5  $10^{-3}$  Mol/L). They last approximately one month to 18 months (Fig. 6). The increases in Cl contents are diversely correlated with other major element variations and pH. The largest Cl anomaly (2009-2010) is also associated with slight increases in other major cations ( $Mg^{++}$ ,  $Ca^{++}$  and  $Na^{+}$ ) and very slight decreases in  $HCO_3^{-}$ ,  $SO_4^{-}$  and pH. The other Cl anomalies are lower in intensity and characterised by slight increases in  $Ca^{++}$  and  $SO_4^{-}$  and slight (or no) decreases in pH. None of these anomalies are correlated to temperature variations which remain low ( $\Delta T = \pm 2^{\circ}C$  around the mean trend) or to the rainfall regime, even in 2010 during which dry and wet periods on La Soufrière dome were particularly extreme. There is also no apparent correlation with seismic

activity and the main anomalies (2001 and 2009) occur during almost aseismic periods. Such anomalies have not been observed in any other spring since 1995.

#### 4.3 Fumaroles: temperature and composition variations.

Temperatures and the ‘dry gas’ compositions of fumaroles at the base of the dome (Route de la Citerne, RC, which almost completely vanished in 2001) and at the summit of the dome (Cratère Sud Central -CSC- since 1992 and Cratère Sud Nord -CSN- since 1995) are reported in Table II. The pH, Cl<sup>-</sup> and SO<sub>4</sub><sup>2-</sup> are also measured in some fumaroles condensates from CSC and CSN (Table Ib and Fig. 7). Few accurate and consistent condensates compositions exist for fumaroles active before 1983, in particular for the 1976 crisis (IPGP, Internal reports, 1976-1984). Since 1992 the evolution of the activity of summit fumaroles has shown a characteristic increase in gas flux from ~1998 to ~2008, followed by a slight decrease. Simultaneously there has been a large increase in total sulfur content (mainly as H<sub>2</sub>S species) relative to CO<sub>2</sub> content (Fig. 3 and 7a). On the basis of the few bulk gas composition measurements (including H<sub>2</sub>O), this is interpreted to result from a significant increase in S-species in the gas, rather than an actual decrease in CO<sub>2</sub>, which has likely remained approximately constant (see also Ruzié et al., 2013). Since 1992, total S content has peaked in early 2008 before initiating a decrease that is ongoing up to the present time. This evolution is roughly correlated to the bulk increase in CSC fumarole temperature.

Temperature and the HCl contents in fumaroles (Table Ib) display three distinct periods of variation, the first one from ~1997 to 2002, the second one from 2003 to the end of 2008, and the third one since the end of 2009 (Fig. 7b). During the first two periods there is a large increase in fumaroles temperatures with maximum values that show transient peaks at ~108°C in mid-1999 and ~125°C in mid-2000, an overall increasing trend until mid-2001 (~115°C) and the highest value at the end of 2007 (~140°C recorded in CSN). Because of infrequent sampling difficulties and frequency (~1/month), these spikes are indicative of periods of high gas temperatures of unknown duration. Since 2009, fumaroles temperatures and vapour flux slightly decrease. HCl contents in fumarole condensates also reached a maximum (~2.5 Mol%) in 2001, but have remained relatively low (< 0.5 Mol%) since 2003. Because H<sub>2</sub>O contents are rarely determined and only ‘dry gas’ compositions of other major species (H<sub>2</sub>, CO, CH<sub>4</sub>, N<sub>2</sub>, H<sub>2</sub>S, CO<sub>2</sub>, SO<sub>2</sub>, O<sub>2</sub>) are measured and normalised to 100%, the absolute variations in HCl contents which are measured in condensates cannot be compared to those of other gas species. However the periods of maximum HCl (2001-2002) and total S contents (2009-2010) do not coincide.

In Fig. 7b, variations of temperatures and Cl contents of CSC fumaroles and Ta spring are compared for the 1998-2008 period. When available, pH measurements of CSC acid ponds are also

reported. Short term variations of Cl and T of both fluids are very closely correlated. They are also correlated to CSC pond pH values. This result clearly indicates that, as for Tarade spring, variations in composition and temperature of Cratère Sud fumaroles are mainly controlled by the rainfall regime. This control occurs through runoff and infiltration in the upper part of the dome. The fumaroles and Ta spring exhibit a similar time delay of ~ 3.5 months (see § 4.2).

## 5. Halogens (F, Cl, Br, I) in hydrothermal fluids.

Halogen (F, Cl, Br and I) contents in spring waters and fumarole condensates have been determined using methods described in Michel and Villemant (2003) and Villemant et al. (2005). Data are reported in Table III and the time-series diagrams of Fig. 8.

### 5.1 Major halogen elements: F and Cl.

All fluids (spring waters, fumarolic condensates) have systematically low F contents. Given that F contents in fumarolic condensates are very low compared to usual detection limits of Ion Chromatography (~0.1 ppm), we have implemented a protocol of pre-concentration by evaporation at low temperature to reduce these detection limits to ~ 0.05 ppm (~2.5  $\mu\text{Mol/L}$ ). F contents of all condensates are now near this new detection limit. In springs outside the Cratère Amic, F contents are almost constant with ~ 2 ppm (0.1 mMol/L) in BCM-EV and about 0.2 ppm (0.01 mMol/L) in HR. F contents in springs inside the Amic structure, are slightly more variable and range between the detection limit and ~1 ppm (0.005 to 0.05 mMol/L). Contrary to F, Cl contents are elevated and highly variable in most sampled fluids. The pre-1998 fumaroles (RC) have very low Cl contents (~ 2 ppm ~ 50  $\mu\text{Mol/L}$ , Fig. 7b), whereas summit fumaroles since 1998 are characterised by very large and highly variable Cl contents (ranging between 20 and 50  $10^3$  ppm, Table 1b). In BCM –EV and HR spring waters the Cl contents are low (< 40 ppm, ~1 mMol/L) and almost constant over the entire sampling period (Fig. 4a). However in all other springs Cl contents are significantly higher and strongly variable in time. In CE spring Cl contents have strongly decreased with time from a maximum of ~20 mMol/L in 1981 to values close to the detection limit at the end of its activity in 2009. In CC and Ga springs Cl variations with time are large and complex (see major element variations, above).

### 5.2 Trace halogen elements: Br and I.

The range of composition of Br and I in hydrothermal fluids is very large (4 to 5 orders of magnitude, Table Ib, Fig. 8a). For the 1979-1998 period no iodine measurements are available, except for Ga spring. Fumaroles have generally much lower Br and I contents than thermal spring

waters: Br contents are lowest in pre-1998 fumaroles (RC, Br < 10 ppb) and they are < 0.1 ppm in most summit fumaroles. Some fumarole condensates however reach Br contents  $\geq$  1ppm. Br contents of thermal springs range between 10 ppb and 1 ppm but, exceptionally, reach higher values (~2 ppm) as in Ga or CC springs. Like Cl, Br and I contents display large temporal variations in fumaroles, in waters of springs located inside the Cratère Amic structure as well as in CC spring.

### 5.3 Halogens ratios.

Although the range in Br and I composition is large, the range of Br/I of all hydrothermal fluids is relatively narrow (5 - 40; mass ratio) compared to analytical errors (~20% relative, Michel and Villemant, 2003). Fumarole condensates have similar Br/I ratios as thermal springs. This ratio is in the lower range of the few Br/I ratios reported for Antilles magmas and other andesitic magmas (~20-100, Balcone-Boissard et al., 2010). Despite the very large temporal Cl variations observed in fumaroles or spring waters, the Br/I ratio remains almost constant (within analytical precision) for each spring. Cl/Br ratios of all thermal springs, with the notable exception of Ga spring for the period 2001-2009, also remain almost constant despite the occurrence of large Cl anomalies (Fig. 8b, see also Villemant et al., 2005). Cl/Br ratios are slightly different from one spring to another and range between 350 and 450. These Cl/Br ratios are in the range of the Cl/Br ratios of most andesitic magmas and high temperature magmatic gases in the Antilles (Villemant and Boudon, 1999). Since 2001, the Cl/Br ratio in Ga spring displays distinctive features (Fig. 8b). The very large increases in Cl contents (up to 700 ppm Cl, 1~20 mMol/L) that have been recorded since 2001 are also accompanied by Br and I enrichments, although they occur with a significant time delay since 2009. The Cl/Br and Br/I ranges in Ga spring before 2000 and after 2009 are ~350-400 and ~5-50 respectively, i.e. in the usual ranges. Conversely, from 2001 to 2008, the few low-amplitude Cl anomalies occurred at low and almost constant Br and I contents (~0.25 ppm and 15 ppb respectively) and lead to very high Cl/Br ratios (up to 3500) and Cl/I ratios (up to 150 000).

Compared to thermal springs, summit fumaroles have much larger Cl contents but are highly depleted in both Br and I. The Cl/Br ratios of summit fumaroles range between  $10^5$  and  $10^6$ , whereas those of the pre-1998 fumaroles are much lower (RC, Cl/Br~750) and close to those of thermal springs. Thus, in comparison to the periods immediately after the 1976 volcanic crisis and since 2009, the 1998 to 2008 period, is characterised by the production of fluids which are strongly fractionated in Br and I relative to Cl and that have fed the summit fumaroles and specifically contaminated only the thermal spring (Ga) located south of the dome and closest to the path of gases that feed fumaroles in the center of the dome (Fig. 1).

## 6 Discussion

### 6.1 Monitoring volcanic unrest at La Soufrière of Guadeloupe.

Geochemical monitoring of volcanic hydrothermal fluids can yield valuable insights, providing that the numerous processes that can affect magmatic gases during their transfer to the surface can be identified. By definition, during unrest periods (pre- or post-eruptive) the interactions of magmatic gas with surrounding wall rock material and pre-existing hydrothermal systems are very large and greatly modify the compositions of both residual gas (if not completely assimilated en route to the surface) and hydrothermal fluids. Scrubbing of soluble magmatic volatile species by hydrothermal systems is likely the most effective process (Symonds et al., 2001). The less soluble major gas-species ( $\text{CO}_2$ ) and the most soluble-gas species (halogen acids) have the simplest behaviors and are the better preserved tracers for geochemical monitoring of magma degassing. At La Soufrière, the evolution over the last 35 years, of the main gaseous species in fumaroles ( $\text{CO}_2$ ,  $\text{H}_2\text{S}$ ,  $\text{SO}_2$ ,  $\text{HCl}$  with the exclusion of  $\text{H}_2\text{O}$  given its complex origins) and of the main ions of magmatic origin in thermal spring waters ( $\text{HCO}_3^-$ ,  $\text{SO}_4^-$ ,  $\text{Cl}^-$ ) clearly shows two or three distinct periods, depending on the location of the spring or the fumarole. For most springs a first period lasted from 1979 (the beginning of the geochemical monitoring) to ~1993-1994, during which time water compositions were significantly affected by the 1976-1977 eruptive crisis; this is followed by a second period which is still going on and during which spring waters reach steady and relatively ion-poor compositions. The only exceptions are the CC and Ga springs. For CC spring the influence of the 1976-1977 crisis lasted until very recently (2004). Ga spring had only a relatively short steady period (~1995 to ~2000) followed by a third (current) period characterised by a complex series of geochemical anomalies. Summit fumaroles were very active in 1976-1977 and then rapidly vanished. They were reactivated in 1991-1992 after a long response time (>10 years) and are currently characterised by an intense activity with highly variable gas compositions and relatively high temperatures (up to  $140^\circ\text{C}$ ).

The thermal and geochemical features of thermal springs during the first period have been consistently interpreted in previous works as the impact of long-lasting degassing of a shallow magma intrusion emplaced in 1976 or slightly earlier on the hydrothermal system confined inside the Cratère Amic structure (Villemant et al., 2005, Boichu et al., 2008, 2011). This interpretation is also consistent with Cl isotopes measurements (Li et al., 2012). The reactivation of seismic activity in mid-1992 and of fumarolic activity at the dome summit beginning in 1997 was relatively rapid. This raises the issue of interpreting geophysical and geochemical signals in terms of: (1) a possible magmatic reactivation at depth, (2) a disturbance of the shallow hydrothermal system in response to

the development of a thermal anomaly (for example related to the assumed 1976-1977 magmatic intrusion), and (3) modification of the properties of the host rock at shallow depth in the volcanic structure (by sealing or fracturing for example, Feuillard et al., 1983, Zlotnicki et al., 1992, Villemant et al., 2005, Boichu et al., 2011). The present unrest period differs from the post-1976-1977 crisis period in that only one spring is affected and also by the nature and characteristics of halogen anomalies. The variations of the geochemistry of Ga spring waters and of summit fumaroles (mainly variations in HCl contents and in Cl/Br and S/C ratios) and the temperatures variations in fumaroles since 1997 have to be combined with phenomenological observations to constrain the possible causes of the current unrest.

## 6.2 Structural control of the shallow hydrothermal system.

The long term geochemical monitoring at La Soufrière of Guadeloupe shows that only fluids emitted by fumaroles at the dome summit and from springs inside a narrow domain delimited by the Cratère Amic structure and at distances  $< 1.5$  km from the dome summit (Fig. 1) display significant variations in composition (Villemant et al., 2005 and this work). In addition, thermal springs inside the Cratère Amic structure have much more variable temperatures but overall lower background temperatures than springs outside the structure. The only exception is CC spring, outside the Cratère Amic structure, which displayed a large chemical anomaly in conservative ions (halogens), but no variation in temperature with time.

### 6.2.1 *The local thermal anomaly.*

The shallow structure of La Soufrière- Grande Découverte volcano is highly controlled by recurrent flank collapse events (Boudon et al., 2008, Komorowski et al., 2005, Fig. 1b) which have created superimposed collapse structures whose basal surfaces constitute zones of preferential fluid circulations. Intense and protracted hydrothermal alteration of the wall rocks leads to progressive sealing of the system of fractures system and confinement of fluid circulation within the collapse structures. This hydrothermal system is confined into a relatively small volume (few  $\text{km}^3$  maximum; Komorowski et al., 2005, Komorowski, 2008, Lesparre et al., 2012) of the volcanic edifice that consists of several zones separated by fracture and structural discontinuities. The hydrothermal system is thus highly reactive to any disturbance by deep magmatic fluids and surficial input of cold meteoric water. Most short term thermal variations in thermal springs are directly related to rainfall (as in Ta spring for example), but some of them, as for CE spring, are clearly induced by convective transport of hot magmatic fluids. The local thermal anomaly related to conductive transport of heat from deep magmatic sources may be estimated from temperatures of springs outside Cratère Amic (BCM-EV, HR and CC) that do not show large variations over the last 35 years (Fig. 4b). The local

thermal anomaly extends over a large zone in the Soufrière-Grande Découverte volcano. Assuming that it is axisymmetric and centred on La Soufrière dome, its extent may be estimated through the almost stable temperatures of thermal springs outside the Cratère Amic : BCM ( $\sim 60^{\circ}\text{C}$ ,  $\sim 1$  km), CC ( $\sim 45^{\circ}\text{C}$ ,  $\sim 1.5$  km), HR ( $\sim 35^{\circ}\text{C}$ ,  $\sim 3$  km; Fig. 9). Inside Cratère Amic, the local thermal anomaly may be highly modified by convective heat transfer through the infiltration and confinement of most of the cold meteoric water falling on the dome summit, and, on the other hand, by fluids in direct transit from the magma source to the dome during periods of volcanic crises. The evolution of thermal anomalies in CE spring (the closest to the dome summit) since the 1976-1977 crisis is an evidence for such confinement effects: a large decrease in temperature, from  $T > 65^{\circ}\text{C}$  to air temperature in less than 20 years and the existence of small thermal ‘spikes’ correlated to Cl anomalies (Fig. 4b,c). The absence of such thermal variations in other springs inside Cratère Amic during the same period is a clear evidence of the partitioning of the summit volcanic structure. The inverse correlation (with a specific time delay) between temperature variations and rain-fall regime in Ta, Ga and BJ springs over the entire survey duration (Fig. 5) is evidence of the significant yet local influence of surface runoff and infiltration of rainwater from La Soufrière dome area. Time delays, which are a measure of the transit time for meteoric water from the summit zone to the different springs, range between 1 and 5 months for the springs (Ta, Ga and BJ) which are at a distance of  $\sim 1$  km from the dome and within the Cratère Amic structure. These values are consistent with those determined by hydrologic tracing from Tarissan pond to BJ spring in 1990 (Bigot et al., 1994). The Cratère Amic structure also acts as a watershed draining a large part of the rainwater falling on the summit area and thus strongly dilutes and cools the thermal waters. The background temperatures of springs inside the Cratère Amic structure show a systematic increase since 1979 (Fig. 4b) that could result from readjustment of the temperature of the edifice to a local conductive thermal anomaly. Indeed the equilibrium values for thermal springs inside Cratère Amic would be higher than  $60^{\circ}\text{C}$  without the effect of meteoric recharge and circulation (Fig. 9). The increase in mean spring temperatures can be explained either by reduction of regional rain-fall since 1994 and particularly over the last decade, or by progressive sealing of the system that can also lead to a reduction of the cold meteoric input into shallow phreatic systems. Assuming that the temperature gradient of the ‘normal’ shallow hydrothermal system as a function of the distance to the dome is defined by springs outside Cratère Amic structure (Fig. 9), one can estimate the mixing mass fraction of thermal waters and rainwater for springs inside the structure. The rainwater temperature is almost constant over the whole year ( $22 \pm 2^{\circ}\text{C}$ ) leading to bulk contributions of cold rainwater varying from 50 to 75% for springs inside Cratère Amic. The increased heat input inferred for the current unrest period from the summit gas flux may not yet have affected the system as a whole..

This inference is consistent with heat flux estimates from aerial infrared thermal imaging (Beauducel et al., . Pers. Com.).

### *6.2.2 Geochemical anomalies in spring waters.*

Springs inside the Cratère Amic structure are slightly acidic, sulfate-rich and have experienced large variations in their Cl contents since the beginning of the geochemical survey in 1979. In contrast, springs outside the Cratère Amic structure (except CC, see below) are neutral, ranging between sulfate-rich (BCM-EV) and carbonate-rich (HR) end-members but never displaying significant geochemical variations: it is an evidence of the partitioning of the upper structure of the volcano and the confinement of the magmatic fluids within the uppermost central parts. For most springs the Cl anomalies observed since 1979 almost completely vanished by 1994-1995. The Cl anomalies recorded in the different springs during this period, are interpreted as resulting from the injection of a series of HCl-rich magmatic gas pulses which have been dissolved and transported by groundwater over distances varying with springs position (see the advection-dispersion model of Villemant et al., 2005). This input of Cl<sup>-</sup> anions in spring waters was balanced by cationic species (Mg, Ca, Na) in varying proportions in the different springs, indicating that acid gas pulses followed different pathways to shallow depth where they chemically interacted with different materials. As with Cl<sup>-</sup>, cations anomalies also vanished in all springs between 1992 and 1995. These results suggest that the large and long-term disturbance of the hydrological system within the Cratère Amic structure that was induced by the 1976-1977 volcanic crisis had ended by about 1994-1995. Either magma degassing at depth had stopped or the surficial hydrologic system became isolated from the magmatic source (Boichu et al., 2011).

The Cl anomaly in CC spring extends over a much longer period of time (~25 years) and is not accompanied by significant temperature anomalies. This may be explained by a similar model by assuming that CC spring is directly related to the shallow hydrothermal system of Cratère Amic through a fracture system. The temperature of the spring is determined by the main local thermal anomaly (Fig. 9) whereas its composition is determined by the transfer of conservative ions of magmatic origin (mainly Cl<sup>-</sup>) over long distances (>2 km) within the edifice; the same series of magmatic gas pulses identified in springs inside Cratère Amic is able to generate the large chemical anomaly of CC spring assuming very long transfer times (~12 years, Villemant et al., 2005). The nested edifice collapse structures of La Soufrière-Grande Découverte volcano are cut by several fault systems: La Ty fault system N-S (Zlotnicki et al., 1992), and arc-transverse i.e. ~E-W normal faults (Feuillet et al., 2001, 2004) which may also act as drains for hydrothermal fluids. The main ~E-W fracturing system is underlined by the series of prominent waterfalls of the Chutes du Carbet.

The marked increase in fumarolic activity in 1997, culminating in 2008, the bulk increase in temperatures (limited to some degrees) of the springs inside Cratère Amic, and the appearance of complex chemical anomalies restricted to a single spring (Ga), is evidence of a new regime of the surficial hydrothermal system at La Soufriere, with no residual effect originating from the 1976-1977 volcanic crisis.

### 6.3 Diversity of chemical and thermal variations in time.

The 1979-1992 and post-1997 fluids inside the Cratère Amic structure exhibit a large diversity of evolution modes and intensities between the different fluid sources (springs and fumaroles) since 1997. From 1979 to 1994 composition and temperature variations of springs were large but consistent with each other if transfer time within each aquifer is taken into account: a unique series of chemical anomalies of magmatic origin is transferred within the different aquifers with time delays that are directly related to the distance between the spring and the dome summit (Villemant et al., 2005). The influence of this magmatic source on the shallow hydrothermal system has dominated other possible sources of chemical variations such as dilution by run-off and infiltration of cold meteoric waters prior its disappearance in ~1994-95. Since that period all springs inside Cratère Amic structure (except Ga) display 'steady' compositions and temperatures that are only affected by periodic dilution by low T meteoric recharge or by a slow and progressive temperature readjustment to the local thermal anomaly. Since 1999-2000 Ga spring displays very specific compositional variations which are not correlated to any thermal anomaly, characteristics that differ from those observed in CE or Ga springs just after the 1976-1977 crisis. For every spring inside Cratère Amic, the mean composition calculated for the steady period provides a good estimate of their chemical background, which can be used in the future for detecting new anomalies (Table IV). These background values allow us, for example, to compare the amount of Cl issued from the degassing of the 1975-1976 magma intrusion to that which has been input in spring waters up to ~1994 and the amount of Cl added in Ga spring since 1999. The two considered periods are similar in Ga spring ( $\sim 2 \cdot 10^5$  Kg) and represent a third of the total estimated amount of Cl injected in all springs from 1979 to 1994 (Villemant et al., 2005). The reactivation of the fumarolic activity at the summit of the dome in 1990-1992 has significantly preceded the chemical anomalies observed in Ga spring and is almost coincident with the seismic activity. Finally, it is to be noticed that a significant delay is also observed between the maximum HCl contents recorded in summit fumaroles (2000-2001) and in the maximum total S contents (2009-2010).

#### 6.4 Magmatic and hydrothermal fluids.

The fluids collected in fumaroles and thermal springs are mixtures in variable proportions of two 'primary' end-members: (1) a pure magmatic gas of likely relatively steady composition (because the magmatic emissions at la Soufrière have a highly homogeneous andesitic composition, Boudon et al., 2008) which however may be more or less strongly modified by decompression, temperature decrease and interaction with conduit walls rocks or aquifers during their transfer to surface (see e.g. Symonds and Reed, 1993) and (2) pure meteoric water. The compositions of hydrothermal waters confined to the shallow edifice over long periods of time, result from complex interaction and thermo-chemical re-equilibration of the two primary components with the edifice rock material. They may be represented by the steady compositions of Cratère Amic spring waters which, which are very similar at similar mean temperatures (SAS waters, Ca(Mg)-SO<sub>4</sub> type, Table IV). The hottest springs (T ~42°C), Ga and Ta, located at altitudes > 1100 m, have slightly higher ion contents (1.5 to 3 times higher, except SO<sub>4</sub><sup>2-</sup>) than colder springs (T~29°C) located at lower altitudes (600-900 m). This suggests that compositions in equilibrium with the surrounding material (of mean andesitic composition) primarily depends on temperature. Temperatures and chemical characteristics of the magmatic and hydrothermal fluids during the 1976-1977 crisis or the current unrest period allow to identify the contributions of these different components.

Very high-flux gaseous emissions through the whole dome fracture system accompanied the seismo-volcanic crisis of 1976-1977.. Gas sampling conditions did not generally ensure reliable analyses, in particular for the ratios SO<sub>2</sub>/H<sub>2</sub>S, CO/CO<sub>2</sub> or H<sub>2</sub>/H<sub>2</sub>O (IPGP Internal Reports, 1976). By the end of the year 1977, improvement of sampling and analytical techniques allowed production of some significant gas analyses (see Javoy et al., 1978, Delorme, 1983 and IPGP, Internal Reports, 1978 and subsequent years, for discussion). The most accurate analyses are those for the Lacroix Inférieur fumarole (1290 m) on the Lacroix fracture (Fig. 1a). This was the hottest summit fumarole which remained active at the end of the volcanic crisis. Its temperature rapidly decreased from ~160°C at the beginning of 1977 to ~96°C at the end of 1978. Temperatures of other fumaroles had already decreased to ~96°C at the end of 1977, which is the ebullition temperature of pure water at the elevation of the dome area (1200 -1467 m). By 1981, almost all fumaroles had completely vanished, and only residual fumarolic activity (mainly the RC and LaTy fumaroles) was still observed at the base of the dome until mid-1997 at the same temperature ~96°C (Fig. 7). From 1990, the fumarolic activity reactivated and migrated to the top of the dome with the first evidences at the Cratère Sud (CS). In 1997, flux increased markedly and new fumaroles started to reactivate on the summit plateau (e.g. Napoléon fumarole, Tarissan). In late 1997 and early 1998, the CS gas emissions became markedly acid (pH mean 1.0 ± 0.6 between Mars 1998 and June 2001 for

example) while intermittent acid boiling greenish ponds (85-109°C, pH mean  $-0.1 \pm 0.5$ , between April 1998 and June 2001 for example) formed in early 1998 at the CS's southern vent and in 2000 in the Tarissan crater, displaying vigorous geyser-like activity (Komorowski et al., 2005; Beauducel Pers. Com.). The summit fumaroles temperatures have strongly increased from that date (from  $\sim 96^\circ\text{C}$  in 1997 with spikes of  $126^\circ\text{C}$  in March 2000,  $118^\circ\text{C}$  in June 2001, and maximum values of  $\sim 140^\circ\text{C}$  in February 1999 and June 2000, Table II). This activity is still going on. Residual fumarolic field at the base of the dome was not affected by the summit reactivation and has even slightly diminished since 1997.

Compositions of all low temperature gases ( $\sim 96^\circ\text{C}$ ) are characterised by low  $(\text{SO}_2+\text{H}_2\text{S})/\text{CO}_2$  and very low or undetectable amounts of HCl,  $\text{SO}_2$  and CO (Figs. 3 and 10). Compositions of gases of higher temperature collected in 1976-1978 (Lacroix Inférieur; Delorme, 1983) and since 1997 at the summit of the dome (CSC) are similar but have higher HCl and total S contents (Table II, Fig. 3). Though the total S and C contents are similar for both activity periods, the 1977-78 Lacroix Inférieure fumaroles have higher  $\text{SO}_2/\text{H}_2\text{S}$ ,  $\text{CO}/\text{CO}_2$  and  $\text{CH}_4/\text{CO}_2$  ratios than present-day summit fumaroles which indicates that more reducing conditions prevailed during gas emissions in 1977-1978 (i.e. closer to pure magmatic gas conditions at depth) than for present activity. The composition domains of fumaroles of La Soufrière are relatively large (especially in  $\text{CO}/\text{CO}_2$  which shows variations of  $\sim 2$  log units for the recent period and up to  $\sim 4$  log units since 1977). Although these variations could be partly explained by sampling difficulties (see section 3.2), they define trends which are close to those defined by Soufrière Hills fumaroles collected at the onset of the eruption (Montserrat, Chiodini et al., 1996, Hammouya et al., 1998; Figs. 3 and 10). Redox conditions and equilibrium temperatures of fumarolic gases may be estimated using  $\text{H}_2/\text{H}_2\text{O}$ ,  $\text{CO}/\text{CO}_2$  and  $\text{CH}_4/\text{CO}_2$  ratios (Giggenbach, 1980, 1987, D'Amore and Panichi, 1980, Chiodini and Marini, 1998) and assuming single fluid phase equilibrium.  $\text{H}_2$  and CO being the more rapidly re-equilibrated species, their abundances reflect the last equilibration steps during the ascent of fumarolic gases or the sampling (see section 3.2.2). Different diagrams have been proposed to represent the  $\text{CO}-\text{CO}_2-\text{CH}_4-\text{H}_2-\text{H}_2\text{O}$  equilibria and are calibrated in temperature and redox conditions for different buffers (Giggenbach, 1987, Chiodini and Marini, 1998); they also allow estimation of steam condensation paths during gas transfer or sampling. High temperature gases of the 1977-1978 crisis have equilibrated at relatively reducing conditions and at temperatures higher than  $400^\circ\text{C}$ ; they plot in the pure vapour domains. Fumaroles emitted at the dome summit in the recent period have equilibrated at progressively increasing temperatures from  $\sim 150^\circ\text{C}$  at the onset of the reactivation of the fumarolic activity in 1997 (Brombach et al., 2000) to values  $> 300^\circ\text{C}$  for the 2000-2010 period. Since 1997, fumaroles compositions also display an evolution towards more

reducing conditions: CO/CO<sub>2</sub> and CO/CH<sub>4</sub> ratios of gases sampled at temperatures higher than 98°C slightly increase from 1997 to 2009 and then seem to decrease. However equilibrium temperatures and reducing conditions have remained slightly lower than those recorded in the 1977-1978 gases, after the main volcanic crisis.

The imprint of long-lived hydrothermal fluids on compositions of volcanic fluids is characterised by (1) H<sub>2</sub>S as the dominant S-bearing species and low or negligible SO<sub>2</sub>, (2) low or negligible HCl contents and (3) CH<sub>4</sub> > CO (Giggenbach, 1980, 1987, Chiodini and Marini, 1998). The fumaroles at the base of the dome (La Ty and RC fumaroles active since the end of the 1976-1977 crisis) have typical hydrothermal characteristics: very low or undetectable CO, H<sub>2</sub>, HCl and SO<sub>2</sub> contents, and temperatures always very close to that of boiling water at the considered altitude. They likely correspond to a boiling hydrothermal aquifer heated by the thermal anomaly and with initial composition represented by the SAS water (Table IV). However, boiling and overheating ('dry gas') of pre-1997 hydrothermal waters alone cannot explain the compositions of summit fumaroles. Indeed such a process should lead to more pronounced decreases in H<sub>2</sub> and CH<sub>4</sub> than in CO<sub>2</sub> and H<sub>2</sub>S, which is not consistent with compositions of the recent summit fumaroles or the 1977-1978 fumaroles (Lacroix Inférieure). Moreover, such a process is not able to produce vapours which are both HCl- and H<sub>2</sub>S-rich with very low SO<sub>2</sub>, as observed in summit fumaroles. Mixing between low temperature hydrothermal fluids and a hot fluid component directly derived from deep magma degassing is required to explain the compositions of the gases emitted at La Soufrière since 1976. The magmatic fluid mainly brings heat, H<sub>2</sub>O, SO<sub>2</sub> and HCl into the shallow edifice. The behaviour of gas species is mainly controlled by the temperature decrease and interaction with shallow phreatic or hydrothermal systems. The efficiency of gas - water interaction depends on the ratio between the mass of magmatic gas and hydrothermal fluids and their bulk solubility in hydrothermal waters, but also on the equilibrium temperature reached by gas before interaction (Fig. 11). At low magmatic fluid/hydrothermal water ratios, almost complete scrubbing of magmatic HCl and SO<sub>2</sub> by surficial hydrothermal aquifers (Symonds et al., 2001) leads to low temperature fumaroles characterised by large H<sub>2</sub>S content and low or undetectable SO<sub>2</sub> and HCl contents. CO<sub>2</sub> content should be less affected by scrubbing. When the proportion of magmatic fluid increases as a result, for example, of drying of the conduit or an increase in the deep magmatic gas flux, the process of scrubbing becomes less efficient. As the gas/water mass ratio approaches or exceeds 1, models for the gas phase predict a significant increase in temperature, (SO<sub>2</sub>+H<sub>2</sub>S)/CO<sub>2</sub> ratio, HCl content, precipitated sulphur and, later, possibly in SO<sub>2</sub> content as well. Because CO<sub>2</sub> is much less affected by scrubbing, it should experience less intense variations than HCl or SO<sub>2</sub>. In addition, the temperature at which the magmatic gas interacts with the groundwater is critical for S-bearing

species, because if the magmatic gas is already significantly cooled (typically  $T < 700^{\circ}\text{C}$ ) the fraction of soluble  $\text{SO}_2$  is negligible and almost all S is in the form of  $\text{H}_2\text{S}$  which is almost insoluble (Fig. 11).

In 1977-1978 high temperature gases were likely very close in compositions to a pure magmatic component as suggested by the comparison with compositions of juvenile gas collected at the onset of Soufrière Hills volcano eruption in Montserrat (Hammouya et al., 1996; Fig. 10). Even the highest temperature gases (up to  $\sim 140^{\circ}\text{C}$ ) emitted during the current unrest period since 1997 never reached the compositions, equilibrium temperatures and redox conditions which prevailed during the 1976-1978 crisis. However, the evolution of temperature and composition of summit fumaroles since 1998, is consistent with a new and progressively increasing influx of magmatic gases into the shallow hydrothermal system with a progressive reduction, though still relatively efficient, of the scrubbing effects: increase in temperature, total S/ $\text{CO}_2$ , and HCl content, and the developments of S precipitates at the gas vents.

Available temperature and chemical composition data of La Soufrière gases cannot be related unambiguously to a unique gas source and evolution path. Indeed the total S content and the  $\text{SO}_2/\text{H}_2\text{S}$  ratios may be modified by numerous processes such as influx of deep magmatic gases, gas scrubbing by meteoric water, variations of redox conditions or condensation- evaporation cycles (Giggenbach 1988, Symonds et al., 2001). However, the simple re-heating of surficial aquifers is not sufficient to explain the range of temperatures and compositions observed since 1977, but a two end-member mixing model involving the periodic influx of hot magmatic gases into the surficial hydrothermal system is consistent with observations. This model is also consistent with studies that have identified sustained passive degassing of  $\text{CO}_2$  and rare gases of deep magmatic origin (Allard et al., 1998, Brombach et al., 2000, Ruzié et al., 2012, 2013). This flux is variable in space and is significantly higher in high-temperature summit fumaroles than in low-temperature fumaroles and thermal springs. The isotopic composition of  $\text{CO}_2$  flux has not significantly varied since 1995 (Ruzié et al., 2013).

## 6.5 Halogen behaviour in volcanic fluids: constraints on degassing-condensation-boiling processes

### *6.5.1 Halogens fractionation, tracer of late evolution processes of volcanic fluids.*

The model discussed in section 6.4, defined on the basis of major gas species chemistry, is poorly constrained due to both the complexity of low-temperature chemistry and poor knowledge of compositions and evolution in time and space. The *a posteriori* model of the evolution of in halogen

species (F, Cl, Br) of thermal springs of La Soufrière between 1979 and ~1995 has allowed us to identify the source and the impact of the 1976-1977 eruptive unrest on the surficial hydrothermal system (Villemant et al., 2005). A consistent interpretative model of the episodic anomalies in Cl- and Br- contents and temperature of thermal springs allows to constrain some chemical and physical characteristics of the magma source (Villemant et al., 2005; Boichu et al., 2008, 2011). Temperature variations and halogen (F, Cl, Br and I) fractionation in post-1995 fluids (spring waters and fumaroles) put significant additional constraints on the recent evolution of the magmatic and hydrothermal system.

Halogen fractionation is very sensitive to low temperature evolution of hydrothermal fluids, but not to their high temperature evolution. It is now well established that the heavy halogens Cl, Br and likely I do not highly fractionate relative to each other during degassing of silicic melts (Villemant and Boudon, 1998, Balcone-Boissard et al., 2010) and during gas cooling and decompression at temperatures higher than  $\sim 120^{\circ}\text{C}$  in dry conditions (Symonds et al. 1998). In addition, due to their high solubility in water, halogen acids produced by degassing of  $\text{H}_2\text{O}$ -rich melts are very efficiently scrubbed by surficial hydrothermal and phreatic systems (Symonds et al., 2001). During such interactions ('wet' path) magmatic gases are thus almost completely depleted in halogens, which are transported as dissolved ions in hydrothermal waters. Halogens are not fractionated relative to each other during their dissolution in water and are transported as conservative ions, which means that they are not affected by the usual chemical evolutions in hydrologic systems (interaction with host-rock leading to mineral precipitation or dissolution, low temperature evaporation, dilution by meteoric water). The relative abundances of Cl, Br and likely I thus should remain constant over large domains of the compositional and thermal evolution of hydrothermal fluids. F has a specific behaviour in magmatic systems because it mainly remains bound to the silicate melt structure during  $\text{H}_2\text{O}$  degassing and is thus much less efficiently extracted from melts than other halogens; this effect leads to high and variable halogens/F ratios in magmatic gases and in all derivatives (Villemant et al., 2003). However, during the subsequent evolution of gases rising to the surface and their interactions with hydrothermal fluids at high temperatures, F behaves as other halogens and is not significantly fractionated.

In contrast, significant fractionations between halogens are expected during evolution at low temperature and pressure (i.e. pressures close to atmospheric pressure and  $T < 130^{\circ}\text{C}$ ) of the gas phase and particularly during vapour/liquid equilibrium. For example, recent studies have shown that low temperature interaction of magmatic gases with the atmosphere at Soufrière Hills (Montserrat) led to high Cl/Br fractionation in the gas plume through the formation of BrO species (Bobrowski et al., 2003, Villemant et al., 2008). It is also well known that azeotropic behaviour of

halogen acids induces significant fractionation between the different halogen during evaporation or condensation cycles (see Azeotrope Data Bank, 2001; Fig. 12). Conversely, evaporation of neutral solutions and brines containing halogen ions causes no significant Cl/Br fractionation over a large range of vapour/liquid ratios, unless extreme degrees of evaporation are reached (see e.g. Liebsher et al., 2006, Shimulovich et al., 2004 and references therein).

Thus fractionation between halogens is a good tracer of the processes involved during magma degassing and further interaction of gases with hydrothermal fluids and the atmosphere. The halogen composition of thermal fluids collected at La Soufrière display characteristic features which are consistent with the model of episodic mixing between two fluid sources (a pure magmatic source and a shallow hydrothermal source). The HCl-rich magmatic component supplies the present day high-temperature summit fumaroles but has suffered significant low-temperature condensation that leads to a drastic depletion in Br and I. When this magmatic gas is completely scrubbed by shallow groundwater, such fractionations do not occur. This means that heavy halogen fractionation only occurs in the very late evolution of the gas phase.

#### *6.5.2 F-Cl fractionation.*

The very low F contents of all volcanic fluids and specifically of the fumaroles at  $T > 96\text{ }^{\circ}\text{C}$  is consistent with a major contribution of magmatic gases to the surficial hydrologic system with no significant contribution of a sea-water component: the magmatic component is F depleted because F is not extracted from melt into the  $\text{H}_2\text{O}$ -vapour during magma degassing and the sea-water has a much higher F/Cl ratio than fumaroles (Fig. 8). The absence of a sea-water component has also been demonstrated for the pre-1995 period using Na/Cl ratios (Villemant et al., 2005). Moreover, the Cl isotopic composition of thermal spring waters (Li et al, 2012) is characteristic of a marked magmatic signature. This result excludes any significant direct contribution of sea-water to the shallow hydrothermal system of La Soufrière in contrast to the Na-Cl fluids of the geothermal area of Bouillante on the western coast of Basse Terre (Brombach et al., 2000). Moreover, the high Cl/F ratios of thermal springs inside the Cratère Amic structure (including CC spring) compared to springs outside the structure (e.g. HR, BCM-EV) can be also simply explained by the imprint of HCl-rich and HF-poor magmatic gases which are channelized and confined to this shallow structure.

#### *6.5.3 Cl-Br and Br-I fractionation.*

Though Cl abundances vary over a very large range in thermal springs inside Cratère Amic, the Cl/Br ratio remains generally constant and close to that of andesitic magmas of La Soufrière

(mass ratio ~400) during the entire survey period (1979-present day), except for Ga spring during a 'transitional period' between ~2000 and 2008 (Fig. 8b). The Ga spring during that period displays a constant Br content ~0.2 ppm regardless of the Cl content, leading to extremely high Cl/Br ratios. Moreover, the large Cl anomaly that culminated in 2009 is again characterized by a Cl/Br ratio in the normal range, which indicates that this enrichment affects Cl and Br similarly. Conversely, all gases from the summit fumaroles since 1998, display a very strong depletion in Br relative to Cl, whereas the Br/I ratio is not modified (Fig. 8).

#### *6.5.4 Mechanisms of halogen fractionation.*

Evaporation or ebullition of near neutral halogen-rich solutions generally produces almost H<sub>2</sub>O-pure vapour and all dissolved ions are enriched in the solution (residual brine) by the same factor: no relative fractionation between halogen ions is expected neither in the brine nor in the vapour phase, except as solubility product constants of salts are reached which only occurs at very high degrees of evaporation (Berndt and Seyfried, 1997 and references therein). An exception is the hydrolysis at high temperature of Cl-rich brines or chloride (Na- or Ca-) salts (Bischoff et al. 1995). In natural systems this occurs at very high temperature by hydrolysis of solid salts or brines, as for example during interaction of basaltic lava flows ( $T > 1000^{\circ}\text{C}$ ) with sea-water leading to the production of HCl-rich vapour known as 'laze' (Edmonds and Gerlach, 2007 and references therein) or through hydrolysis at high temperature ( $>400^{\circ}\text{C}$ ) and depth of CaCl<sub>2</sub> produced by water-rock interaction as suggested for Vulcano island (Di Liberto et al., 2002). Though not documented by in situ measurements, such processes very likely induce large halogen fractionation, as is usually observed during analysis of halogen contents in solids by pyrohydrolysis. In this method, halogens are extracted as halogen acids by high temperature hydrolysis and extraction kinetics are much slower for heavy halogens than for light halogens (see e.g. Michel and Villemant, 2003 and references therein). These processes are unlikely in the surficial hydrothermal system of La Soufrière where temperatures do not exceed 300 - 400°C (see Fig. 10b). If they occur at depth they probably require the interaction of a high temperature magmatic source with salts or brines of hydrothermal origin. But the halogen signature of these gases produced at depth would likely be highly fractionated in heavy halogens and should be recovered in both thermal springs and fumarolic gas, which is not the case. Though experimental data on heavy halogen fractionation during hydrolysis do not yet exist, in view of our current knowledge this process is highly unlikely at La Soufrière.

Boiling or condensation of acid solutions may lead to significant halogen fractionation since mixtures between halogen acids and H<sub>2</sub>O have azeotrope solution with a temperature maximum

(Fig. 12). Mixtures of H<sub>2</sub>O with HI and HBr have similar azeotrope maxima, whereas mixtures of H<sub>2</sub>O with HF and HCl have azeotrope maxima of lower temperature and halogen acid contents. The phase diagrams predict that cooling of high-temperature halogen acid vapours with initial compositions less concentrated than azeotrope maxima will produce highly concentrated liquids and residual vapours which are progressively impoverished in halogen acids. In addition, due to the shapes of the various ebullition and dew curves and the initial halogen contents, less impoverishment in HCl relative to heavy halogen acids (which are much less concentrated) is expected in magmatic gases. Finally, the phase diagrams predict that vapour condensation preserves a Br/I ratio close to that of the initial vapour. This simple process may explain the large heavy halogen depletion in the summit fumaroles.

Conversely, if a model involving acid lake evaporation is considered, the high ionic strength of these solutions has to be taken into account. The phase diagrams of all halogen azeotropes are well known only for pure acid solutions; for solutions of high ionic strength there is a significant shift of the azeotrope maxima towards higher temperatures and more halogen-rich compositions (Fig. 12b). The shift in temperature is likely similar to that of pure H<sub>2</sub>O, and the increase of the ionic strength and shifts in azeotrope composition are likely similar for all halogens. Classical thermodynamic laws show that the boiling-point elevation of aqueous solutions is directly proportional to the molal concentration of non-volatile solutes (C) according to the equation  $\Delta T \sim 0.512 \times C$ . If the most concentrated hydrothermal solutions measured at la Soufrière of Guadeloupe (i.e. the Tarissan pond waters,  $C_{\max} \sim 3$  mol/L; Table I) are evaporated by a factor  $\sim 20$ , the ebullition temperature will increase by  $\sim 30^\circ\text{C}$ , consistent with the maximum temperatures observed for summit fumaroles (Table I, Fig. 7). If the relative positions of the azeotrope maxima of halogen acids are preserved, the ratio of halogen content in the vapour phase over that in the liquid phase is much greater for Cl than for Br (Br content in the vapour phase in these conditions is negligible) and the Cl/Br ratio of the vapour should be much higher than the initial ratio ( $\sim 400$ ). The Br/I ratios should remain similar. Such a mechanism could also explain most observed characteristics of La Soufrière summit fumaroles (CSC and CSN) which have very high HCl contents (up to 1.5 mol/L let  $\sim 0.5\text{wt}\%$ ) with a rough correlation between HCl content and ebullition temperature (up to  $130^\circ\text{C}$ , Fig. 7b), very high Cl/Br (and Cl/F) ratios and no significant Br/I fractionation relative to spring waters or low temperature fumaroles (RC, Table III). The production of such HCl-rich vapours has however never been observed at Tarissan, where temperature has remained lower than boiling temperature. The production of such highly HCl-rich vapours also requires extreme HCl contents in solutions (Fig. 12b), far above those observed in Tarissan or other acid ponds. Such a process could however occur below the CSC and CSN vents, where intermittent acid ponds have been observed

and may reach such extreme compositions when close to total evaporation. Maintaining a high gas flux at the dome summit since 1997 by this mechanism would require the existence of permanent acid lakes of very large volume heated to high temperature. In addition, long term preservation of such acid lakes requires the continued input of new magmatic gas to maintain a low pH, which tends to increase by reaction with the wall-rock material. These conditions are inconsistent with observations and such a process may, if it exists, represent only a small and occasional contribution.

### 6.6 Ga spring contamination.

The special chemical features of Ga spring waters since ~2000 may be explained by contamination by derivatives from magmatic gases of variable composition through time (Fig. 6 and 8). During a transitional period from 2000 to 2008,  $\text{Cl}^-$  anomalies were relatively low with very high Cl/Br ratios and accompanied by  $\text{SO}_4^{2-}$  anomalies of similar amplitude, with only minor variations in other anions or cations and an occasional slight decrease of pH. The  $\text{Cl}^-$  anomaly developed in Ga spring waters since 2009 is large and has a characteristic magmatic Cl/Br ratio and is accompanied by large increases in  $\text{Ca}^{++}$  and  $\text{Mg}^{++}$  but only slight decreases in  $\text{SO}_4^{2-}$ ,  $\text{HCO}_3^-$  and pH. During the transitional period, the  $\text{Cl}^-$  and  $\text{SO}_4^{2-}$  anomalies suggest a contamination by gas of magmatic origin and containing significant amounts of soluble HCl and  $\text{SO}_2$ . The large fractionation in Cl and Br indicates that significant condensation has affected the HCl-rich component. These fluids may represent high temperature gas condensates (equivalent to aerosols) that are rich in  $\text{Cl}^-$  and  $\text{SO}_4^{2-}$  but less acid than their gaseous source. They do not contain  $\text{HCO}_3^-$  because condensation and dissolution in liquid water mainly affects halogen acids and  $\text{SO}_2$  but not  $\text{CO}_2$  with its very low solubility. Since 1998, because the dominant low altitude wind direction is E-W, gas plume condensates have destroyed the vegetation on the western flank of the dome and could potentially contaminate all surficial aquifers in that sector, which is however not observed. Thus, the pre-2009 contamination of Ga spring was more likely generated by gas condensation inside the edifice during percolation at shallow depth through the Ga spring aquifer. The main fracture system affecting the southern flank of the volcano (Fig. 1) likely represents the connection between the sealed central feeding system for volcanic fluids and the phreatic system of Ga spring. Note that in order to generate  $\text{SO}_4^{2-}$  anomalies in a phreatic system the  $\text{SO}_2$  content in the gas must be significant, which is strongly in favour of a magmatic origin.

Since the end of 2008 the contamination of Ga spring has grown significantly more intense and the contaminant composition is modified: waters are slightly more acid and rich in  $\text{Cl}^-$ ,  $\text{Ca}^{++}$  and  $\text{Mg}^{++}$  and display a magmatic Cl/Br ratio, but no  $\text{SO}_4^{2-}$  anomaly. A contaminating fluid of magmatic origin should have lower  $\text{SO}_2$  contents and scrubbing of acid gas (mainly HCl) should be

followed by a significant interaction with rock material. This suggests that interaction of the magmatic gas with surficial aquifers occurs at temperatures lower than  $\sim 700^{\circ}\text{C}$ , where conversion of  $\text{SO}_2$  into insoluble  $\text{H}_2\text{S}$  is almost complete, but at sufficiently high temperature to prevent significant gas condensation, which would have led to Cl-Br fractionation. The absence of a positive  $\text{HCO}_3^-$  anomaly also indicates that  $\text{CO}_2$  scrubbing was, as expected, inefficient. The dissolved acids are progressively neutralised during transfer to the spring, by reaction with surrounding rocks and exchange of  $\text{H}^+$  ions with  $\text{Ca}^{++}$  and  $\text{Mg}^{++}$ . These characteristics are similar to those observed in CE spring shortly after the 1976-1977 volcanic crisis (Villemant et al., 2005), but the absence of anomalies in  $\text{SO}_4^-$  and  $\text{HCO}_3^-$  confirms that present-day magmatic gases scrubbed in the Ga aquifer have lower  $\text{CO}_2$  content and are more depleted in soluble  $\text{SO}_2$  contents than those during the 1976-1977 crisis, consistent with gas plume compositions (see section 6.4).

We thus propose that the geochemical characteristics of Ga spring waters since 2000 result from the contamination by a fluid the composition of which evolve in time with magmatic gas flux and gas interaction conditions inside the upper feeding conduit. The contamination occurs through a specific pathway to the phreatic system of Ga spring which is controlled by the main 'La Ty fault system'. At the onset of the fumarolic reactivation, progressively increasing amounts of high temperature and HCl- and  $\text{SO}_2$ -rich magmatic gases were injected at shallow depth contaminating the Ga spring in both  $\text{Cl}^-$  and  $\text{SO}_4^-$ . This transitional period was followed by more active magmatic gas production leading to greater contamination of the surficial phreatic system of Ga spring. The temperature of gases interacting with groundwater was low enough (i.e.  $< 700^{\circ}\text{C}$ ) for almost all  $\text{SO}_2$  to be converted into insoluble  $\text{H}_2\text{S}$ . More intense cooling and condensation of these magmatic gases en route to the surface through 'dry conduits' (preventing scrubbing) led to the summit fumaroles which are thus  $\text{SO}_2$ -poor and  $\text{H}_2\text{S}$ - and HCl-rich and highly fractionated in Br relative to Cl. The initial high temperature magmatic gases are also likely less rich in  $\text{CO}_2$  than the fumaroles of the 1976 volcanic crisis. The shape and duration of the Cl anomalies recorded in Ga spring since 2000 suggest that they result from a series of contaminating gas pulses injected within the edifice and transported to Ga spring. Because of these long transfer duration the geochemical anomalies time series recorded in Ga spring are strongly delayed relative to the gas pulse time series recorded in summit fumaroles. Given the efficient conversion of magmatic  $\text{SO}_2$  to insoluble  $\text{H}_2\text{S}$  with decreasing temperature, scrubbing does not significantly affect the variation in total S flux at the dome summit, which represents a good record of the gas pulse time series.

6.7 HCl pulse time series, relative behaviours of halogens,  $\text{SO}_2$  and  $\text{CO}_2$  and seismicity: evidences for a new shallow magma intrusion?

The preceding discussion suggests that the total S flux in summit fumaroles and Cl anomalies in Ga spring are related to the same series of magmatic gas pulses. Transport of these fluids within the shallow edifice of la Soufrière to Ga spring may be described using the advection dispersion model developed by Villemant et al. (2005) for the post-1976 volcanic crisis (1979-1992 period). Time series evolution of the bulk seismic activity (total number of earthquakes/month), the Cl content in three key springs (CE, BJ and Ga) as corrected for advection delays (Villemant et al., 2005), and variations in total S content of summit fumaroles is shown in Fig. 13a. The clear correlation between the total S content of summit fumaroles and the Cl content in Ga spring corrected for transfer duration indicate a common origin for  $\text{SO}_2$  (+ $\text{H}_2\text{S}$ ) and HCl in the current crisis. Using the same physical characteristics of the transport model of Villemant et al (2005) (in particular transfer time of  $\sim 2$  years), we have calculated the best fitting dates and relative amplitudes of a series of gas pulses recorded by Cl contents in Ga spring for the 2000-present period (Fig. 14a and Supplementary Material). The fit of the same series of pulses to the Cl-time series in Ga spring and the total-S contents in CSC fumarole (using very low gas transfer durations and large dispersion factors compared to those for Cl-pulses in Ga aquifer) leads to a highly consistent model (residues equal to 0 within analytical errors; Fig. 14b). In addition, this model shows that the flux of  $\text{SO}_2$ + $\text{H}_2\text{S}$  is significantly less variable than that of HCl, suggesting some disconnect between the sources of the two magmatic gases (i.e. mafic vs andesitic magma sources; Fig. 14c).

The gas pulse time series calculated for both crises are compared with the seismic activity in Fig. 13a. HCl,  $\text{SO}_2$  and  $\text{CO}_2$  degassing after the 1976-1977 volcanic crisis and during the present unrest period are compared in Fig. 13b. In the absence of reliable gas composition data for the 1976-1977 volcanic crisis, we have used the  $\text{Cl}^-$  and  $\text{HCO}_3^-$  records in CE spring, which is the closest to the dome, as a proxy for HCl and  $\text{CO}_2$  degassing some years (4-5) after the crisis. These proxies are compared to total S ('dry gas' composition) and HCl time series measured in summit fumaroles for the current volcanic crisis. Both records display the same fundamental characteristics:  $\text{SO}_2$  and  $\text{CO}_2$  display long-term buffered-like variations and HCl displays pulsatory variations which, as discussed above, cannot be solely attributed to surficial effects. Such contrasting behaviours have also been described for example at the active Soufrière Hills volcano (Montserrat) nearby (Edmonds et al., 2002, 2003, Villemant et al., 2008). The behaviour of these different gas species is directly related to their solubilities in andesitic or dacitic magmas and to the degassing regime such that  $\text{CO}_2$  and  $\text{SO}_2$  (in that order) have much lower melt solubilities than  $\text{H}_2\text{O}$  and HCl, which exsolve at much lower pressure and from more differentiated melts. It is thus likely that intrusions of new magma at shallow depth are at the origin of both volcanic crises and the simultaneous degassing of  $\text{SO}_2$  (+ $\text{H}_2\text{S}$ ) and HCl. Although  $\text{CO}_2$  was produced in large amounts in 1976-1977 as testified by gas

compositions and  $\text{HCO}_3^-$  anomalies in CE spring, this is likely not the case during the present unrest (i.e. other than that recorded in diffuse degassing around the dome since the 1980's; Allard et al., 1998, Ruzié et al., 2013). Rhyolitic melts of acid andesites, which are dominant in La Soufrière-Grande Découverte volcano since 200 ka, contain large amounts of  $\text{H}_2\text{O}$  and  $\text{HCl}$  but almost no  $\text{CO}_2$  and  $\text{SO}_2$  (Boudon et al., 2008).  $\text{CO}_2$  and  $\text{SO}_2$  necessarily originate from deeper and more basic magma sources. Following a scenario frequently proposed (Doukas and Gerlach, 1995; Crider et al., 2011; Edmonds et al., 2010 as examples) the reactivation of the seismo - volcanic activity in 1976-1977 and since 1992 at La Soufrière of Guadeloupe may be explained by input of new basic magma batches within the deep magma chamber, triggering ascent of small differentiated (andesite or dacite) magma intrusions and that stall at shallow depth. Rejuvenation of the magma feeding conduits facilitates the ascent of  $\text{SO}_2$  and possibly  $\text{CO}_2$  of deep origin through the edifice, with a degassing regime characterized by relatively long time constants.

Every emplacement of a new differentiated magma intrusion leads to a two-step degassing regime (Villemant et al. 2005) mainly involving  $\text{H}_2\text{O}$  and  $\text{HCl}$ . The first degassing step is synchronous with emplacement of a new magma batch and characterized by large production of  $\text{HCl}$ -rich  $\text{H}_2\text{O}$  vapour. Subsequently, when an intrusion stalls, a second, long lasting regime may occur which corresponds to pulsatory degassing induced by magma crystallization. This second regime is characterised by regular increase of the time interval between successive degassing pulses and regular decrease of their intensity (Boichu et al., 2008, 2011). From 1979 to 1995, after the 1976 volcanic crisis, the time delays between successive gas pulses increased with time (from  $\sim 2$ -4 months in 1979 to  $\sim 8$  months in  $\sim 1990$ ) and intensities also decreased with time. Since 1997, time delays between  $\text{HCl}$  degassing pulses have been longer but more stable (mean  $\sim 13 \pm 3.5$  months) although their intensities have increased from 1994 to 2005-2006 to a more or less steady state (Fig. 14a). The present unrest conditions may represent progressive feeding of a system of shallow and differentiated magma intrusions since 1994-1995.

However, the degassing of such acid andesitic magma is not able to produce significant amounts of magmatic S-bearing gas, which requires the presence of more basic  $\text{SO}_2$ -rich magmas. Thus the volcanic activity recorded in 1976 and the current period may have been triggered by involvement of more basic magmas which produce  $\text{SO}_2$ -rich gases emitted at a similar rate, at least during the initial degassing stages. Among the different models proposed to explain the volcanic activity at La Soufrière since the 17<sup>th</sup> century, this model best explains both the clear magmatic character of expelled gas pulses and the main physical characteristics of the pulsatory degassing regimes observed after the 1976-1977 crisis and in the present unrest.

The relative amounts of magmatic gas involved since 1995 may be estimated from the spring flow rates and the Cl contents of contaminated springs, and the gaseous HCl emissions. These estimates indicate that the amounts of magmatic gas scrubbed within the Ga aquifer during the current crisis (1997-2013) represents ~25% of that scrubbed in all springs inside Crater Amic from ~1979 to ~1994. The amounts of gaseous HCl emitted at the dome summit since 1997 is much more difficult to evaluate due to the large errors in the estimates of gas fluxes and HCl contents. Using the H<sub>2</sub>O flux data of 2005 and 2010 (Beauducel et al., pers. com.<sup>1</sup>) and assuming a linear increase in H<sub>2</sub>O flux from 1997 to 2010 followed by a steady state to present day, and a mean HCl content in fumaroles of ~ 5-10 mol% (dry gas, Table II) the total amount of gaseous HCl emitted at the dome summit since 1997 may be estimated at ~20x10<sup>6</sup> Kg. Thus the amount of HCl scrubbed in the Ga spring aquifer over the same period of time represents only ~ 1% of the total HCl emitted by summit fumaroles. Similar calculations (involving more basic magmas) may be performed for total S and CO<sub>2</sub> emissions and indicates production of ~ 100 x10<sup>6</sup> Kg of SO<sub>2</sub> and ~ 200 x10<sup>6</sup> Kg of CO<sub>2</sub> since 1997.

Since the 1976-1977 volcanic crisis seismic activity has been characterised by a regular decrease in intensity reaching a quiescence period from ~ 1983 to 1991 (< 30 earthquakes/month or < 50 VT/year, Fig. 14), followed by renewal of the activity in 1992 that was not immediately accompanied by significant surficial volcanic manifestations. The renewal of fumarolic activity at the dome summit became significant at the end of 1997. During the 1979-1995 period a close correlation between the chemical and thermal anomalies generated in the shallow geothermal system and the seismic activity was observed (Villemant et al., 2005). Reactivation of seismic activity from 1992 to 1997 was concomitant with progressive migration of fumarolic activity from the basement to the summit of the dome, with no direct evidence of new magmatic gas input and no geochemical imprint in thermal springs until 1995. However, the sealing of the shallow edifice and the scrubbing effects of shallow aquifers can delay components of magmatic origin. A series of magma intrusions likely began in 1994-1995 (Fig. 13). We thus suggest that renewal of the seismic activity in 1992 was related to reactivation of the deep magmatic activity and progressive emplacement of a new small magma intrusion. Ascent and degassing of this intrusion reactivated fracturing of the surficial parts of the edifice which progressively allowed juvenile gases generated by at least two types of magmas (acid andesite and a more basic magma) to reach the surface and to generate the summit fumarolic activity beginning in 1997.

---

<sup>1</sup> During the process of review of the article, Allard and co-workers (Allard et al., in press) have published independent estimates of the gas flux from composition gradients measurements in the plume and wind speed. These data lead to production rates 8 times lower. Comparing these estimation methods is beyond the scope of this paper. This is discussed in a forthcoming paper by Beauducel and co-workers (submitted).

## 7. Conclusions: unrest conditions at La Soufrière of Guadeloupe and implications for volcanic hazard assessment.

The shallow hydrothermal system of La Soufrière of Guadeloupe is confined to the Cratère Amic structure inherited from a series of flank collapse event affecting the upper parts of La Soufrière-Grande Découverte volcano (Figs. 1 and 15; Komorowski et al., 2005, Boudon et al., 2008). The low permeability of the volcanic edifice and the existence of numerous major discontinuities in the dome and the host-rock generates small, discrete hydrothermal reservoirs. Hence, different parts of this complex hydrothermal system are highly reactive to two major disturbances: the rainfall at the dome summit which is particularly intense (average ~10-12 m/year and currently ~ 6-7 m/year) and episodic input of magmatic gas from deep magma reservoirs or shallow intrusions. Monitoring the composition and temperature of the hydrothermal fluids (hot springs, fumaroles, acid ponds) thus provides a particularly effective technique to track the evolution of magmatic activity and volcanic crises (phreatic, phreato-magmatic or magmatic) and provides constraints for hazard assessment. Geochemical monitoring over ~35 years shows that the major modification of the shallow hydrothermal system related to the seismo-volcanic crisis of 1976-1977 ended in ~1991, about 15 years after the onset of the crisis (Fig. 15). After a period of seismic quiescence (1983-1991), renewed seismic unrest (of much lower intensity) occurred in 1992, followed by the reactivation of fumarolic activity at the summit of the dome which then further increased in 1997-98. Both unrest (1976-1977; 1992-present) were likely triggered by emplacement of shallow magma intrusions.

We can estimate present day volatile fluxes through the summit fumaroles using recent gas flux and composition measurements (Beauducel et al., pers. com. and this work) to obtain total fluxes of  $\text{CO}_2 \sim 100$  T/day,  $\text{HCl} \sim 10$  T/day and S expressed as  $\text{SO}_2 \sim 40$  T/day. These can be compared for example, to present day total S fluxes at Soufrière Hills (Montserrat) of ~ 300-500 T/day (expressed as  $\text{SO}_2$ ; MVO Website). On the basis of the composition of summit fumaroles ( $\text{HCl}$ ,  $\text{H}_2\text{S}$  and  $\text{SO}_2$ ), contents of  $\text{Cl}^-$  and  $\text{SO}_4^-$  in thermal springs, and the  $\text{Cl}/\text{Br}/\text{I}$  ratios in all the fluids, the gas flux has a juvenile magmatic origin and cannot be generated by fluctuations of the shallow hydrothermal system in response to a pure thermal disturbance, or by the interplay of shallow sealing/fracturing processes. The apparent low variation in  $\text{CO}_2$  flux and the high  $\text{HCl}/\text{total S}$  ratio of the magmatic gas implies that the intrusion generating the major  $\text{Cl}^-$  anomalies consists of a differentiated acid andesite or dacite magma.

The mass of H<sub>2</sub>O vapour ( $M_{\text{H}_2\text{O}}$ ) extracted from the acid andesitic magma since 1997 may be roughly estimated assuming a Cl content of the melt of  $\sim 3000$  ppm and  $D_{\text{vapour/melt}}^{\text{Cl}} \sim 20$  (Villemant et al., 1999) at  $\sim 2 \times 10^8$  Kg, which represents  $\sim 10\%$  of the estimated total mass of H<sub>2</sub>O vapour produced since 1997 at the dome summit (i.e. summit fumaroles emit 90% of the H<sub>2</sub>O which however is of meteoric origin). This value is also in the same range as the estimated mass of H<sub>2</sub>O vapour produced at the dome summit during the 1976-1977 crisis ( $\sim 10^8$  Kg; P. Allard, personal communication). The corresponding mass of acid andesitic magma ( $M_{\text{m}}$ ) able to produce this mass of H<sub>2</sub>O vapour at emplacement may be roughly estimated from the ratio  $M_{\text{m}}/M_{\text{H}_2\text{O}}$  ( $\sim 200$ ) as proposed in the model of Villemant et al. (2005). This mass ( $\sim 50 \times 10^9$  Kg) is also in the same range as the mass of magma involved in the 1976-1977 volcanic crisis as deduced from the pulsatory crystallisation-degassing model proposed by Boichu et al. (2011): 0.05 to 0.1 km<sup>3</sup> equivalent to  $\sim 100 - 200 \times 10^9$  Kg of magma. All these estimates must however be considered with caution due to the large number and possible range of assumed parameters.

In addition, the involvement of more basic magmas (basic andesites?) is likely because of the production of magmatic SO<sub>2</sub>. This contribution should be eventually identifiable through increases in total S fluxes (and possibly - but not necessarily- in CO<sub>2</sub> fluxes), SO<sub>2</sub>/total S ratio, and a decrease in HCl content relative to other major species. The trends observed since 2011 argue in favour of such a contribution, with a decrease in HCl production and a sustained flux of total S (Fig. 13). Such a balance between the contributions from two types of magmas is observed at the ongoing eruption of Soufrière Hills (Montserrat): a pulsatory production of HCl directly related to explosive activity and dome growth period involving a dacitic magma superimposed on a continuous production of SO<sub>2</sub> corresponding to degassing of a deep more basic andesite (Villemant et al., 2008, Edmonds et al., 2010). Such evolution increases the hazard of a future magmatic or phreato-magmatic eruption. Continuous determination of these key parameters represents a major challenge for geochemical monitoring of unrest conditions at La Soufrière of Guadeloupe.

The estimated masses of gas and magma involved in the current unrest (from 1997 to the end of 2013) are thus similar to those estimated for the  $\sim 2$  year long 1976-1977 crisis, but gas emissions and magma input are distributed over a much longer period of time ( $\sim 17$  years) such that overpressures generated in the system are likely lower and the mean flux of magmatic gas is at least one order of magnitude lower than during the 1976-1977 volcanic crisis. However, both the progressive confinement of the fumarolic activity to the dome summit and the restricted distribution of the hydrothermal features indicate that the upper volcanic edifice is highly sealed, and has probably been only slightly fractured by the recent seismic activity. This result is consistent with VLF and electrical tomography surveys of La Soufrière dome (Zlotnicki et al., 2006, Nicollin et al.,

2006, 2007), and with the recent increase in rainfall transfer durations within the edifice<sup>2</sup>. The decreasing flux of cold rain water associated with a sealed and compartmented upper volcanic edifice promotes, the development of fumarolic activity and concentrated acid ponds at the expense of gas scrubbing by the upper phreatic system. This contrasts with after the aftermath of the 1976-1977 crisis, when intense seismic activity and phreatic explosions led to an intense fracturing of the upper edifice and favoured widespread circulation of magmatic gas. Relative to the post 1976 situation, the current unrest situation may last even longer if the system does not become more highly fractured in the future. However, if current unrest conditions are the consequence of a new magma production at depth, similar magma intrusions may occur over a relatively short interval of time, as suggested by Villemant et al. (2005) for the period preceding the 1976-1977 crisis. Conversely, if emplacement of deep magma intrusions has stopped, we may expect long-lasting (decades) degassing of the current stalled intrusion, according to the model proposed by Villemant et al. (2005) and Boichu et al. (2008, 2011). A direct consequence of the confinement in volcanic and hydrothermal activity and the reduction of rainfall is a local increase of the hydrothermal alteration that likely favours continued sealing and development of zones of mechanical weakness within the upper edifice. The combination of sealing and injection of a new intrusion in a fragile edifice could lead to over-pressurisation of the shallow hydrothermal system, increasing the likelihood of partial edifice collapse and explosive activity at La Soufrière volcano as theoretically modelled for a different setting by Reid (2004) and proposed by Komorowski (2008). Edifice collapse and associated phenomena have been recognized as one of the most frequent hazards of the volcano over the last 10 000 years (LeFriant et al., 2006, Komorowski et al., 2005, 2008).

Reconstruction of the evolution of the shallow and deep evolution of the volcanic and hydrothermal system was made possible by the remarkably long term high resolution monitoring of a set of geochemical and phenomenological data. Measurements of time series of the same parameters (T, SO<sub>2</sub>, CO<sub>2</sub>, HCl and their main derivatives H<sub>2</sub>S, SO<sub>4</sub><sup>2-</sup>, HCO<sub>3</sub><sup>-</sup>, Cl<sup>-</sup>) in all of the different hydrothermal fluids provides the data necessary to reconstruct the extremely complex history of volcanic fluids from the magma source to the surface. The complex succession of condensation and scrubbing processes affecting magmatic fluids in the shallow edifice leads to fumarolic activity which is highly variable in temperature and composition, and whose thermal and chemical history cannot be unambiguously reconstructed. The utility of the contrasted behaviours of S-bearing species (SO<sub>2</sub>, H<sub>2</sub>S, SO<sub>4</sub><sup>2-</sup>) and Cl-bearing species is particularly well illustrated in this system. Although S species

---

<sup>2</sup> In addition, a recent tracing experiment using the injection of KI inside the Tarissan lake performed in April 2010, with a systematic survey of iodine recovery in the different springs around La Soufrière dome (ANR DOMOSCAN, D. Gibert, pers. com.) indicates very low recovery even 2 years after injection. This indicates a significant sealing of the surrounding of volcanic fluids feeding conduits.

(mainly  $\text{H}_2\text{S}$ ) and  $\text{CO}_2$  are almost entirely transported in the gas phase from depth to the surface, gaseous  $\text{HCl}$  (and other halogen acids), because of their very high solubility in water, are almost dissolved in phreatic systems wherever the magmatic gas interacts with them (scrubbing effect of Symonds et al., 2001). Because of these contrasting behaviours it is necessary to combine measurement of S species (and specifically to survey the eventual increase of the  $\text{SO}_2/\text{total S}$  ratio) in the gas plume and  $\text{Cl}^-$  in the thermal springs to identify a common magmatic origin and reconstruct the time series of magma degassing pulses (Fig. 14).

The systematic and accurate high resolution measurement of halogen ratios in volcanic fluids, used in combination with the measurement of major species, provides a very efficient tool to determine the possible magmatic origin of the fluids and to reconstruct their complex evolution in the shallow volcanic edifice.

**Acknowledgments:** We thank all the teams that have succeeded for several decades in the Observatoire Volcanologique et Sismologique de Guadeloupe (OVSG-IPGP) to maintain a high quality the monitoring data acquisition. The recent eruptive history of the volcano and scenarios of possible activity have been improved in the framework of the CASAVA and RiskVolcAn ANR projects (Agence Nationale de la Recherche, France). We thank D. Gibert (ANR DOMOSCAN) for information on Tarissan survey data and P. Agrinier for fruitful discussions on gas composition acquisition and interpretation. We wish also to thank B. Caron and A. Salaün for critical review and discussions. This article benefited from the constructive comments of an anonymous reviewer and of S. Ingebritsen. Special thanks to the latter for his very enthusiastic and comprehensive comments and corrections of the manuscript.

## References

- Aiuppa, A., Baker, D.R., Webster J.D., 2008. Halogens in volcanic systems, *Chem. Geol.*, doi:10.1016/j.chemgeo.2008.10.005
- Aiuppa, A., Federico, C., Franco. A., Giudice, G., Gurrieri S., Inguaggiato S., Liuzzo, M. McGonigle, A. J. S., Valenza, M., 2005. Emission of bromine and iodine from Mount Etna volcano. *Geochemistry, Geophysics, Geosystems* 6, Q08008, doi:10.1029/2005GC000965.
- Allard P., Hammouya, G., Parello, F., 1998. Dégazage magmatique diffus à la Soufrière de Guadeloupe, Antilles, *C. R. Acad. Sci. Paris, Earth and Planetary sciences* 327(315-318).
- Allard P., Aiuppa A., Beauducel F., Calabrese S., Di Napoli R., Crispi O., Gaudin D., Parello F., Steam and gas emission rate from La Soufriere volcano, Guadeloupe (Lesser Antilles): implications for the magmatic supply during degassing unrest. *Chem. Geol.* In press.
- Azeotrope Data Bank (2001). [eweb.chemeng.ed.ac.uk/chemeng/azeotrope\\_bank.html](http://eweb.chemeng.ed.ac.uk/chemeng/azeotrope_bank.html)
- Balcone-Boissard, H., Villemant, B. Boudon, G., 2010. Behavior of halogens during the degassing of felsic magmas, *Geochem. Geophys. Geosyst.*, 11, Q09005, doi:10.1029/2010GC003028.
- Beauducel, F., Gaudin, D., Coutant, O., Delacourt, C., Allemand, P., Richon, P., de Chabalier, J.B., Hammouya, G., 2013. Mass and heat flux balance of La Soufrière volcano (Guadeloupe) from aerial infrared thermal imaging. (submitted)
- Beauducel, F., Anténor-Habazac, C., Mallarino, D., 2004. WEBOBS : Integrated monitoring system interface for volcano observatories. Paper presented at IAVCEI General Assembly, Pucon, Chile, Nov 2004, abstract S08A-PF-072.
- Beauducel F., Bosson, A. , Randriamora, F., Anténor-Habazac, C., Lemarchand, A., Saurel, J.-M., Nercessian, A., Bouin, M.-P., de Chabalier, J.-B., Clouard, V., 2010. Recent advances in the Lesser Antilles observatories Part 2 : WebObs - an integrated web-based system for monitoring and networks management, Paper presented at European Geophysical Union General Assembly, Vienna, May 2010.
- Beauducel F., Bazin, S., Bengoubou-Valérius, M., Bouin, M-P., Bosson, A., Anténor-Habazac, C., Clouard, V., de Chabalier, J-B., 2011. Empirical model for rapid macroseismic intensities prediction in Guadeloupe and Martinique. *CR Geoscience (Elsevier)*, 343:11-12, 717-728, doi:10.1016/j.crte.2011.09.004, 2011.
- Beauducel, F., 2013, <http://www.ipgp.jussieu.fr/~beaudu/soufriere/forum76.html>; À propos de la polémique de Soufrière 1976...Rappel des faits et point de vue personnel sur les événements qui ont marqué la Guadeloupe et la communauté volcanologique.

Bernard M.L., Molinié J., Petit R., Beauducel, F., Hammouya, G., Marion, G., 2006. Remote and in situ plume measurements acid gas release from La Soufrière volcano, Guadeloupe. *J. Volcanol. Geotherm. Res.*, 150,395-409. doi:10.1016/j.jvolgeores.2005.08.001

Berndt M.E., Seyfried W. E., 1997. Calibration of Br/Cl fractionation during subcritical phase separation of seawater : possible halite at 9 to 10°N East Pacific Rise. *Geochim. Cosmochim. Acta*, 61, 14, 2849-2854

Bischoff, J.L., Rosenbauer, R.J., Fournier, R.O., 1996. The generation of HCl in the system CaCl<sub>2</sub>-H<sub>2</sub>O: Vapor-liquid relations from 380-500 °C. *Geochim. Cosmochim. Acta.* 60,1, 7-16.

Bigot, S., Hammouya, G., 1987. Surveillance hydrogéochimique de la Soufrière de Guadeloupe, 1978-1985: diminution de l'activité ou confinement?, *C. R. Acad. Sci. Paris 304(Sér. II)*, 757-760,.

Bigot, S., Boudon, G., Semet, M.P., Hammouya, G., 1994. Traçage chimique de la circulation des eaux souterraines sur le volcan de la Grande Découverte (la Soufrière), Guadeloupe, *C. R. Acad. Sci. Paris 318(Sér. II)*, 1215-1221.

Bobrowski, N., Hönninger, G., Galle, B., Platt, U.,2003. Detection of bromine monoxide in volcanic plumes, *Nature* 423, 273-276.

Boichu, M., Villemant, B., Boudon, G., 2008. A Model for Episodic Degassing of an Andesitic Magma Intrusion, Part 1., *J. Geophys. Res.*,113, B7, B07202 doi: 10.1029/2007JB005130.

Boichu, M., Villemant, B., Boudon, G., 2011. Degassing at la Soufrière de Guadeloupe Volcano (Lesser Antilles) since the Last Eruptive Crisis in 1976-77 : Result of a Shallow Magma Intrusion. *J. Volcanol. Geotherm. Res.*, 202: 102-112. doi:10.1016/j.jvolgeores.2011.04.007

Boudon, G., Semet, M.P., Vincent, P.M., 1989. The evolution of la Grande Découverte (La Soufrière) volcano, Guadeloupe, F.W.I., in: *Volcano hazards: Assessment and Monitoring*, J. Latter, ed., pp. 86-109, Springer-Verlag.

Boudon, G., Le Friant, A., Komorowski, J.C., Deplus, C., Semet, M.P., 2007. Volcano flank instability in the Lesser Antilles Arc: diversity of scale, processes, and temporal recurrence. *J. Geophys. Res.* 112, B08205. doi:10.1029/2006JB004674

Boudon G., Komorowski J.-C., Villemant B, Semet M.P., 2008. A new scenario for the last magmatic eruption of La Soufrière de Guadeloupe (Lesser Antilles) in 1530 A.D.: evidence from stratigraphy, radiocarbon dating and magmatic evolution of erupted products. *J. Volcanol. Geotherm. Res.* 178,3, 474-490. DOI: 10.1016/j.jvolgeores.2008.03.006

Brombach T., Marini, L., Hunziker, J.-C., 2000. Geochemistry of the thermal springs and fumaroles of Basse-Terre Island, Guadeloupe, Lesser Antilles, *Bull. Volcanol.* 61, 477-490.

Chen J-B., Gaillardet, J., Dessert, C., Villemant, B., Louvat, P., Crispi, O., Birck, J-L., Wang Y-N., 2013. Zn isotope compositions of the thermal spring waters of La Soufrière volcano, Guadeloupe Island) *Geochim. Cosmochim. Acta* . 127:67–82.

Chiodini G., Marini, L., 1998. Hydrothermal gas equilibria: The H<sub>2</sub>O-H<sub>2</sub>-CO<sub>2</sub>-CO-CH<sub>4</sub> system. *Geochimica et Cosmochimica Acta*, Vol. 62, No. 15, pp. 2673–2687.

Chiodini G., Cioni, R., Frullani, A., Guidi, M., Marini, L., Prati F., Raco, B., 1996. Fluid geochemistry of Montserrat island, West Indies, *Bull. Volcanol.* 58, 380-392.

Chiodini G., Todesco, M., Caliro, S., Del Gaudio, C., Macedonio, G., Russo M., 2003. Magma degassing as a trigger of bradyseismic events: The case of Phlegrean Fields (Italy), *Geophys. Res. Lett.*, 30(8), 1434, doi:10.1029/2002GL016790.

Chiodini G., Caliro S., Cardellini, C., Granieri, D., Avino, R., Baldini, A., Donnini, M., Minopoli, C., 2010. Long-term variations of the Campi Flegrei, Italy, volcanic system as revealed by the monitoring of hydrothermal activity, *J. Geophys. Res.*, 115, B03205, doi: 10.1029/2008JB006258.

Crider J.G., Frank, D., Malone, S.D., Poland, M.P., Werner, C., Caplan-Auerbach, J., 2011. Magma at depth: a retrospective analysis of the 1975 unrest at Mount Baker, Washington, USA. *Bull. Volcanol.* (2011) 73:175–189 DOI 10.1007/s00445-010-0441-0

D'Amore, F., Panichi, C., 1980. Evaluation of deep temperatures of hydrothermal systems by a new gas geothermometer *Geochim. Cosmochim. Acta.* 44, 549-556.

Delorme H., 1983. Composition chimique et isotopique de la phase gazeuse des volcans calco-alcalins: Amérique Centrale et Soufrière de Guadeloupe. PhD thesis, Université Paris-Diderot, 418p

Dupont, A., 2010. Étude du son produit par la Soufrière de Guadeloupe et le Piton de la Fournaise : implications pour la dynamique éruptive et la surveillance volcanique, PhD Thesis, , 153 p. IPGP, Paris.

Doukas, M. P., Gerlach, T.M., 1995. Sulfur dioxide scrubbing during the 1992 eruption of Crater Peak, Mount Spurr, Alaska, in Keith, T., ed., *The 1992 eruptions of Crater Peak Vent, Mount Spurr volcano, Alaska: U.S. Geological Survey Bulletin* B-2139, p. 47-57.

Edmonds M., Gerlach, T.M., 2006. The airborne lava–seawater interaction plume at Kīlauea Volcano, Hawai‘i. *Earth Planet. Sci. Letters.* 244 (2006) 83–96. doi:10.1016/j.epsl.2006.02.005

Edmonds, M., Pyle, D., Oppenheimer C., 2001. A model for degassing at the Soufriere Hills Volcano, Montserrat, West Indies, based on geochemical data. 186 , 159-173.

Edmonds M., Aiuppa, A., Humphreys, M., Moretti, R., Giudice, G., Martin, R.S., Herd, R. A., Christopher, T., 2010. Excess volatiles supplied by mingling of mafic magma at an andesite arc volcano. *Geochem. Geophys. Geosyst.* 11, Q04005. doi:10.1029/2009GC002781

Feuillard, M., Allègre, C.J., Brandeis, G., Gaulon, R., Le Mouél, J.-L., Mercier, J.-C., Pozzi, J.-P., Semet, M.P., 1983. The 1976-1977 crisis of la Soufrière de Guadeloupe (F.W.I.): a still-born magmatic eruption, *J. Volcanol. Geotherm. Res.* 16, 317-334.

Feuillard, M., 2011. *La Soufrière de Guadeloupe, un volcan et un peuple*, Edition Jasor, Pointe-à-Pitre, 1-246 pp, 26 planches

Feuillet, N., Manighetti, I., Tapponnier, P., 2001. Extension active perpendiculaire à la subduction dans l'arc des Petites Antilles (Guadeloupe, Antilles françaises). *C. R. Acad. Sci. Paris, Earth and Planetary Sciences*, 333 (2001) 583–590

Feuillet, N., Tapponnier, P., Manighetti, I., Villemant, B., King, G. C. P., 2004. Differential uplift and tilt of Pleistocene reef platforms and Quaternary slip rate on the Morne-Piton normal fault (Guadeloupe, French West Indies). *J. Geophys. Res.* 109-126, B02404, doi:10.1029/2003JB002496.  
Gerlach, T.M., 2004. Volcanic sources of tropospheric ozone-depleting trace gases. *Geochem. Geophys. Geosyst.* 5, Q09007. doi:10.1029/2004GC000747.

Feuillet N., Beauducel, F., Jacques, E., Tapponnier, P., Delouis, B., Bazin, S., Vallée, M., King, G., 2011. The Mw = 6.3, November 21, 2004, Les Saintes earthquake (Guadeloupe): Tectonic setting, slip model and static stress changes. *Jour. Geophys. Res.*, 116, B10301, doi:10.1029/2011JB008310, 2011.

Giggenbach W. F., 1980. Geothermal gas equilibria. *Geochim. Cosmochim. Acta* 44, 2021–2032.

Giggenbach W. F., 1987. Redox processes governing the chemistry of fumarolic gas discharges from White Island, New Zeland. *Appl. Geochem.* 2, 143–161.

Giggenbach W.F., 1988. Geothermal solute equilibria. Derivation of Na-K-Mg-Ca geoindicators, *Geochim. Cosmochim. Acta* 52, 2749-2765.

Giggenbach, W.F., Tedesco, D., Sulistiyo, Y., Caprai, A., Cioni, R., Favara, R., Fischer, T.P., Hirabayashi, J.I., Korzhinsky, M., Martini, M., Menyailov, I., Shinohara, H., 2001. Evaluation of results from the fourth and fifth IAVCEI field workshop on volcanic gases, Vulcano Island, Italy, and Java, Indonesia. *J. Volcanol. Geotherm. Res.* 108,157–172.

Hammouya, G., Allard, P., Jean-Baptiste, P., Parello, F., Semet, M.P., Young, S.R., 1998. Pre- and syn-eruptive geochemistry of volcanic gases from Soufriere Hills of Montserrat, West Indies, *Geophys. Res. Letters* 25(19), 3685-3688.

Hincks, T., Komorowski J-C., Sparks, R.S.J., Aspinall, W.P., 2014. Retrospective analysis of uncertain eruption precursors at La Soufrière volcano, Guadeloupe, 1975-77: volcanic hazard assessment using a Bayesian Belief Network approach. *Journal of Applied Volcanology.* 3:3, doi: 10.1186/2191-5040-3-3

Hurwitz, S., Lowenstern, J.B., Heasler, H., 2007. Spatial and temporal geochemical trends in the hydrothermal system of Yellowstone National Park: Inferences from river solute fluxes. *J. Volcanol. Geotherm. Res.* 162, 149-171. doi:10.1016/j.jvolgeores.2007.01.003

IPGP, Internal Reports (1976-1984) Rapports d'activité des Observatoires Volcanologiques des Antilles (Gadeloupe-Martinique), IPGP. Nov. 1976-April 1977, April 1977-Dec. 1978, 1979, 1980, 1981, 1982, 1983-1984, Paris, France.

IPGP website (public access) <http://volobsis.ipgp.fr> and <http://centredonnees.ipgp.fr/index.php>

Komorowski, J.C., Boudon, G., Semet, M., Beauducel, F., Anténor-Habazac, C., Bazin, S.Hammouya, G., 2005. Guadeloupe, in: *Volcanic Hazard Atlas of the Lesser Antilles*, J. Lindsay, R. Robertson, J. Shepherd and S. Ali, eds., pp. 65-102, University of the West Indies, Seismic Research Unit, Trinidad and IAVCEI, 2005.

Komorowski, J.-C., Legendre, Y., Caron, B., Boudon, G., 2007. Reconstruction and analysis of sub-plinian tephra dispersal during the 1530 A.D. Soufrière (Guadeloupe) eruption: Implications for scenario definition and hazards assessment. *J. Volcanol. Geotherm. Res.* 178 (2008) 491–515. doi:10.1016/j.jvolgeores.2007.11.022

Komorowski, J.-C., 2008. De l'édifice au pyroclaste: une approche pluridisciplinaire de la compréhension des processus volcaniques et de l'évaluation des aléas. HDR, IPGP-Paris Diderot ; 552 p.

Komorowski, J.-C., Boudon, G., Antenor-Habazac, C., Hammouya, G., Semet, M., David, J., Beauducel, F., Cheminée, J.-L., Feuillard, M., 2001. L'activité éruptive et non-éruptive de la Soufrière de Guadeloupe: problèmes et implications de la phénoménologie et des signaux actuellement enregistrés, Atelier sur les aléas volcaniques – Les volcans antillais : des processus aux signaux. PNRN (CNRS) – INSU, BRGM, CEA, CEMAGREF, CNES, IRD. 18-19 janvier 2001, Paris, abstract volume, p. 18-21

Kuster, D., Silve, V., 1997. *Guadeloupe, Canyons, Gouffres, Découverte*. Editions Gap, La Ravoire, Chambéry, France, 256 pp.

Le Friant A., Boudon, G., Komorowski, J.-C., Heinrich, P., Semet, M.P., 2006. Potential Flank-Collapse of Soufrière Volcano, Guadeloupe, Lesser Antilles? Numerical Simulation and Hazards. *Natural Hazards.* 39: 381–393. DOI 10.1007/s11069-005-6128-8

Di Liberto V., Nuccio P.M., Paonita A., 2002. Genesis of chlorine and sulphur in fumarolic emissions at Vulcano Island (Italy) : assessment of pH and redox conditions in the hydrothermal system. *J. Volcanol. Geotherm. Res.* 116, 137-150.

Long Li, Jendrzewski, N., Aubaud, C., Bonifacie, M., Crispi, O., Dessert, C., Agrinier, P., 2012. V53B-2831: Isotopic evidence for quick freshening of magmatic chlorine in the Lesser Antilles arc volcanoes, AGU fall meeting, <http://fallmeeting.agu.org/2012/eposters/eposter/v53b-2831/>

Liebsher A., Heinrich, C. A., 2007. Fluid–Fluid Interactions in the Earth’s Lithosphere. *Reviews in Mineralogy & Geochemistry*. Vol. 65, pp. 1-13.

Lowenstern, J.B., Smith, R.B., Hill, D.P., 2006. Monitoring super-volcanoes: Geophysical and geochemical signals at Yellowstone and other large caldera systems. *Philosophical Transactions of the Royal Society A364*: 2055-2072

Melián, G., Tassi, F., Pérez, N., Hernández, P., Sortino, F., Vaselli, O., Padrón, E., Nolasco, D., Barrancos, J., Padilla, G., Rodríguez, F., Dionis, S., Calvo, D., Notsu, K., Sumino H., 2012. A magmatic source for fumaroles and diffuse degassing from the summit crater of Teide Volcano (Tenerife, Canary Islands): a geochemical evidence for the 2004–2005 seismic–volcanic crisis. *Bull. Volcanol.* doi:10.1007/s00445-012-0613-1

Michel, A., Villemant, B., 2003. Determination of halogens (F, Cl, Br, I), sulphur and water in 17 reference geological material, *Geostandard Newsletter* 27(2), 163-171.

Millard, G.A., Mather, T.A., Pyle, D.M., Rose W. I., Thornton, B., 2006. Halogen emissions from a small volcanic eruption: Modeling the peak concentrations, dispersion, and volcanically induced ozone loss in the stratosphere. *Geophys. Res. Letters*, 2006, 33, L19815, doi: 10.1029/2006GL026959

Moretti, R., Arienzo, I., Civetta, L., Orsi, G., Papale P., 2013. Multiple magma degassing sources at an explosive volcano. *Earth Planet. Sci. Letters* 367; 95–104. doi: 10.1016/j.epsl.2013.02.013.

MVO Website: <http://www.mvo.ms/>

Newhall, C., Dzurisin, D., 1988. Historical unrest at large calderas of the world, *U.S. Geol. Surv. Bull.*, 1855, 1108 pp.

Nicollin, F., Gibert, D., Beauducel, F., Boudon, G., Komorowski, J.-C., 2006. Electrical tomography of La Soufrière of Guadeloupe Volcano: Field experiments, 1D inversion and qualitative interpretation. *Earth and Planetary Science Letters*, 244 (3-4): 709-724.

Nicollin, F., Gibert, D., Beauducel, F., Boudon, G., Komorowski, J.-C., 2007. Reply to comment on "Electrical Tomography of La Soufriere of Guadeloupe Volcano: Field experiments, 1D inversion and qualitative interpretation" by N. Linde and A. Revil. *Earth and Planet. Sci. Letters*, 258 (3-4): 623-626.

Oppenheimer, C., Tsanev, V.I., Braban, C.F., Cox, R.A., Adams, J.W., Aiuppa, A., Bobrowski, N., Delmelle, P., Barclay, J., McGonigle, A.J.S., 2006. BrO formation in volcanic plumes, *Geochim. Cosmochim. Acta* 70, 2935–2941.

OVSIG – IPGP Website: Volcano and seismic activity bulletin of La Soufrière of Guadeloupe: <http://www.ipgp.fr/pages/0303.php>

OVSIG-IPGP, 1978–2012. Bilan mensuel de l'Activité volcanique et de la sismicité régionale de l'Observatoire Volcanologique de la Soufrière. <http://volcano.ipgp.fr/guadeloupe/Infos.htm>.

OVSIG-IPGP, 1999-2013. Bulletin mensuel de l'activité volcanique et sismique de Guadeloupe. Monthly public report, Observatoire Volcanologique et Sismologique de Guadeloupe - Institut de Physique du Globe de Paris, Gourbeyre, ISSN 1622-4523

Ruzié L., Moreira, M., Crispi, O., 2012. Noble gas isotopes in hydrothermal volcanic fluids of La Soufrière volcano, Guadeloupe, Lesser Antilles arc. *Chemical Geology* 304-305, 158–165. doi: 10.1016/j.chemgeo.2012.02.012

Ruzié, L., Aubaud, C., Moreira, M., Agrinier, P., Dessert, C., Gréau, C., Crispi, O. 2013. Carbon and helium isotopes in thermal springs of La Soufrière volcano (Guadeloupe, Lesser Antilles): Implications for volcanological monitoring. *Chem. Geol.* 359, 70–80. doi: 10.1016/j.chemgeo.2013.09.008

Reid M. E., 2004. Massive collapse of volcano edifices triggered by hydrothermal pressurization. *Geology*; 32; 5; 373–376. doi: 10.1130/G20300.1

Salaün, A., Villemant, B., Gérard, M., Komorowski, J.C., Michel A., 2011. Hydrothermal alteration in andesitic volcanoes: a study of trace element redistribution in active- and paleohydrothermal systems of Guadeloupe (Lesser Antilles). *Journal of Geochemical Exploration GEXPLO Special Issue on Geochemical Sampling Media for Various Geological-Environmental Studies. Jour. Geo. Expl.* 111, 59-83. doi:10.1016/j.gexplo.2011.06.004.

Shimulovich, K.I., Graham, C.M., 2004. An experimental study of phase equilibria in the systems H<sub>2</sub>O–CO<sub>2</sub>–CaCl<sub>2</sub> and H<sub>2</sub>O–CO<sub>2</sub>–NaCl at high temperatures and pressures (500–800 °C, 0.5–0.9 GPa) geological and geophysical applications. *Contrib. Mineral. Petrol.* 146, 450–462.

Sorey, M., McConnell, V., Roeloffs, E., 2003. Summary of recent research in Long Valley caldera, California, *J. Volcanol. Geotherm. Res.*, 127(3–4), 165–173, doi: 10.1016/S0377-0273(03)00168-9.

Symonds, R.B., Reed, M.H., 1993. Calculation of multicomponent chemical equilibria in gas-solid-liquid systems: calculation methods, thermochemical data and applications to studies of high temperature volcanic gases with examples from Mount St. Helens, *Amer. J. Sci.* 293, 758-864.

Symonds, R.B., Rose, W.I., Bluth, G.J.S., Gerlach, T.M., 1994. Volcanic-gas studies: methods, results and applications. In: Carroll, M.R., Holloway, J.R. (Eds.), *Volatiles in Magmas*. *Rev. Mineral.*, vol. 30, pp. 1–66.

Symonds, R.B., Rose, W.I., Gerlach, T.M., Briggs, P.H., Harmon, R.S., 1990. Evaluation of gases, condensates, and SO<sub>2</sub> emissions from Augustine volcano, Alaska: the degassing of a Cl-rich volcanic system, *Bull. Volcanol.* 52, 355– 374.

Symonds, R.B., Gerlach, T.M., Reed, M.H., 2001. Magmatic gas scrubbing: implications for volcano monitoring, *J. Volcanol. Geotherm. Res.* 108, 2749-2765.

Todesco, M., 2008. Hydrothermal fluid circulation and its effects on caldera unrest, in *Caldera Volcanoes: Analysis, Modeling and Response*, *Dev. Volcanol.*, vol. 10, edited by J. Gottsmann and J. Marti, pp. 393–416, doi:10.1016/S1871-644X(07)00011-3, Elsevier, Amsterdam.

Todesco, M., 2009. Signals from the Campi Flegrei hydrothermal system: Role of a “magmatic” source of fluids, *J. Geophys. Res.*, 114, B05201, doi:10.1029/2008JB006134.

Traineau, H., Sanjuan, B., Beaufort, D., Brach, M., Castaing C., Correia, H., Genter, A., Herbrich, B., 1997. The Bouillante geothermal field (F.W.I.) revisited: new data on the fractured geothermal reservoir in light of a future stimulation experiment in a low productive well. *Proc 22nd Workshop on Geothermal Reservoir Engineering*, Stanford University, SGP-TR-155

Villemant, B., Boudon, G., 1999. H<sub>2</sub>O and halogen (F, Cl, Br) behaviour during shallow magma degassing processes, *Earth Planet. Sci. Letters* 168, 271-286.

Villemant B., Boudon, G., Nougriat, S., Poteaux, S., Michel, A., 2003. H<sub>2</sub>O and halogen in volcanic clasts: tracers of degassing processes during plinian and dome-forming eruptions, in: *Volcanic Degassing*, C. Oppenheimer, D. Pyle and J. Barclay, eds., Special Publication 213, pp. 63-79, *Geol. Soc. London*.

Villemant B., Hammouya G., Michel A., Semet M.P., Komorowski, J.C., Boudon, G., Cheminée, J.L., 2005. The memory of volcanic waters: shallow depth magma degassing revealed by long-term monitoring of hydrothermal springs at la Soufrière volcano (Guadeloupe, Lesser Antilles) *Earth Planet. Sci. Lett.* doi:10.1016/j.epsl.2005.05.013.

Villemant, B., Mouatt J., Michel A., 2008. Andesitic Magma Degassing Investigated Through H<sub>2</sub>O Vapour-Melt Partitioning of Halogens at Soufrière Hills Volcano, Montserrat (Lesser Antilles) *Earth Planet. Sci. Lett.* 269,1-2, 212-229. doi:10.1016/j.epsl.2008.02.014.

von Glasow, R., Bobrowski, N., Kern, C., 2008. The effects of volcanic eruptions on atmospheric chemistry. *Chem. Geol.* doi:10.1016/j.chemgeo.2008.08.020.

Webster, J.D., Kinzler, R.J., Mathez, E.A., 1999. Chloride and H<sub>2</sub>O solubility in basalt and andesitic melts and implications for magmatic degassing. *Geochimica and Cosmochimica Acta* 63, 729-738.

Zlotnicki J., Boudon G., Le Mouél, J.-L., 1992. The volcanic activity of la Soufrière of Guadeloupe (Lesser Antilles): structural and tectonic implications, *J. Volcanol. Geotherm. Res.* 49, 91-104.

Zlotnicki, J., Vargemesis, G., Mille, A., Bruère, F., Hammouya, G., 2006. State of the hydrothermal activity of Soufrière of Guadeloupe volcano inferred by VLF surveys. *J. Applied Geophys.* 58, 265– 279. doi:10.1016/j.jappgeo.2005.05.004

ACCEPTED MANUSCRIPT

## Table captions

Table I: Temperature, pH and major element compositions of hot springs, acid ponds and fumarole condensates of La Soufrière of Guadeloupe.

Maximum, minimum and mean values ( $1 \sigma$  error) are calculated for different periods of time corresponding to the different regimes observed in the temperatures and Cl content time series (see Fig. 2 and Fig. 5). n: number of measurements (fortnight based sampling for most springs). n.d.: not determined.

## Ia: Thermal springs

For springs outside Cratère Amic structure (HR, BCM-EV) temperature and composition variations are low during the whole survey. Other springs inside the Cratère Amic structure display at least two different variation regimes, generally corresponding to 1979- 1995 and 1996 - present day. Ga spring displays three distinct regimes. CC spring (outside Cratère Amic) displays two regimes with time periods different from other springs (see text for explanations). For data sources see OVSG-IPGP website and Villemant et al. (2005) and Chen et al. (2013). See also Brombach et al. (2000) for comparison. See Fig. 1 for source locations.

## Ib: Acid ponds and fumaroles condensates

Acid ponds (Tarissan and Cratère Sud Central) and gas condensates (Cratère Sud Central and Napoléon) are irregularly sampled, depending on accessibility. Gas compositions are recalculated to 100%, on an anhydrous basis by combining compositions of dry gas and condensates (HCl) when available on the same sampling.

Table II: Temperature and major gas compositions of fumaroles. Comparison with 1977-1978 fumaroles.

CSC: summit fumarole (sampling period: 1997-2010); mean values and means for different temperature ranges. RC: Route de la Citerne fumaroles (sampling period: 1983-2010). (\*) The composition of the summit fumarole in 1997 is from Brombach et al. (2000). (§) Compositions of summit fumaroles (Lacroix) sampled in 1977 and 1978 are recalculated from IPGP Internal reports (see text for explanations).

Sampling in  $P_2O_5$  bottles; measurements by gas chromatography (OVSG-IPGP websites).

Compositions are in mol% (anhydrous basis).  $N_2$ ,  $O_2$  and Ar have been corrected from air pollution (calculated on the basis of  $N_2$  contents).  $H_2O$  contents are higher than 95-96 mol% but not systematically determined. (\*\*)  $N_2 + O_2$ . Bold: mean values; lower case:  $1 \sigma$  errors. n.d. not

determined; b.d.l. below detection limit. Extensive CSC (1999-2012) and Lacroix (1977-1978) fumarole gas compositions are given in Annex 2.

Table III: Halogen contents in spring waters, acid ponds and fumarole.

Maximum, minimum and mean values of halogen contents; Cl/Br and Br/I mass ratios. F, Cl and Br are in ppm, I in ppb. Abbreviations and explanations as in Tables I and II.

III a: Thermal springs. Values are calculated for the different regimes observed in the temperatures and Cl contents time series (see also Table I). (\*) For Galion spring, two different Cl-Br correlations are observed from 1996.

III b: Acid ponds and fumaroles. Halogen compositions in fumaroles are determined on condensates.

Table IV: Steady compositions of Amic Crater spring waters (SASW). Comparison with pre-1976 compositions and estimates of the Cl contamination of phreatic systems.

IV a: SASW are calculated as the mean steady compositions of spring waters inside Cratère Amic structure with similar T and altitudes. SASW1: BJ, CE and PR (alt. ~600 m, T ~28°C); SASW2: Ga and Ta (alt. ~1100 m, T ~41°C). BJ (1968) and CE (1968) data from Feuillard, 2011).

IV b: estimates of Cl contaminations of spring waters (CE, CC, BJ, Ga) after the 1976-1977 crisis and of Ga spring since the beginning of the current crisis. These are calculated as the difference between Cl compositions of SASW's and Cl -time series and multiplied by the flow rate (expressed in Kg). This shows, for example, that the current Cl contamination by volcanic gases of Ga spring (since 2002) is similar to that estimated for Ga spring from 1979 to 1996 (~2 10<sup>5</sup> Kg, Villemant et al., 2005, Table 2), and one third of the total estimated for all springs (see text for further explanations).

## Figure captions

Fig. 1: The active hydrothermal system at La Soufriere of Guadeloupe

1a: Main volcano-tectonic structures and distribution of thermal springs and fumaroles:

(1) Thick black lines : flank collapse scars ; the most internal is Cratère Amic; (2) thick red dashed line: La Grande Découverte Caldera; (3) La Soufrière lava dome. (4) black double straight lines: summit fractures; (5) black dotted line: La Ty fault system. (6) small open red circles: 1976-19777 fumaroles active up to to 1981 (L : Lacroix, CDE: col de l'Echelle) ; (7) small light red circles: Route de la Citerne or La Ty fumarolic field (weakly active up to 1997); (8) small red dots: active summit fumaroles since 1997; (9) small blue-red circles: fumaroles with intermittent acid lakes (CSC: Cratère Sud Central, Tr: Tarissan); (10) black dots Savane à Mulets (SAM) and Col de l'Echelle (CDE) wells. Yellow zones: hydrothermally altered areas. Large circles: thermal springs; see text for name abbreviations. The equidistance between the thick contour lines is 100 m (1000: altitude 1000 m).

Fig 1b (inset): Interpretative cross section of the dome structure and hydrothermal circulations.

(Redrawn from Villemant et al., 2005, Komorowski, 2008, Salaün et al., 2011)

Fig. 2: Compositions of spring waters and acid ponds.

Compositions in major anions ( $\text{SO}_4^{2-}$ ,  $\text{Cl}^-$ ,  $\text{HCO}_3^-$ ) and cations ( $\text{Ca}^{++}$ ,  $\text{Mg}^{++}$ ,  $\text{Na}^+$ ) of thermal springs and acid ponds recorded from 1995 to 2012. Coloured domains correspond to 1979-1994 records for CE, BJ and Ga springs and to 1979-2004 for CC spring. See Fig. 1 for springs and ponds locations; labels are explained in Table I and text. RM is not represented for simplification. Tarissan composition (mean value) is from IPGP-OVSG (IPGP Website, unpublished). Large crosses correspond to calculated steady Amic Crater waters at different equilibration temperatures (SASW at 28°C and 45°C; see text for explanation). Notice that numerous springs were not sampled before 1995.

Compositions of springs outside the Cratère Amic structure (HR and BCM-EV, except CC) are represented for the whole sampling period because they do not display significant composition variations. Cations composition variations are low, with no major differences (except CC) between the two sampling periods. Most springs inside Cratère Amic structure and CC spring display large variations in  $\text{Cl}^-$  (and to a lesser degree in  $\text{SO}_4^{2-}$ ) during the first (CE, CC) or the second (Ga) sampling periods. Acid ponds are very similar in composition with extremely high  $\text{Cl}^-$  contents and  $\text{Ca}^{++}/\text{Mg}^{++}/\text{Na}^+$  ratios close to 1/1/1 and are clearly distinct from fumarole condensates

compositions (CSC) Composition variations of springs during the first sampling period (1979-1995) have been described and interpreted by Villemant et al. (2005).

Fig. 3: Fumaroles of La Soufriere dome: temperature and composition of major components since 1977.

The composition of fumaroles collected at the dome summit after 1997 (red domains, CSC and CSN: Cratère Sud Central and Nord) and the low temperature fumaroles collected at the base of the dome (RC, Route de la Citerne) since 1983 (yellow domain) define two distinct trends. The HCl-S-CO<sub>2</sub> compositions of post-1997 summit fumaroles with  $T > 96^{\circ}\text{C}$  are similar to those of fumaroles collected at the end of the 1976-1977 crisis (Lacroix fumaroles) and define a trend towards a HCl-rich pole at constant S/CO<sub>2</sub> ratio. This trend is similar to that defined by high temperature gases of Soufrière Hills (Montserrat) measured in 1996 (onset of the eruption composition close to HCl apex, Hammouya et al., 1998) and 2008 (eruptive hiatus, estimate from Edmonds et al. 2010). This evolution trend at Soufrière Hills from 1996 to 2008 is interpreted as the result of increasing contribution of unerupted mafic magmas (Edmonds et al., 2010). Low temperature fumaroles collected at the dome summit in 1997 (red solid diamond, Brombach et al., 2000), just before the production of a highly acid summit gas plume, have compositions similar to those of RC. CSC gas and condensates compositions are represented by both individual measurements and mean values calculated for different temperature ranges (see Table II). Compositions of fumarolic gases collected in 1997 at La Ty (RC) and at the dome summit are from Brombach et al. (2000).

Fig. 4 : Cl<sup>-</sup> and temperature time series of thermal springs since 1979.

Fig 4a: Time series of Cl<sup>-</sup>. Long term variations clearly differentiate springs inside and outside Cratère Amic structure. Most springs outside the structure (HR, BCM-EV, but not CC) display no Cl<sup>-</sup> anomaly. Inside Cratère Amic structure springs (CE, Ga, Ta, BJ to which must be associated CC spring) display short term variations with similar frequency but highly different amplitude variations (see also Fig. 5 and 6 for details). Two main periods may be distinguished (from 1979 to ~1994 and from 2000 to present day); during the second period only Ga spring displays a series of Cl<sup>-</sup> anomalies, whereas other springs display steady compositions. Cl<sup>-</sup> contents in CC spring display a distinct characteristic behavior. All Cl<sup>-</sup> anomalies (except in Ta) are interpreted as resulting from scrubbing of magmatic gas component (HCl). Those in the Ta spring which mainly result from variation in precipitation (see also Fig. 5). Symbols as in Fig. 2. RM spring not represented. See also Supplementary Material (Fig. D).

Fig. 4b: Temperatures time series; comparison with precipitations. Symbols as in Fig. 4a. Black line: precipitations at the dome summit (reverse scale). All springs outside Cratère Amic structure (BCM, HR, CC) display only smooth and very low amplitude variations with time, with very low variations at long time scale (~35 y). Springs inside the structure display either long term variations or both long term and short term variations. Short term temperature (and Cl<sup>-</sup>, Fig. 4a) variations in Ta spring are clearly related to precipitation variations, which is not the case for other springs. However, the increasing temperature of spring waters inside the Cratère Amic structure since the 1990's is directly related to a decrease in precipitation.

Fig. 4c: comparison of Cl<sup>-</sup> and temperature anomalies for CE spring during the first period.  $\Delta T$  is measured as the difference between a smooth polynomial fit over the whole time series and individual values. There is a close correlation between the main T and Cl<sup>-</sup> anomalies. This evolution is not related to the precipitation regime (see text for explanations).

Fig. 5 : Composition and temperatures time series for Ta, Ga and BJ springs; comparison with precipitation regime.

Fig. 5a : (top) Co-variations of major element compositions of Tarade waters and (bottom) close anti-correlation between temperature, Cl<sup>-</sup> content and precipitation regime (dashed line). The dilution effect of rain-water affects both temperature and all major elements. Close adjustment between composition and temperature data variations and rainfall regime black dashed line requires delays in rain-water transfer times varying by step from 1.1 to 3.5 months (thick black line: rainfall corrected from transfer time delays).

Fig. 5b: Anti-correlation between temperature variations since ~1992 in Galion (Ga) and Bain Jaune (BJ) springs and rainfall regime. T Anti-correlations between Cl<sup>-</sup> and rainfall variations (not shown) are much less clear for Tarade spring : composition variations in these springs are likely dominated by other factors (see e.g. Fig. 6). No relationships between composition or temperature and rainfall regime exist for the other main springs, which are at greater distance from the dome summit.

Fig. 6: Composition and temperature anomalies in Ga spring since ~2000.

Ga spring displays a series of chemical anomalies since 2001 (top), the main one occurred from ~2009 to 2012. These anomalies (vertical dashed lines) are not correlated with rainfall regime (black continuous line) unlike the temperature variations. The main anomaly affects Cl<sup>-</sup>, Ca<sup>++</sup>, Mg<sup>++</sup> but also weakly pH, SO<sub>4</sub><sup>-</sup> or HCO<sub>3</sub><sup>-</sup>. The lower amplitude anomalies (arrows) between 2000 and 2006 affect both Cl<sup>-</sup> and SO<sub>4</sub><sup>-</sup>. See also Fig. 8b.

Fig. 7: Temperature and composition variations in fumaroles.

Fig. 7a: Variations of T, total S and CO<sub>2</sub> contents. Notice the anti-correlation between CO<sub>2</sub> and total S contents which likely corresponds to an absolute increase in S content rather than a depletion in CO<sub>2</sub> (see text for explanation).

Fig. 7b: Comparison between variations in Cl contents and temperatures of summit fumaroles and Ta spring and the precipitation regime (not to scale, inverted scale). The clear inverse correlation indicates that precipitations directly control (by dilution and with no time delay) both the composition and the ebullition temperature of hydrothermal fluids at the fumaroles.

Dome summit fumaroles: CSN, Cratère Sud Napoléon; CSC, Cratère Sud Central. Fumaroles at the base of the dome: RC, route de la Citerne.

Fig. 8 Halogens compositions of La Soufrière hydrothermal fluids

Fig. 8a: Correlations between F, Cl, Br and I. Concentrations in ppm for F, Cl and Br and in ppb for I; log scales. F contents in summit fumaroles are close to or lower than detection limits. Domains: blue: spring waters (notice the relatively high F content of BCM-EV spring); yellow: low temperature fumaroles (RC, since 1983); light red: fumaroles (T > 96°C) at the dome summit, CSC, CSN); dark red: high temperature volcanic gas of Lesser Antilles magmas (model, from Villemant and Boudon, 1998, Balcone et al., 2010). Open blue square and blue arrow: sea-water and low temperature (< magmatic T) vapours.

Fumarole gas is characterised by very low F, Br and I contents at similar Cl contents compared to high temperature volcanic gas. The Cl/Br and Cl/F ratios of fumaroles are extremely high ( $>10^5$ ), whereas the Br/I ratios are in the same range as that of spring waters and high T volcanic gas.

Fig. 8b: Cl, Br and Cl/Br time series of Ga spring; comparison with other spring waters.

Red line : Cl/Br ratio of magma and high T gas compositions (from Villemant et al. 2008) ; blue line Cl/Br ratio of sea water. The Cl enrichments related to the 1976-1977 and present day crises are characterised by the absence of Cl-Br fractionation except during the 2001-2009 period in Ga spring where Cl enrichments occur at almost constant Br content leading to extremely high Cl/Br ratios.

Fig. 9: Thermal anomaly around La Soufrière dome.

Spring waters and well temperatures as a function of the distance to the dome summit. Red dots: springs outside the Cratère Amic structure. Blue dots and coloured bars: springs inside the structure. Black line and black dotted line: Savane à Mulets (SAM) and Col de l'Echelle wells. Arrows

indicate the evolution of temperatures with time. Symbols and labels as in Fig. 1. The lower temperature inside Cratère Amic structure is interpreted as the effect of the large input of low temperature precipitations from the dome summit (see also Fig. 1a).

Fig. 10: CO-CO<sub>2</sub>-H<sub>2</sub>-H<sub>2</sub>O-CH<sub>4</sub> compositions of La Soufrière fumaroles.

Fig 10 a, b: Thermodynamic equilibrium grids are from Giggenbach (1987, Fig. 10a) and Chiodini and Marini (1998, Fig. 10 b). Fig. 10 c: evolution of CO/CO<sub>2</sub> and CO/CH<sub>4</sub> of fumaroles for the 1998-2013 period.

Red dashed lines correspond to rock buffered vapour-liquid equilibrium (FeO-FeO<sub>1.5</sub> buffer, Giggenbach, 1987), red dotted line are composition paths of vapours separated at different temperatures from liquid and equilibrated at different initial temperatures (see Chiodini and Marini, 1987). Other rock buffers: FMQ: fayalite-magnetite-quartz; NNO: nickel-nickel oxide. La Soufrière fumaroles: light blue domain summit fumaroles (CSC); blue dots refer to gas compositions with air contamination < 10% and sampling T > 98°C; yellow diamonds are 1997 fumaroles (data from Brombach et al., 2000); red triangles are highest temperature (T > 130°C) fumaroles of 1976-1977 (data from compilation of Delorme, 1983). Soufrière Hills data (Montserrat; Hammouya et al., 1998): solid square is 720°C fumarole (1996); open triangles are low temperature fumaroles. White Island fumaroles as a reference (Giggenbach et al., 1987): black dots in Fig. 10 a; ellipses of increasing intensity of grey indicate increasing sampling temperatures (< 120°C, 120-500°C; > 500°C). See text for explanations.

Fig. 11: Schematic evolution of the composition of a high temperature andesitic (HCl-rich) gas with cooling and scrubbing.

Fig. 11a: Cooling: Theoretical evolution of a volcanic gas of andesitic composition from 900°C to 100°C is characterised by the absence of significant variations in H<sub>2</sub>O, CO<sub>2</sub> and HCl contents and a conversion of SO<sub>2</sub> to H<sub>2</sub>S below 700°C.

Fig. 11b: Scrubbing: Theoretical evolution of the composition *of the gas phase* during interaction of a high temperature (900°C) andesitic gas with low temperature (20°C) water. When the gas/liquid (water) ratio is close to or exceeds 1, contents of the gas phase in soluble and reactive species (SO<sub>2</sub>, HCl, CO, H<sub>2</sub>) rapidly increase, whereas contents of other major species (H<sub>2</sub>O, H<sub>2</sub>S and CO<sub>2</sub>) do not vary significantly. If scrubbing affects a volcanic gas cooled to T < 700°C, S-bearing species are mainly represented by H<sub>2</sub>S, which is insoluble, and the total S content of the gas phase is not significantly affected by scrubbing. No SO<sub>2</sub> emission can be expected even if the gas/water ratio is very large.

Adapted from Symonds et al., 1998, 2001). Compositions in mol fractions (log units). The initial gas composition is only indicative.

Fig. 12: Halogens behaviour during evaporation of HCl-rich solutions

Fig. 12 a: Halogen acid azeotropes. Halogen acids-water mixtures behave as azeotrope with maxima. HBr and HI have close azeotrope points and similar dew and boiling curves on the diluted acid side; the azeotrope point of a HCl-H<sub>2</sub>O mixture has significantly lower temperature and HCl content (Azeotrope Data Bank, 2001). The phase diagrams predict the absence of significant Br-I fractionation and large Cl fractionation relative to other halogens in vapours in equilibrium with acid solutions. Red arrow: typical HCl-H<sub>2</sub>O composition of acid ponds (CSC or Tarissan). Boiling of such HCl-rich and ion-rich hydrothermal waters leads to acid vapours with high HCl contents and very high HCl/HBr and HCl/HF mass ratios ( $>10^5$ ) and display a rough correlation between Cl content and temperature. The relative positions of dew and boiling curves and the azeotrope maxima are strongly shifted towards higher temperatures and higher acid contents with increasing amounts of non-volatile species in solution. The red and black double arrows indicate the T and [Cl] ranges in condensates expected for pure HCl-H<sub>2</sub>O solutions and actually observed in gas condensates (see text for further explanations).

Fig. 12b: T-Cl diagram for fumarole gases of La Soufrière; comparison with azeotrope curves. Red dots: CSC fumaroles; blue dots: CSN fumaroles; diamonds: pre-1998 fumaroles (data from Brombach et al., 2000); red triangle: 1977-1978 Lacroix fumarole; black dots: Tarissan pond. Solid and dotted lines are boiling and dew curves of HCl-H<sub>2</sub>O mixtures with different contents in non-volatile ions: 1mol/L, 15 mol/L and 50 mol/L (~100g/L), at a pressure corresponding to the dome summit altitude (1465m, let - 4.8°C relative to temperatures in 1 atm experiments). Tarissan pond data fit the boiling curve of the 1mol/L solution. Fumaroles emitted between 1978 and 1998 correspond to boiling of almost pure aqueous solutions. The 1977-1978 Lacroix fumaroles and post 1998 summit fumaroles (CSC, CSN) display a large range of temperatures and HCl contents: they correspond to ebullition of more or less concentrated acid solutions by evaporation of ponds-like hydrothermal solutions. The 50 mol/L solutions would correspond to a 90% evaporated Tarissan solution.

Fig. 13: Composition time series of magmatic gaseous species in fumaroles and springs since 1976 at la Soufrière.

13a: Reconstruction of magma degassing history: comparison with seismic activity and phenomenology. Fluid compositions (gas and thermal waters) are plotted dimensionless. Time series of springs (BJ, GA, CE) are delayed by a factor depending on their distance to dome summit (see Table IV and text for explanations). Time series for summit fumaroles compositions are real time measurements: mean value for total S and maximum value for HCl for time intervals of 2 months. Seismicity (grey lines) is the total number of recorded seisms per month. Phenomenology: red circles are reactivation dates of summit fumaroles ; CS: Cratère Sud, TA: Tarissan, NA: Napoléon, G: Gouffre 1956, LS: Lacroix Supérieur, NB: Nord Breislak. Blue circles: acid ponds. Gas flux trend is deduced from Beauducel (Pers. Com.). The gas pulse (black bars) injection models (1971-1995 and 1997-present day) are both calculated to fit the Cl anomalies observed in thermal springs (CE, BJ, Ga and CC for the 1971-1999 period -Villemant et al., 2005- and Ga spring since 1997 – Fig. 14 and Supplementary Material). The advection-dispersion model and the input parameters used are described in the text and in more detail in Villemant et al. (2005). The dashed black bars correspond to poorly constrained calculations (pre-1974). Unfortunately no high-resolution geochemical data exist for the pre-1976 period and the 1976-1977 volcanic crisis. Red bars: S-bearing gas pulse time series calculated from the previous model (see text for explanations).

13b: Chemical signatures of magmatic gaseous species ( $\text{CO}_2$ ,  $\text{SO}_2$ , HCl) in fumaroles and thermal springs for the 1976-1977 and current crises. Fumaroles: total S (dry composition) and HCl. Springs:  $\text{Cl}^-$ ,  $\text{HCO}_3^-$  and  $\text{SO}_4^{2-}$  (as proxies of HCl,  $\text{CO}_2$  and  $\text{SO}_2$  scrubbing respectively). For the 1976-1977 crisis complete composition time series are available only for the nearest spring to the dome (CE). For the current crisis total S and HCl time series are measured in the summit fumaroles; imprints of gas species in aquifers (Ga spring) are significant only for the most soluble gas species (HCl and sometimes  $\text{SO}_2$  expressed as  $\text{Cl}^-$  and  $\text{SO}_4^{2-}$ ). In addition this signal is altered by the long transportation time for Ga spring water ( $\sim 2$  y delay) within the edifice (see Fig. 14a). The geochemical records display contrasting features for proxies of the poorly soluble (S-species and  $\text{CO}_2$ ) and highly soluble (HCl) gas species for both fumaroles and proximal springs). For a given volcanic degassing activity  $\text{CO}_2$  and  $\text{SO}_2$  proxies display long-term buffered-like variations and the HCl proxy displays pulsatory variations. This reflects the difference in solubility thresholds of  $\text{SO}_2$ ,  $\text{CO}_2$ , HCl (and  $\text{H}_2\text{O}$ ) in melts, the composition of magma sources, and the degassing mechanisms at depth (see text for further explanation).

The evolution of the composition of the summit fumaroles and Ga spring show significant differences for Cl- and S- bearing species: the first period corresponds to influx of HCl- and  $\text{SO}_2$ -rich magmatic gas, followed by a higher flux of magmatic gas less rich in HCl but initially enriched

in SO<sub>2</sub>; this gas however has suffered enough cooling to convert most SO<sub>2</sub> to insoluble H<sub>2</sub>S. This evolution suggests an increasing contribution from deep basic andesite magma and complete degassing of the acid andesitic magma source (through freezing or nearly complete crystallisation). This situation may be compared to the present day situation at Soufrière Hills where gas flux of deep origin (SO<sub>2</sub> bearing gas from basic magmas) is more or less steady since the beginning of the eruption and likely controlled by the fracturing induced by the magmatic activity, whereas HCl productions is related to a dacitic magma

Fig. 14: Modeling gas pulses based on Cl-time series in Ga spring and total S time series in CSC summit fumaroles.

14a: Gas pulses (dates and relative amplitudes) contaminating Ga spring between 1979 and 2013 are fitted to Cl-time series using the advection dispersion model developed by Villemant et al. (2005): 1979-1994 (Villemant et al., 2005), 1994-2013 (this work, see Supplementary material). Model parameters: time delay (transfer duration): ~27 months; flow: 140 l/mn; indicative path length (flow distance) within the aquifer: ~650 m (estimation using a normalised flow rate of 10<sup>-5</sup> ms<sup>-1</sup>). Residues are within analytical errors for most measurement points. See Villemant et al. (2005) and Boichu et al. (2011) for further explanations of the model.

14b: Gas pulse (total S content) time-series in CSC fumarole since 1994 calculated from the previous model. The model uses the same advection-dispersion formalism as for Cl time-series and the same pulse injection dates, but it is assumed that transfer time for gas pulses is negligible compared to those for Cl within Ga aquifer and that, in contrast, dispersion is much larger (and set arbitrarily 3 times higher). Only relative amplitudes are chosen for the fit of the total-S time series. Residues are low and within analytical errors. See text for further explanations.

14c: Model time-series of degassing pulses: comparison of calculated relative intensities in the production of HCl (from Cl measurements in Ga spring) and of total S in CSC fumarole.

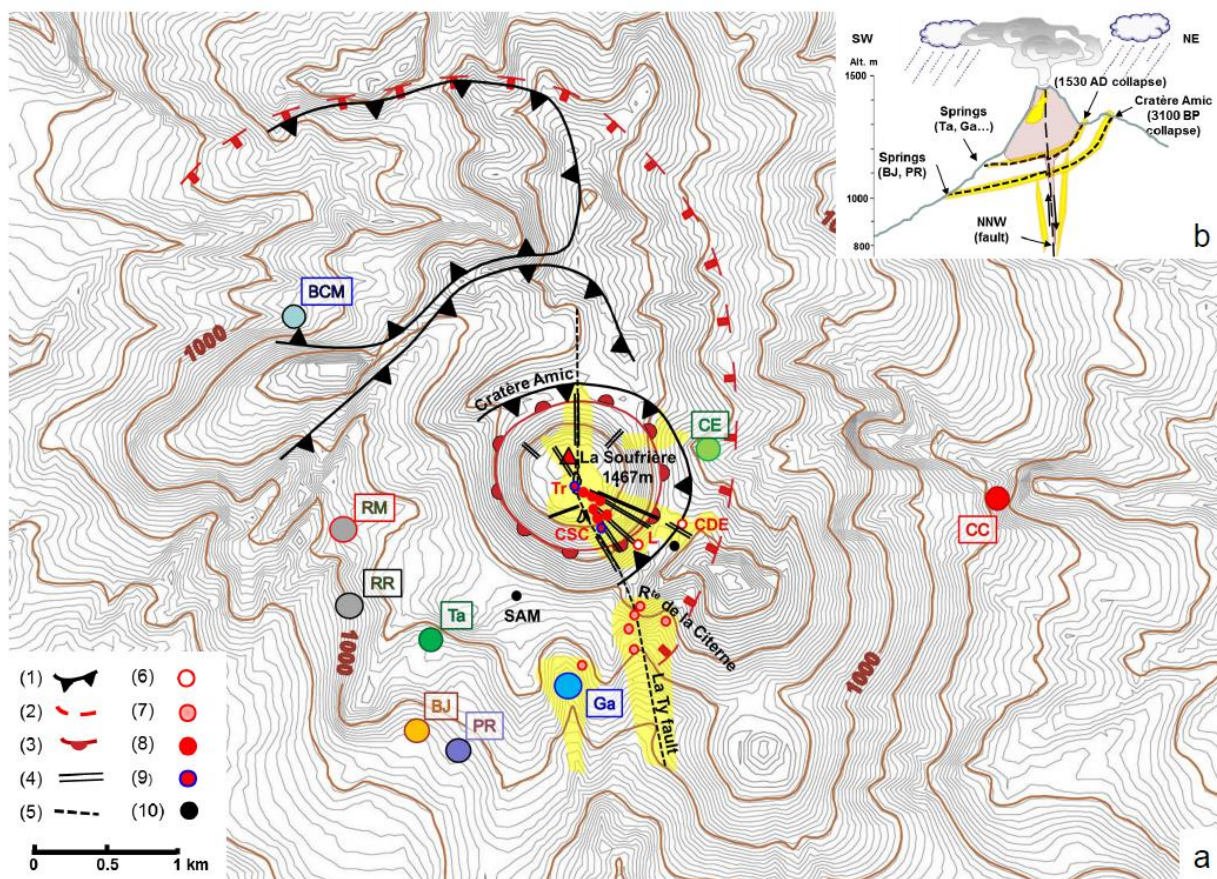
Fig. 15: Evolution of the shallow magmatic and hydrothermal systems of La Soufrière of Guadeloupe, since the seismo-volcanic crisis of 1976-1977.

La Soufrière Dome (brown) was emplaced during the 1530 AD eruption in a nested structure of flank collapse (3100 BP, 1530 AD) defining the Cratère Amic, which contains a low volume hydrothermal system. The rainfall regime strongly affects the composition and temperature of this system, which is only episodically modified by the volcanic activity. However, a more or less permanent CO<sub>2</sub> flux is generated by the deep magmatic system

1976-1977: During the seismo-volcanic crisis of 1976-1977 and perhaps slightly earlier, a magma intrusion was emplaced at shallow depth (~3 km?) and the volcanic feeder system was strongly fractured. The crisis produced strong gas emissions and a few phreatic explosions which ended in 1977.

1978-1992: The fumarolic activity generated by the volcanic crisis rapidly decreased and almost completely vanished in ~1981. Further degassing of the shallow magma intrusion produced a series of volcanic gas pulses over a long time period. These gas pulses were almost completely scrubbed by the hydrothermal system. This activity also led to sealing of the feeding conduit by hydrothermal alteration.

1993 - present day: At the end of 1992 a new seismic crisis occurred, likely corresponding to emplacement of a new magma intrusion (smaller than in 1976-1977). Degassing through a highly confined system led to a highly evolved gas plume and contamination of the shallow hydrothermal system observed at a single spring (Ga). This unrest may lead to phreatic explosions and flank collapse hazards, as a consequence of over pressurisation of a strongly sealed system by active hydrothermal alteration.

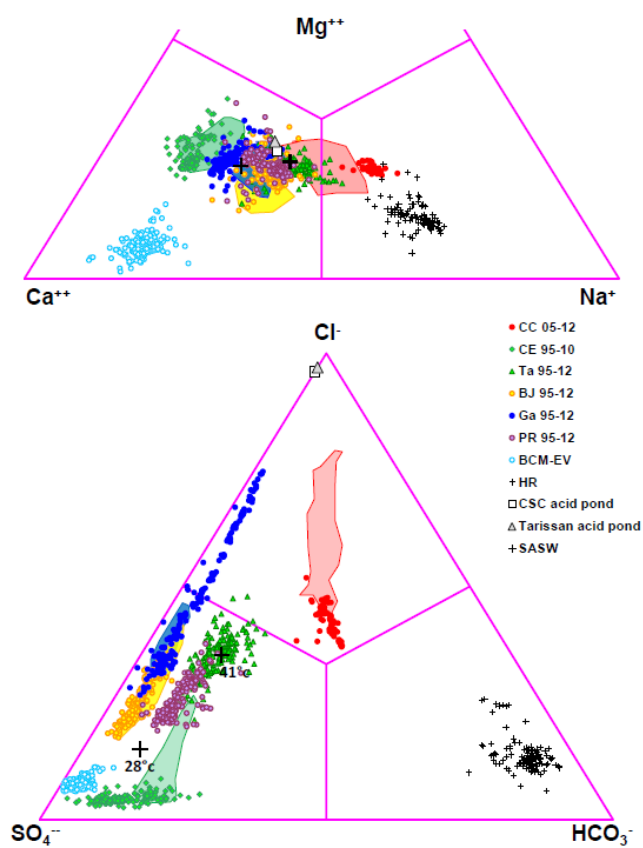


31/03/2014

Fig. 1

ACCEPTED

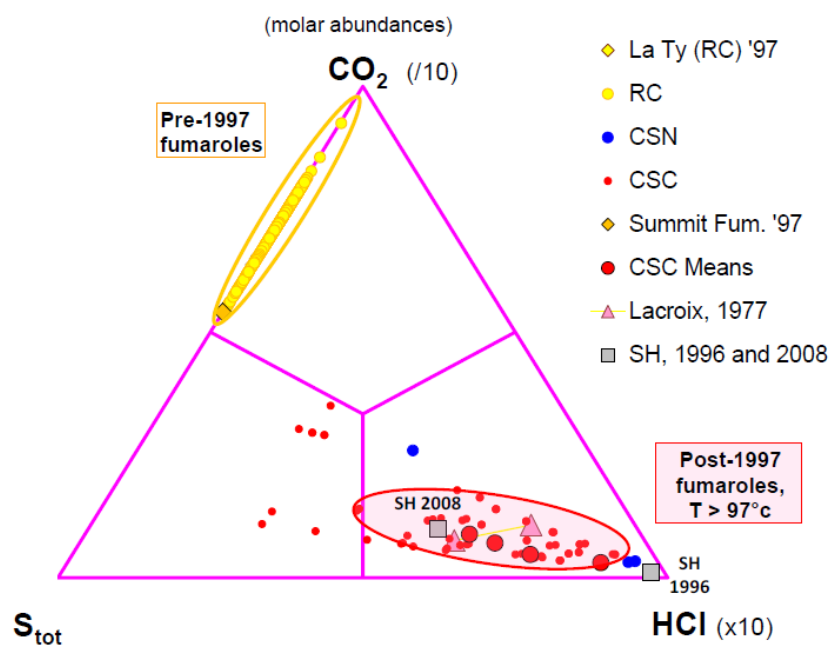
Fig. 2



31/03/2014

ACCEP

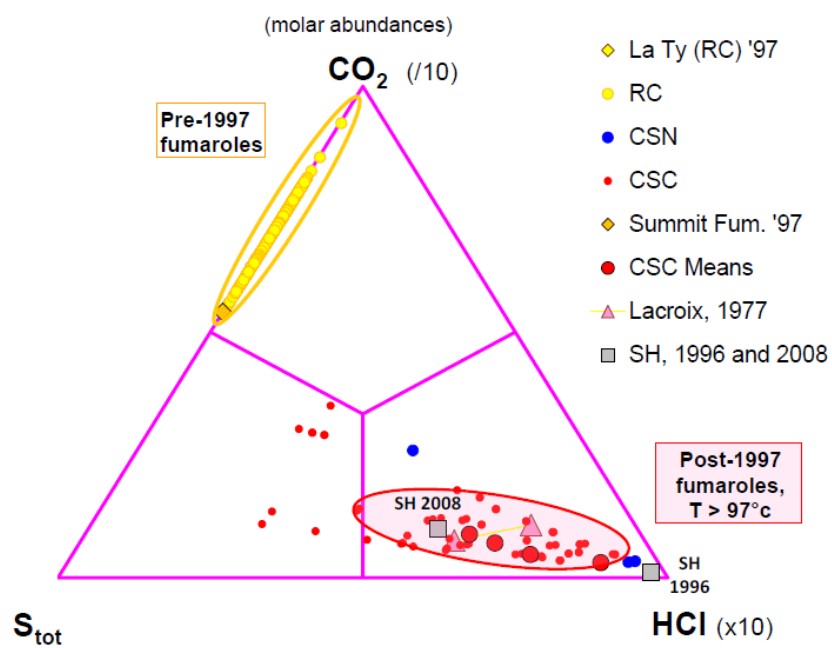
Fig. 3



31/03/2014

ACCEPTED

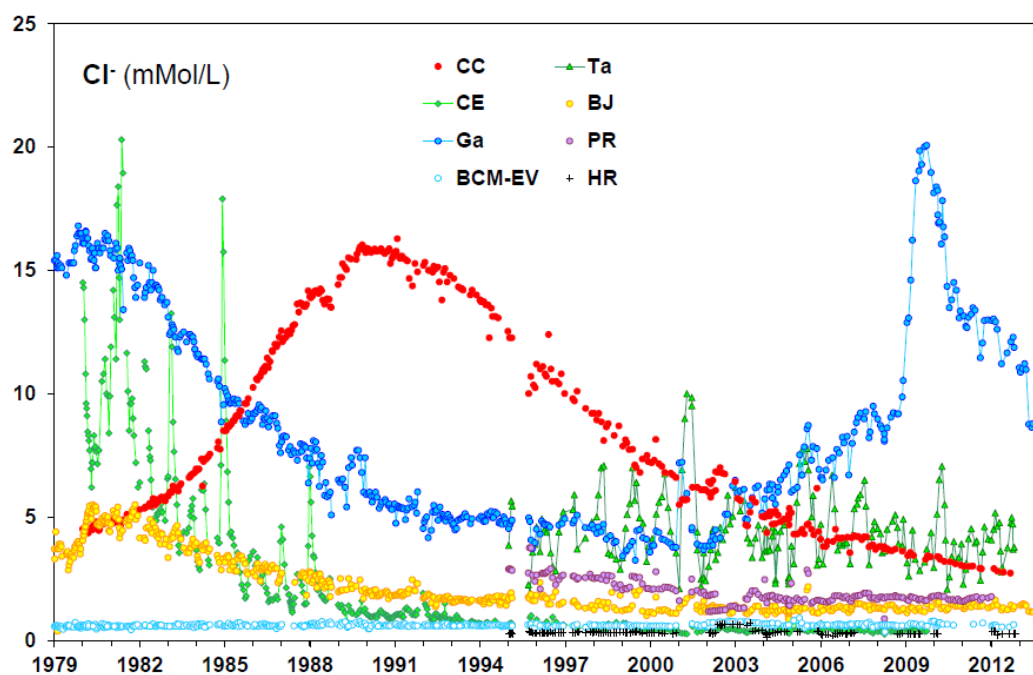
Fig. 3



31/03/2014

ACCEPTED

Fig. 4 a



31/03/2014

ACCEPTED

Fig. 4b

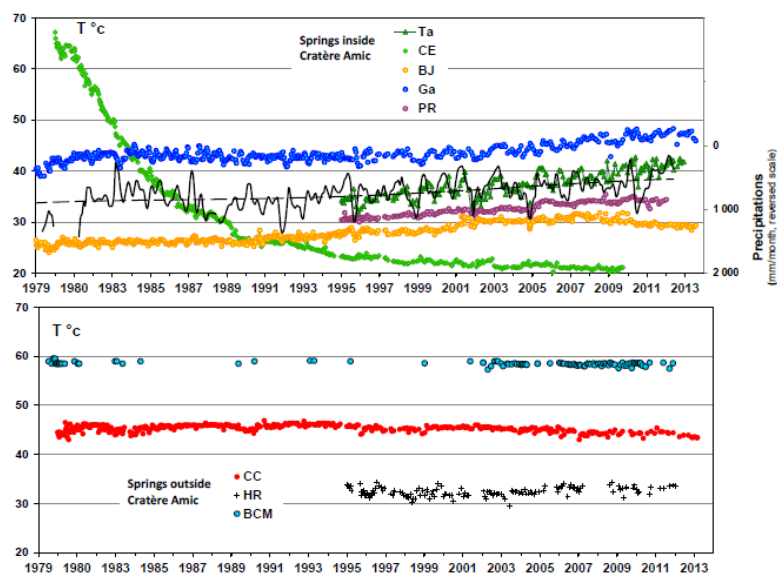


Fig. 4c

31/03/2014

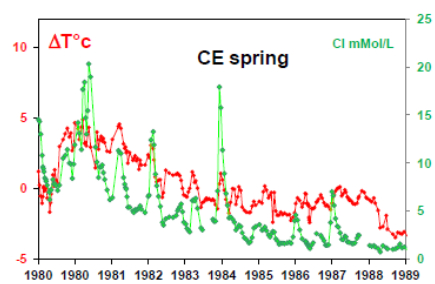
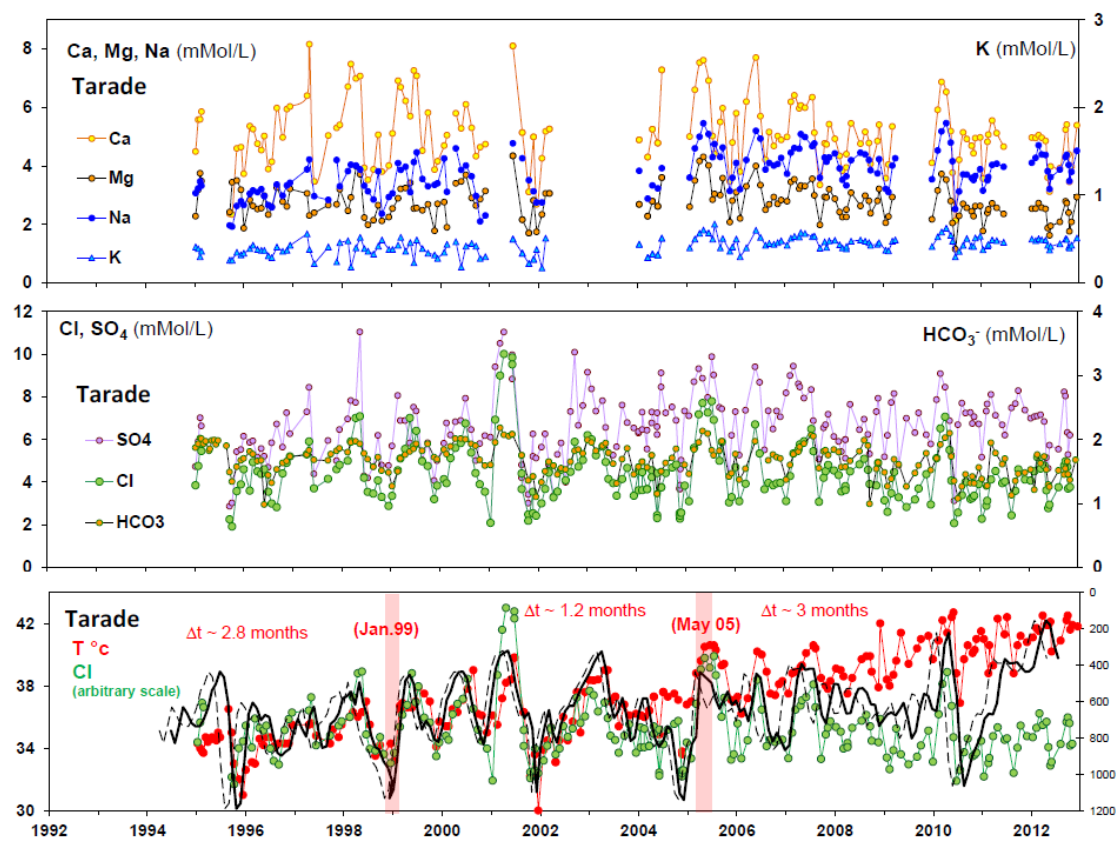


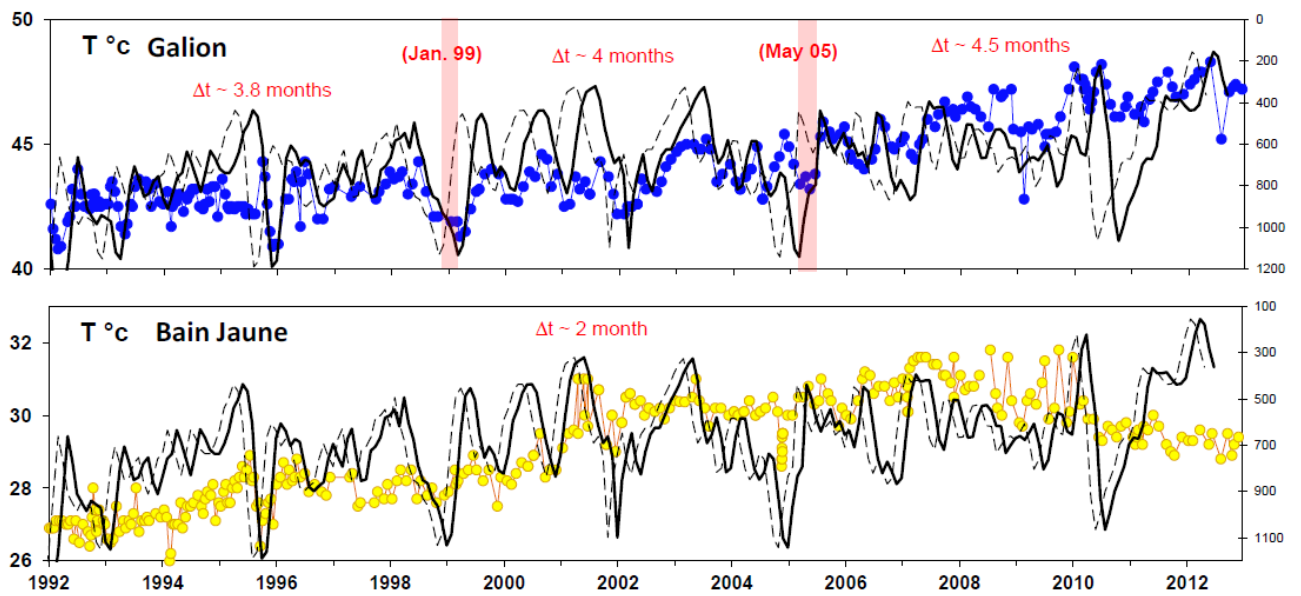
Fig. 5a



31/03/2014

ACCEPTED

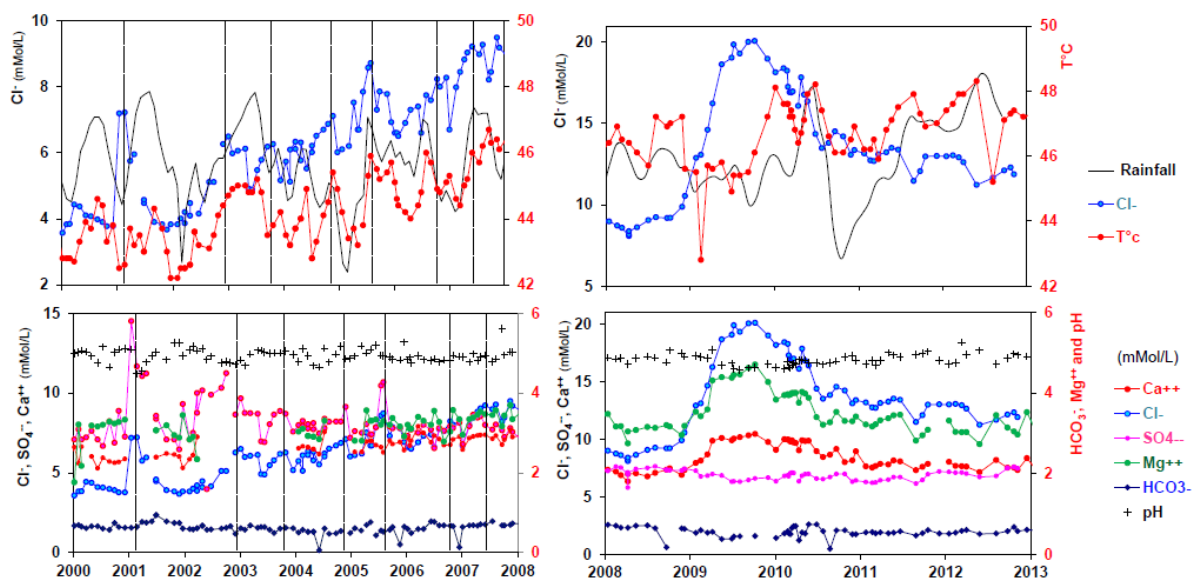
Fig. 5b



31/03/2014

ACCEP

Fig. 6



31/03/2014

ACCEPTED

31/03/2014

Fig. 7a

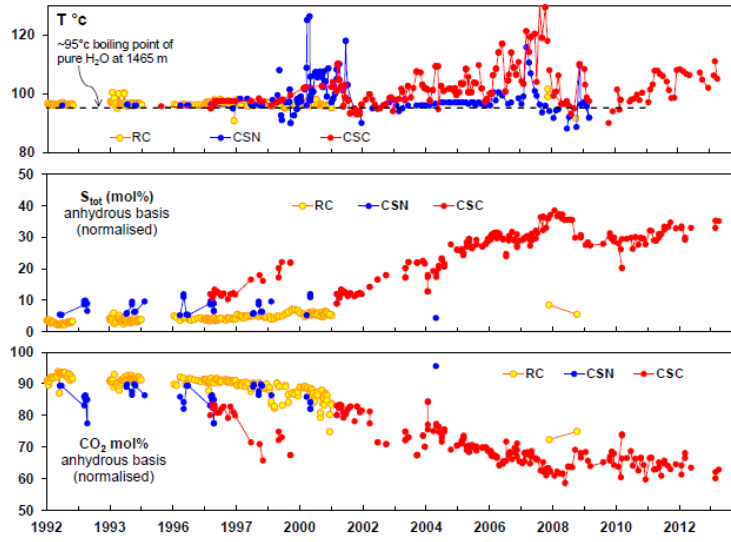
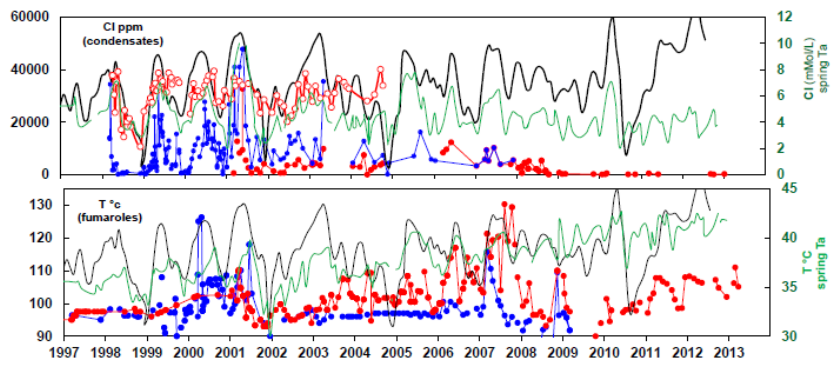


Fig. 7b



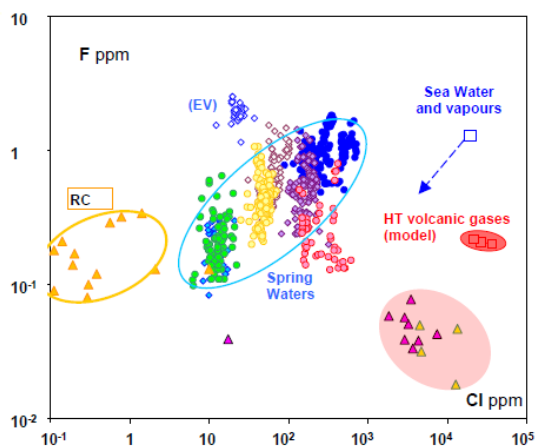
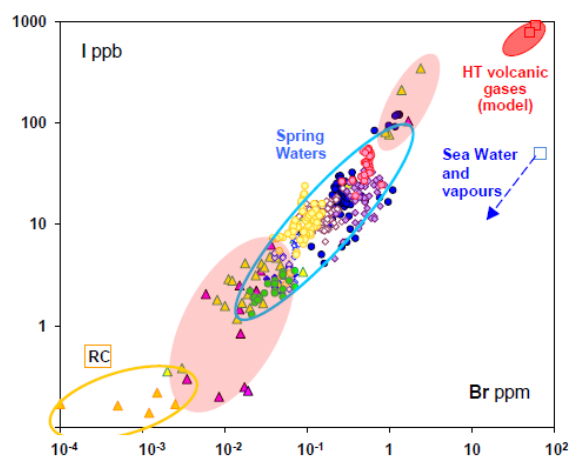
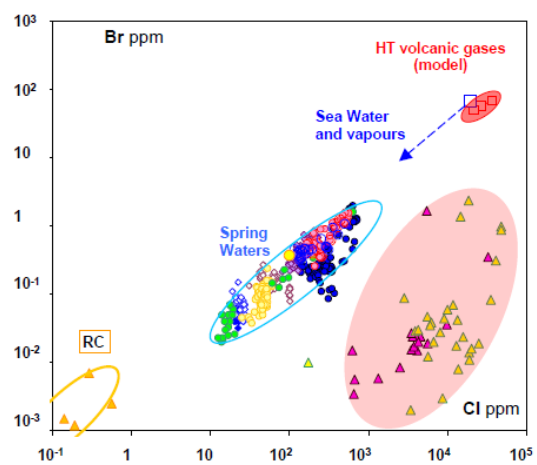


Fig. 8a

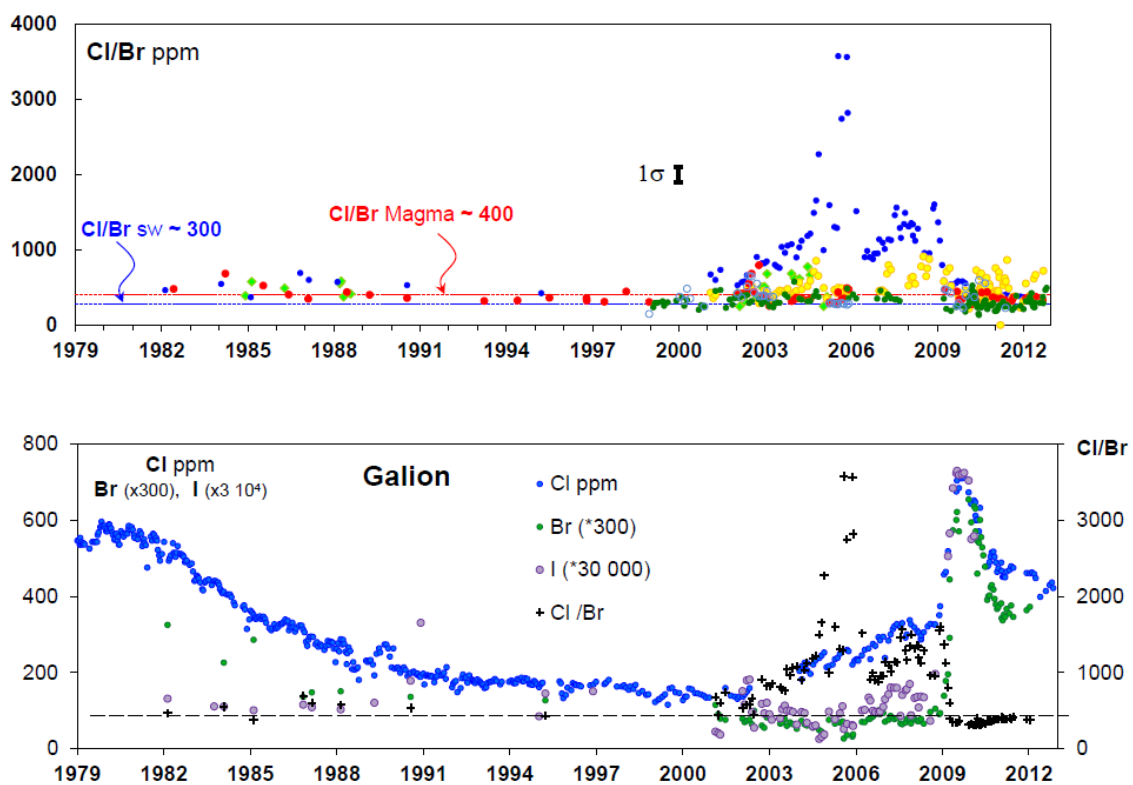
31/03/2014



ACCEPTED

Fig. 8b

31/03/2014



ACCEPTED

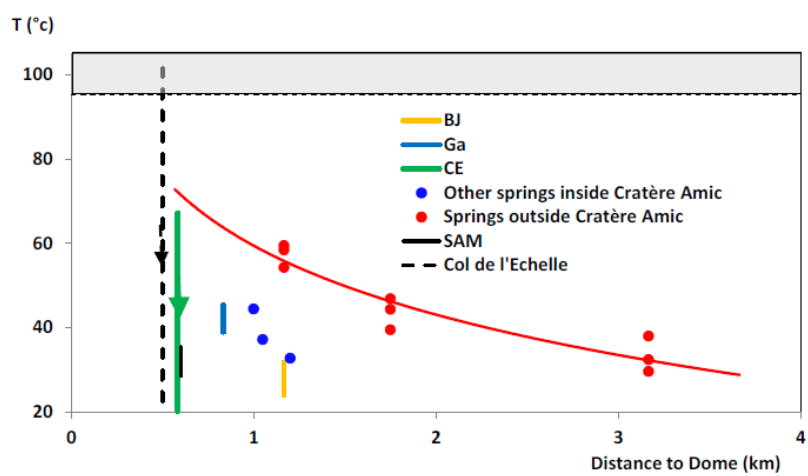


Fig. 9

ACCEP

Fig. 10a

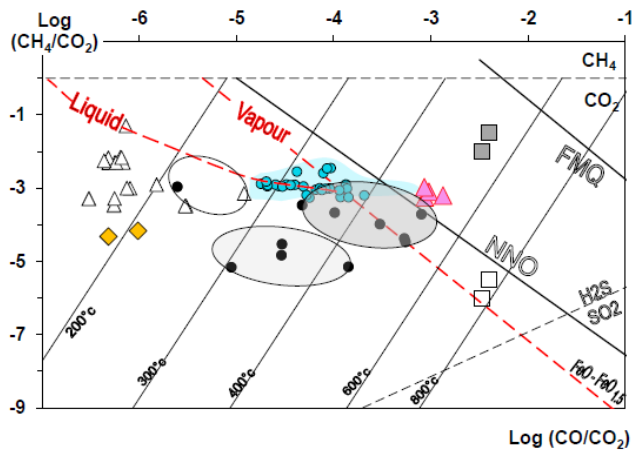


Fig. 10b

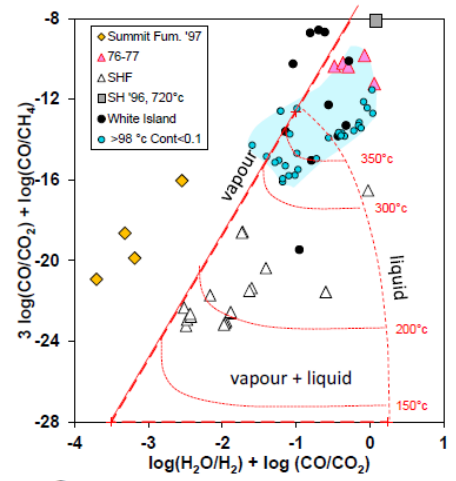
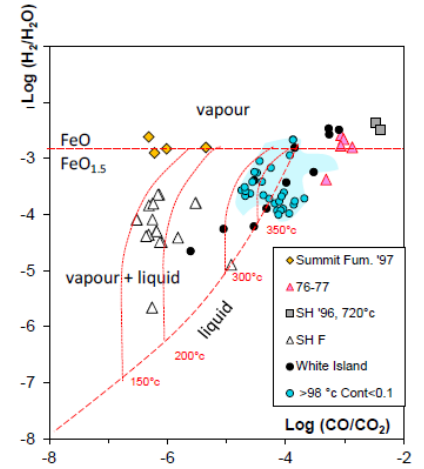
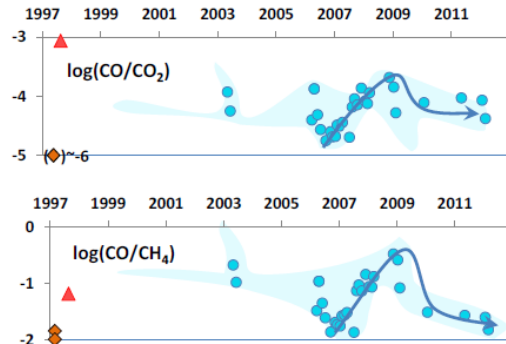


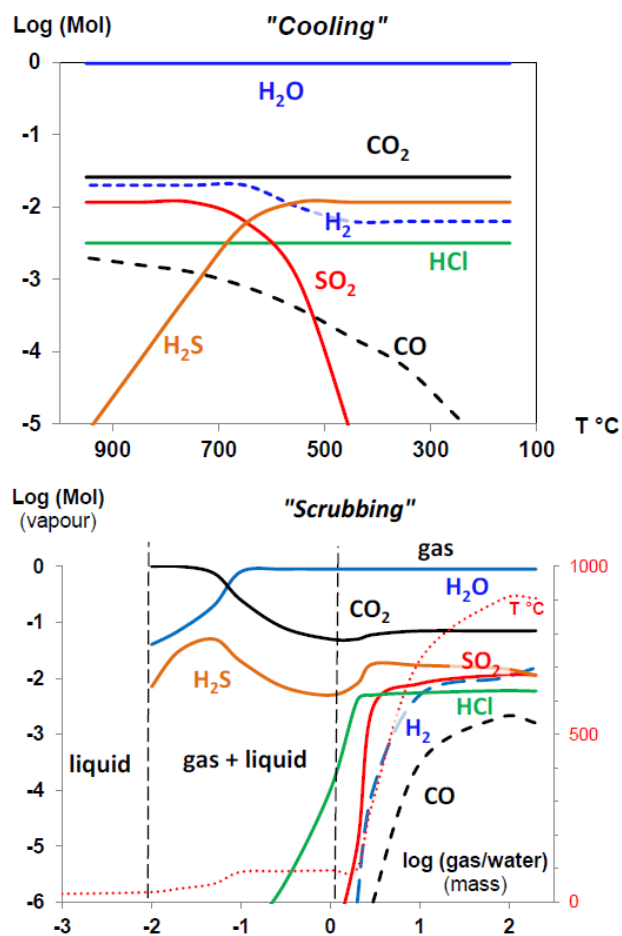
Fig. 10c



31/03/2014

ACCEPTED MANUSCRIPT

Fig. 11

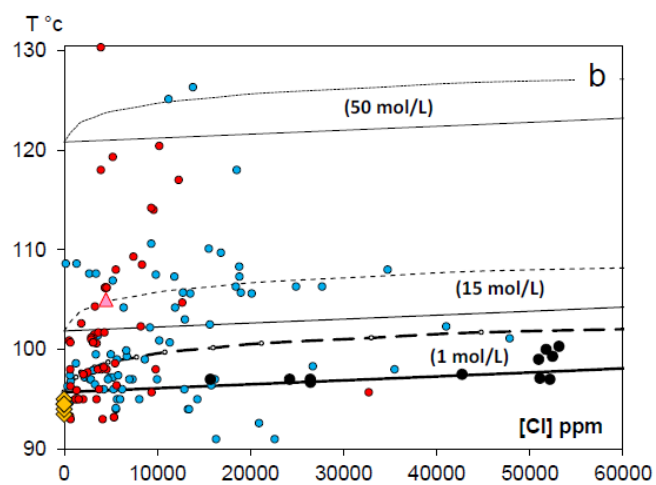
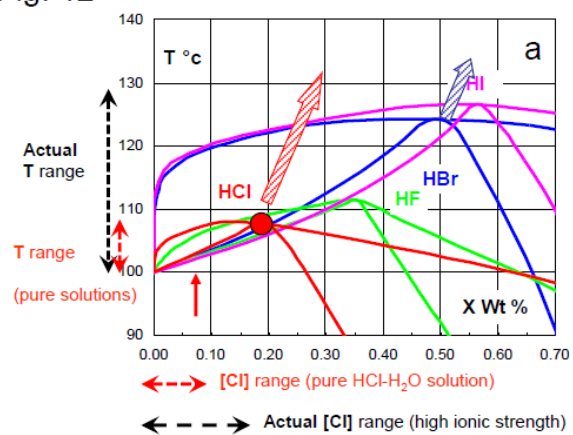


31/03/2014

ACCEPTED

Fig. 12

31/03/2014



ACCEPTED

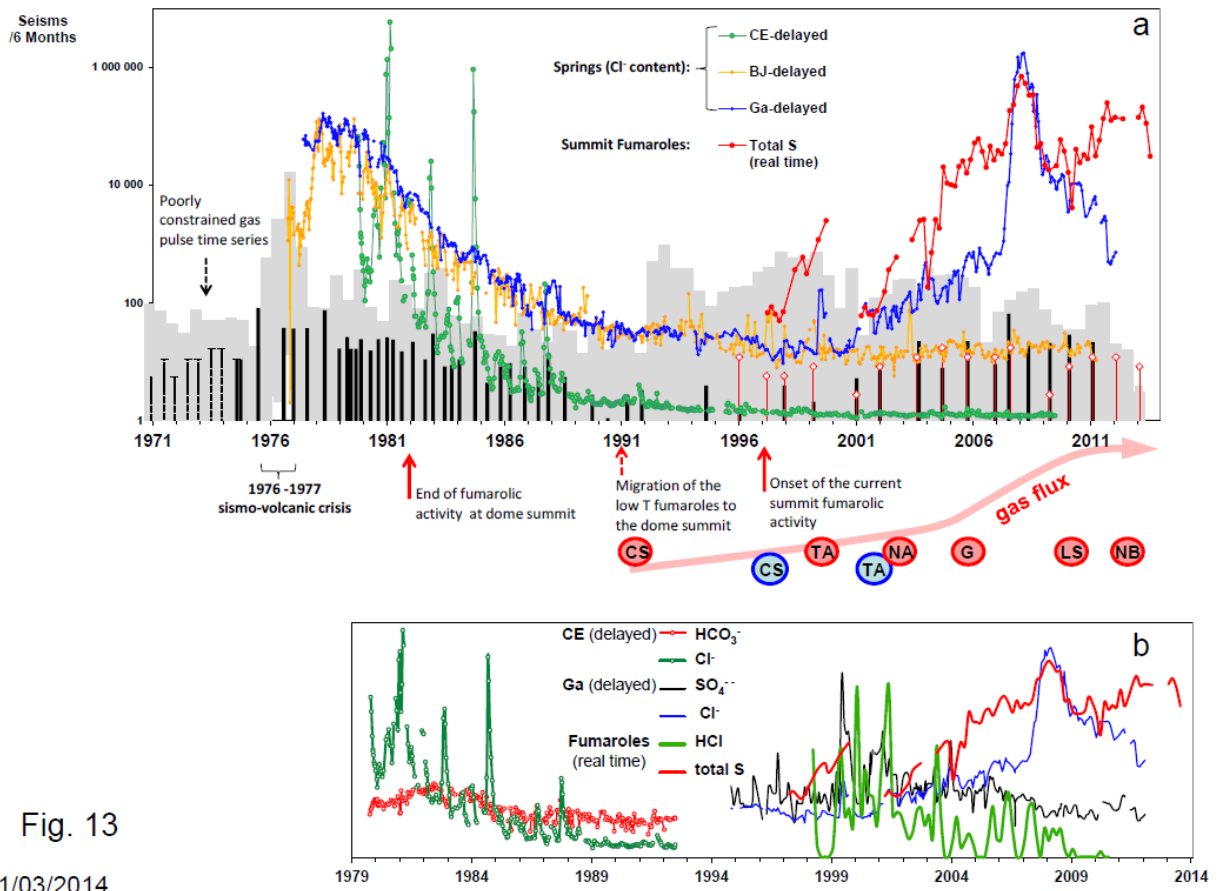
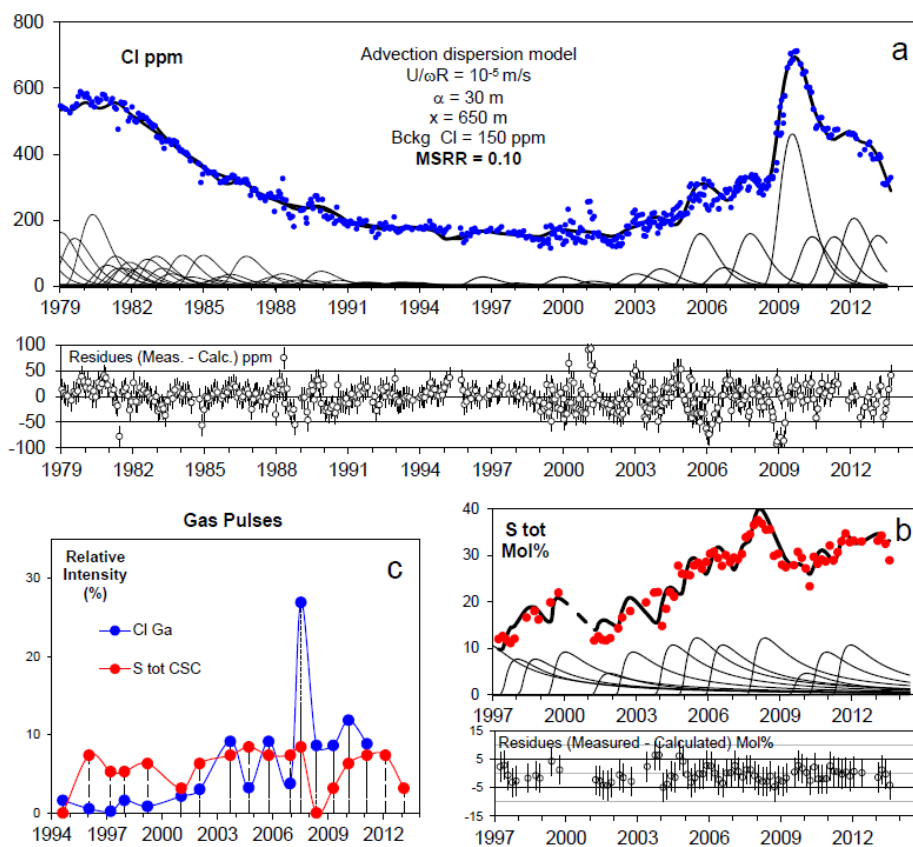


Fig. 13

31/03/2014

ACCEPTED

Fig. 14



31/03/2014

ACCEPTED

Fig. 15

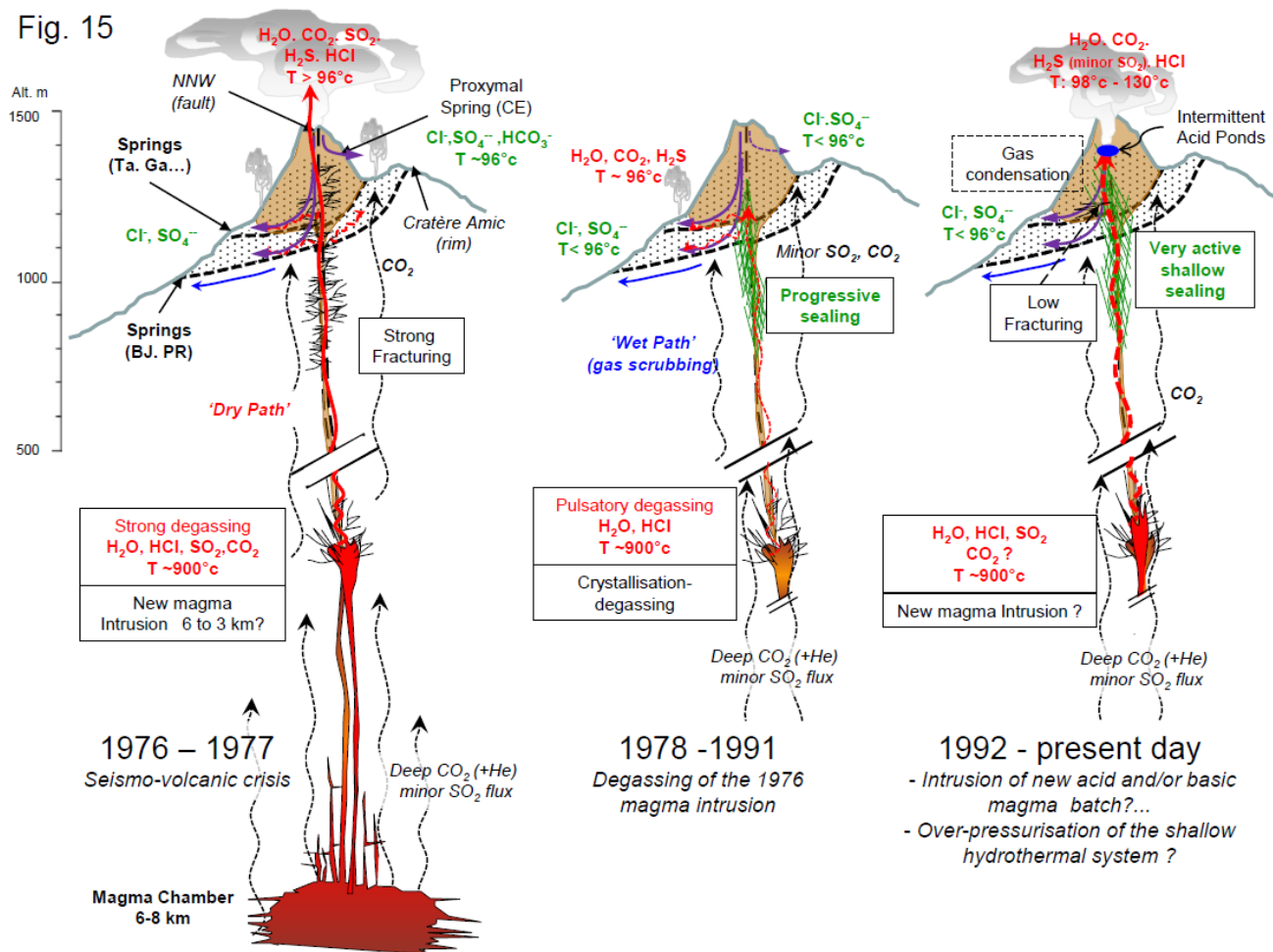


Table 1 a

Tab. la: springs		Composition (mMol/L)											
Spring	Regime (dates)	flow rate /l/m	Conductivity (µS)	T (°C)	pH	Na+	K+	Mg++	Ca++	F-	Cl-	SO4--	HCO3-
<b>Bains Jumeaux</b>													
<b>BJ 1979-1995</b>													
n=411	m	n.d.	n.d.	26.3	5.0	1.7	0.2	1.4	3.1	0.018	3.1	4.7	0.2
	σ			0.8	0.2	0.1	0.0	0.4	0.8	0.003	1.2	1.5	0.1
	Max			28.9	5.6	2.4	0.3	0.4	0.6	0.03	5.5	9.9	0.6
	min			24.0	4.5	1.3	0.0	0.1	2.4	0.01	0.4	3.1	0.1
<b>BJ 1995-2012</b>													
n=228	m	164	884	28.7	5.3	1.6	0.2	1.2	2.6	0.02	1.3	3.8	0.2
	σ	85	108	1.1	0.2	0.2	0.1	0.3	0.4	0.00	0.2	0.8	0.1
	Max	600	1105	31.8	6.1	2.5	0.5	2.1	3.8	0.04	2.3	7.9	0.4
	min	87	494	27.5	4.7	1.1	0.0	0.7	1.8	0.01	0.9	2.5	0.1
<b>Pas du Roy</b>													
<b>PR 1995-2012</b>													
n=222	m	30	1184	32.4	5.7	2.3	0.2	1.9	3.7	0.03	1.9	4.9	0.9
	σ	21	149	1.3	0.1	0.3	0.1	0.3	0.4	0.01	0.5	0.7	0.1
	Max	116	1575	35.4	6.4	3.3	0.8	3.6	4.6	0.05	3.8	8.7	1.7
	min	4	641	30.0	5.3	1.3	0.1	1.3	2.7	0.01	0.9	2.9	0.4
<b>Ravine Marchand</b>													
<b>RM 2000-2012</b>													
n=34	m	25.4	1365	44.5	5.4	2.1	0.4	1.6	3.7	0.02	1.7	5.4	1.2
	σ	14.3	290	1.9	0.2	0.3	0.1	0.2	0.7	0.01	0.6	1.1	0.2
	Max	62.4	1855	48.4	6.1	3.1	0.8	2.5	6.6	0.03	2.7	9.6	1.9
	min	8.9	925	42.0	4.8	1.7	0.3	1.3	3.1	0.01	0.8	4.5	0.6
<b>Tanda</b>													
<b>Ta 1995-2012</b>													
n=218	m	66.6	1811	37.4	6.0	3.8	0.4	2.8	5.1	0.02	4.4	6.6	1.7
	σ	46.4	409	2.7	0.2	0.7	0.1	0.6	1.2	0.01	1.4	1.5	0.2
	Max	154.8	3350	42.7	6.6	5.5	0.7	4.3	8.2	0.05	10.0	11.0	2.2
	min	0.2	922	30.0	5.5	1.9	0.2	1.2	2.1	0.01	1.9	2.9	1.0
<b>Gallon</b>													
<b>Ga 1979-1995</b>													
n=368	m	7.8	n.d.	42.6	4.7	3.4	0.5	3.4	6.0	0.03	9.7	8.6	0.3
	σ	1.9		1.0	0.2	0.4	0.1	0.4	0.4	0.00	4.3	0.6	0.1
	Max	11.1		45.2	5.8	4.4	0.9	5.0	7.2	0.04	16.9	9.6	0.9
	min	5.6		38.0	3.9	2.4	0.3	2.9	5.2	0.01	3.7	6.5	0.0
<b>Ga 1995-2004</b>													
n=101	m	112	1758	43.4	4.9	2.8	0.4	3.0	6.0	0.04	4.9	8.1	0.6
	σ	10	361	0.9	0.2	0.4	0.1	0.4	0.5	0.01	1.0	1.4	0.1
	Max	140	2630	45.4	5.3	3.7	0.8	3.8	7.6	0.06	7.2	14.5	0.9
	min	88	1055	41.0	4.5	2.1	0.1	1.8	4.4	0.03	3.2	4.0	0.1
<b>Ga 2005-2012</b>													
n=125	m	138	3147	45.3	4.8	3.1	0.5	3.4	7.8	0.05	11.6	6.9	0.5
	σ	21	750	2.0	0.2	0.4	0.1	0.4	1.2	0.01	3.8	0.9	0.2
	Max	183	4630	48.3	5.6	4.4	0.8	4.7	10.4	0.08	20.1	10.7	0.8
	min	103	1088	38.8	4.6	2.5	0.4	2.6	5.4	0.03	5.4	4.6	0.1
<b>Carbet Echelle</b>													
<b>CE 1979-1995</b>													
n=360	m	n.d.	n.d.	37.3	5.7	2.5	0.2	3.6	6.5	n.d.	4.0	11.3	2.9
	σ			1.2	0.2	0.4	0.1	0.5	0.8		4.0	1.4	0.3
	Max			39.2	6.5	5.8	0.5	5.8	9.3		20.3	15.9	4.7
	min			22.7	5.3	1.1	0.0	2.5	5.0		0.5	7.4	1.2
<b>CE 1995-2009 (*)</b>													
n=151	m	7.1	1374	21.7	5.5	1.4	0.2	2.4	5.3	0.009	0.5	8.5	1.3
	σ	5.9	246	0.8	0.1	0.2	0.1	0.6	0.8	0.005	0.1	1.3	0.4
	Max	25.5	2330	23.9	6.0	2.1	0.5	3.6	8.3	0.023	0.9	12.4	2.4
	min	0.1	751	20.2	5.1	1.0	0.1	1.4	4.0	0.001	0.2	4.5	0.3
<b>Chute du Carbet</b>													
<b>CC 1979-2004</b>													
n=387	m	n.d.	1381	45.4	6.6	4.3	0.6	3.0	4.1	0.005	9.5	2.5	2.2
	σ		226	0.6	0.2	0.4	0.1	0.6	0.9	0.002	4.6	0.4	0.1
	Max		1960	46.9	7.3	5.3	0.8	4.3	6.9	0.02	16.3	4.2	2.8
	min		880	43.0	6.2	3.0	0.3	1.8	2.5	0.002	4.3	1.7	1.8
<b>CC 2005-2012</b>													
n=70	m	n.d.	1406	44.4	6.5	3.4	0.5	1.6	2.2	0.010	3.8	2.5	2.5
	σ		155	0.6	0.2	0.3	0.0	0.2	0.3	0.002	0.6	0.3	0.1
	Max		1700	45.6	7.0	3.9	0.7	2.0	3.0	0.02	6.2	3.6	2.7
	min		1057	43.0	5.9	2.7	0.4	1.3	1.7	0.01	2.7	2.1	2.1
<b>Bain Chaud du Matouba (s.s.)</b>													
<b>BCM 1979-2012</b>													
n=158	m	121	1811	57.5	5.8	1.5	0.2	0.5	6.7	0.10	0.6	7.3	0.3
	σ	14	420	2.4	0.2	0.2	0.1	0.1	0.8	0.01	0.1	0.7	0.1
	Max	2405	59.5	6.5	2.2	0.5	1.2	13.6	0.12	0.9	10.0	0.7	0.7
	min	1028	50.0	5.1	0.8	0.1	0.3	6.0	0.06	0.3	4.9	0.0	0.0
<b>Habitation Revet</b>													
<b>HR 1995-2012</b>													
n=151	m	60	288	32.4	6.6	1.1	0.1	0.2	0.5	0.005	0.3	0.2	1.8
	σ	55	58	0.9	0.2	0.1	0.1	0.1	0.1	0.004	0.1	0.1	0.1
	Max	247	459	34.4	7.2	1.4	0.6	0.5	0.7	0.020	0.7	0.5	2.2
	min	3	155	28.6	6.1	0.7	0.0	0.1	0.3	0.000	0.1	0.1	1.2

(\*) not sampled since 2010

Table I b

Tab 1b: Cratère Sud : fumaroles condensates and acid pond			Composition (mMol/L)									
			T (°c)	pH	Na <sup>+</sup>	K <sup>+</sup>	Mg <sup>++</sup>	Ca <sup>++</sup>	F <sup>-</sup>	Cl <sup>-</sup>	SO <sub>4</sub> <sup>-</sup>	HCO <sub>3</sub> <sup>-</sup>
Fumaroles condensates (1998-2009)												
CSC	m		102	1.32	n.d.	n.d.	n.d.	n.d.	<l.d.	142	1	n.d.
n= 285	σ		7	0.70						128	1	
	Max		130	4.30						921	6	
	min		90	0.50						0.5	0.1	
CSN	m		104	1.0	n.d.	n.d.	n.d.	n.d.	< l.d.	261	1.1	n.d.
n= 210	σ		11	0.6						260	1.8	
	Max		140	3.6						1329	7.9	
	min		90	0.1						3	0.0	
Acid pond:												
Cratère Sud Central	10/07/2007		n.d.	n.d.	0.15	0.04	0.14	0.23	< l.d.	246	10.02	n.d.

ACCEPTED MANUSCRIPT

Table II

	Nb Val	T (°C)	pH	Concentrations (Mol %) Anhydrous basis											Total	Total S	Total C
				H <sub>2</sub>	He	CO	CH <sub>4</sub>	N <sub>2</sub>	H <sub>2</sub> S	HCl	Ar	CO <sub>2</sub>	SO <sub>2</sub>	O <sub>2</sub>			
<b>CSC fumarole (1997-2012)</b>																	
Mean		105.2	1.5	0.7	b.d.l.	0.006	0.08	-	29.1	4.5	0.3	64.5	0.4	0.4	100.0	29.5	64.5
	92	9.5	0.8	1.1		0.009	0.05		5.0	6.4	0.5	4.6	0.3	0.2			
T < 98°C		95.1	2.1	0.5	b.d.l.	0.011	0.08	-	28.6	4.1	0.8	64.8	0.42	0.7	100.0	29.1	64.8
	20	2.3	1.2	0.6		0.015	0.05		6.0	8.9	1.0	5.5	0.3	-			
T ≥ 98°C		108.7	1.3	0.8	b.d.l.	0.005	0.08	-	29.0	5.2	0.2	64.0	0.42	0.3	100.0	29.4	64.0
	57	9.5	0.7	1.1		0.009	0.05		5.0	4.9	0.5	4.6	0.3	0.2			
14-08 & 18-10 2007 (T max)	2	129.9	~ 0.7	0.2	0.018	0.004	0.05	1.68	31.8	9.1	0.1	56.6	0.46	-	100.0	32.2	56.6
<b>Lacroix Sup. Fumarole (1977)<sup>§</sup></b>				3.2	n.d.	0.07	0.04	1.04	13.2	4.7	n.d.	67.4	10.4	n.d.	100.0	23.6	67.5
<b>Lacroix Inf. Fumarole (1978)<sup>§</sup></b>				1.6	n.d.	0.06	0.05	1.2	19.8	b.d.l.	n.d.	68.7	8.6	n.d.	100.0	28.4	68.8
	20	20.4		0.8		0.03	0.05	0.7	6.1			7.4	5.7				
<b>RC fumaroles (1983-2012)</b>																	
Mean		96.4	4.1	9.7	b.d.l.	b.d.l.	0.01	2.6	3.7	b.d.l.		91.6	0.5	0.3		4.2	91.6
	700	0.8	0.4	21.6			0.02	4.5	1.0			2.8	0.1	0.6			
Summit Fumarole (1997)*		93.5	n.d.	5.2	n.d.	0.0004	b.d.l.	0.9**	7.3	b.d.l.	n.d.	86.5	b.d.l.	**	99.1	7.3	86.5

ACCEPTED MANUSCRIPT

Tab IIIa: Springs

Spring Names dates	F ppm	Cl ppm	Br ppm	I ppb	Cl/Br	Br/I
<b>Bains Jaunes</b> <b>1979-1995</b>	<b>m</b> <b>0.3</b>	<b>109</b>	n.d.	n.d.	-	-
	$\sigma$ 0.1	43				
	Max 0.5	195				
	min 0.2	48				
	<i>n</i> = 234	<i>n</i> = 342				
<b>1996-2012</b>	<b>m</b> <b>0.4</b>	<b>49</b>	<b>0.17</b>	<b>10.2</b>	<b>528</b>	<b>9.7</b>
	$\sigma$ 0.2	7	0.05	4.2	157	3.5
	Max 1.1	83	0.28	24.0	<i>n</i> = 60	<i>n</i> = 61
	min 0.2	30	0.10	2.6		
	<i>n</i> = 144	<i>n</i> = 186	<i>n</i> = 24	<i>n</i> = 62		
<b>Pas du Roy</b> <b>1995-2012</b>	<b>m</b> <b>0.7</b>	<b>71</b>	<b>0.17</b>	<b>12.5</b>	<b>439</b>	<b>14</b>
	$\sigma$ 0.2	18	0.04	3.1	250	4
	Max 1.6	133	0.27	22.6	<i>n</i> = 47	<i>n</i> = 49
	min 0.3	41	0.08	6.8		
	<i>n</i> = 131	<i>n</i> = 178	<i>n</i> = 49	<i>n</i> = 49		
<b>Tarade</b> <b>1995-2012</b>	<b>m</b> <b>0.5</b>	<b>160</b>	<b>0.50</b>	<b>20</b>	<b>341</b>	<b>28</b>
	$\sigma$ 0.2	46	0.15	8	70	12
	Max 1.2	357	0.86	39	<i>n</i> = 58	<i>n</i> = 44
	min 0.2	68	0.21	4.6		
	<i>n</i> = 138	<i>n</i> = 192	<i>n</i> = 58	<i>n</i> = 45		
<b>Galion</b> <b>1979-1995</b>	<b>m</b> <b>0.6</b>	<b>345</b>	<b>0.64</b>	<b>22.7</b>	<b>526</b>	<b>33</b>
	$\sigma$ 0.1	151	0.26	10.9	103	15
	Max 0.8	596	1.08	55.0	<i>n</i> = 8	<i>n</i> = 8
	min 0.2	132	0.42	14.0		
	<i>n</i> = 201	<i>n</i> = 329	<i>n</i> = 8	<i>n</i> = 12		
<b>1996-2004</b>	<b>m</b> <b>0.8</b>	<b>181</b>	<b>0.23</b>	<b>15.3</b>	(*) <b>~ 500 and</b> <b>1100 ± 400</b>	<b>18</b>
	$\sigma$ 0.2	34	0.05	6.9		10
	Max 1.4	266	0.38	30.2		<i>n</i> = 26
	min 0.5	88	0.11	4.1		
	<i>n</i> = 62	<i>n</i> = 94	<i>n</i> = 27	<i>n</i> = 27		
<b>2005-2012</b>	<b>m</b> <b>1.1</b>	<b>413</b>	<b>0.75</b>	<b>39</b>	(*) <b>~ 500 and</b> <b>1400 ± 400</b>	<b>14</b>
	$\sigma$ 0.3	137	0.67	39		4
	Max 1.8	712	2.18	122		<i>n</i> = 41
	min 0.6	234	0.09	8		
	<i>n</i> = 83	<i>n</i> = 87	<i>n</i> = 65	<i>n</i> = 44		
<b>Carbet Echelle</b> <b>1979-1995</b>	<b>m</b> n.d.	<b>141</b>	<b>0.40</b>	n.d.	<b>485</b>	-
	$\sigma$	142	0.54		90	

	Max		720	1.62		<i>n</i> = 7	
	min		19	0.13			
			<i>n</i> = 315	<i>n</i> = 7			
<b>1996-2012</b>	<b>m</b>	<b>0.2</b>	<b>16</b>	<b>0.04</b>	<b>2.1</b>	<b>462</b>	<b>17</b>
	<b><math>\sigma</math></b>	<b>0.1</b>	<b>4</b>	<b>0.02</b>	<b>0.8</b>	<b>162</b>	<b>5</b>
	Max	0.7	33	0.07	3.5	<i>n</i> = 21	<i>n</i> = 21
	min	0.0	6	0.02	0.3		
		<i>n</i> = 101	<i>n</i> = 151	<i>n</i> = 21	<i>n</i> = 26		
<b>Chute du Carbet</b>							
<b>1979-2003</b>							
	<b>m</b>	<b>0.2</b>	<b>344</b>	<b>0.75</b>	<b>39</b>	<b>412</b>	<b>14</b>
	<b><math>\sigma</math></b>	<b>0.08</b>	<b>141</b>	<b>0.36</b>	<b>10</b>	<b>116</b>	<b>5</b>
	Max	0.8	628	1.58	56	<i>n</i> = 38	<i>n</i> = 19
	min	0.0	154	0.26	25		
		<i>n</i> = 221	<i>n</i> = 350	<i>n</i> = 38	<i>n</i> = 19		
<b>2005-2012</b>							
	<b>m</b>	<b>0.2</b>	<b>140</b>	<b>0.37</b>	<b>41</b>	<b>367</b>	<b>14</b>
	<b><math>\sigma</math></b>	<b>0.07</b>	<b>31</b>	<b>0.12</b>	<b>11</b>	<b>60</b>	<b>4</b>
	Max	0.5	246	0.59	53	<i>n</i> = 27	<i>n</i> = 9
	min	0.1	97	0.25	19		
		<i>n</i> = 56	<i>n</i> = 66	<i>n</i> = 27	<i>n</i> = 9		
<b>Bain Chaud du Matouba-Eau Vive</b>							
<b>1979-2012</b>							
	<b>m</b>	<b>1.9</b>	<b>22</b>	<b>0.07</b>	<b>5.4</b>	<b>369</b>	<b>14</b>
	<b><math>\sigma</math></b>	<b>0.2</b>	<b>2</b>	<b>0.02</b>	<b>1.8</b>	<b>118</b>	<b>6</b>
	Max	2.4	37	0.15	8.5	<i>n</i> = 45	<i>n</i> = 23
	min	1.1	15	0.04	2.3		
		<i>n</i> = 339	<i>n</i> = 470	<i>n</i> = 45	<i>n</i> = 23		
<b>Habitation Revel</b>							
<b>1995-2012</b>							
	<b>m</b>	<b>0.2</b>	<b>11</b>	<b>0.05</b>	<b>3.3</b>	<b>233</b>	<b>17</b>
	<b><math>\sigma</math></b>	<b>0.1</b>	<b>1</b>	<b>0.01</b>	<b>0.8</b>	<b>53</b>	<b>3</b>
	Max	0.4	14	0.07	5.0	<i>n</i> = 12	<i>n</i> = 12
	min	0.1	5	0.03	2.1		
		<i>n</i> = 50	<i>n</i> = 127	<i>n</i> = 12	<i>n</i> = 14		

(\*) Two distinct correlations are observed within Cl-Br compositions of Ga Thermal springs (see Fig. 7).

(\*\*) EV is the capture of BCM spring- Chemical compositions are preserved but not temperature

Table III b Cratère Sud: fumaroles condensates and acid pond

		T (°C)	pH	F ppm	Cl ppm	Br ppm	I ppb	Cl/Br	Br/I
<b>Fumaroles condensates</b>									
<b>RC</b> (1983-2010)	<b>m</b>	<b>96.4</b>	<b>4.1</b>	<b>0.16</b>	<b>1.74</b>	<b>0.001</b>	<b>0.11</b>	~ 750	<b>10</b>
	$\sigma$	<b>0.8</b>	<b>0.4</b>	<b>0.08</b>	<b>2.42</b>	<b>0.002</b>	<b>0.05</b>		
	Max	100.4	5.1	0.34	9.87	0.01	0.22		
	min	90.8	2.7	0.08	0.02	b.d.l.	0.03		
	Nb values	739	124	18	27	18	13		
<b>CSC</b> (1997-2010)	<b>m</b>	<b>102.3</b>	<b>1.3</b>	<b>0.05</b>	<b>3604</b>	<b>0.13</b>	<b>9</b>	~ 200 000	<b>23</b>
	$\sigma$	<b>6.7</b>	<b>0.7</b>	<b>0.01</b>	<b>4538</b>	<b>0.40</b>	<b>25</b>		
	Max	130.3	4.3	0.08	32700	1.67	104		
	min	90.0	0.5	0.03	17	0.003	0.1		
	Nb values	285	123	9	85	17	17		
<b>CSN</b> (1997-2009)	<b>m</b>	<b>99.6</b>	<b>1.0</b>	<b>0.04</b>	<b>9410</b>	<b>0.23</b>	<b>28</b>	~ 600 000	<b>10</b>
	$\sigma$	<b>6.3</b>	<b>0.6</b>	<b>0.01</b>	<b>9381</b>	<b>0.52</b>	<b>73</b>		
	Max	126.3	3.6	0.05	47830	2.37	345		
	min	88.1	0.1	0.02	100	0.002	0		
	Nb values	211	162	4	145	30	30		
<b>Acid Pond</b>									
<b>CSC</b>	<b>m</b>	<b>88.8</b>	<b>-0.08</b>	(1 measurement 14/08/2007)				-	-
	$\sigma$	<b>8.6</b>	<b>0.50</b>	n.d.	<b>8745</b>	n.d.	n.d.		
	Max	109.2	1.61						
	min	72.0	-0.84						
	Nb values	33	88						

Table IV

IV a Standard Amic Hydrothermal waters (SASW)			Composition (mMol/L)							
	T°c	pH	Na+	K+	Mg++	Ca++	F-	Cl-	SO4--	HCO3-
<b>SASW1</b>	29	5.5	1.7	0.2	1.6	3.6	0.02	1.2	5.6	0.8
σ %	22	3	29	27	39	41	60	57	46	66
BJ (1968)	27	5.1	2.2	0.2	1.7	3.9	-	3.3	4.3	0.2
<b>SASW2</b>	41	5.8	3.2	0.4	2.4	4.3	0.0	3.9	5.6	1.5
σ %	8	12	18	3	39	51	60	25	54	61
Ga (1968)	24	4.3	1.7	0.2	1.7	4.0	-	1.3	6.0	-

IV b Contaminations (Kg)		Na	K	Mg	Ca	F	Cl	S	C
<b>BJ</b>	<b>2002-2011</b>	1 543	301	1 842	5 611	16	217 169	17 210	-
<b>Ga</b>	<b>1995-2001</b>	18 404	6 616	16 970	41 036	66	216 146	45 289	7
<b>Ga</b>	<b>2002 - 2011</b>	11 623	5 021	15 836	61 561	206	147 511	30 503	5
<b>CE</b>	<b>1998-2009 (*)</b>	585	65	1 216	2 963	-	4 813	5 604	1 393
<b>CC</b>	<b>1979-2004</b>	323	94	111	78	-	2 324	0	183

ACCEPTED